Effects of Ivermectin and Perfluorobutanesulfonic Acid (PFBS) on Lipid Metabolism

EFFECT OF IVERMECTIN AND PERFLUOROBUTANESULFONIC ACID ON LIPID METABOLISM

A Dissertation Presented

by

WEIPENG QI

Submitted to the Graduate School of the
University of Massachusetts Amherst in partial fulfillment
of the requirements for the degree of

DOCTOR OF PHILOSOPHY

SEPTEMBER 2019

The Department of Food Science

EFFECT OF IVERMECTIN AND PERFLUOROBUTANESULFONIC ACID ON LIPID METABOLISM

A Dissertation Presented

by

WEIPENG QI

Approved as to style and content by:

_____
Yeonhwa Park, Chair

_____
John M. Clark, Member

_____
Guodong Zhang, Member

_____
Lili He, Member

_____
Erick A. Decker, Department Head
Department of Food Science

ACKNOWLEDGMENTS

Undertaking this Ph.D. degree has been and will always be one of the most challenging obstacles in my life, and it would not be possible to do without support from many people.

First, I would like to thank my advisor, Dr. Yeonhwa Park, for being so patient and always willing to help whenever I need. I see your as my life-time role model for your dedication to work and your kindness to people.

My sincere thanks go to my dissertation committee members, Dr. John M. Clark, Dr. Guodong Zhang and Dr. Lili He, for your support and guidance.

Many thanks to all my lab members, past and present: Dr. Yoo Kim, Dr. Xiao Xiao, Dr. Quancai Sun, Dr. Peiyi Shen, Mr. Tsung-Hsiu Hsieh, Mr. Daniel Colmenares, Dr. Ou Wang, Ms. Yiren Yue, Dr. Phoebe Chen, Dr. Szu-Hao Yang, Dr. Ye Peng, Mr. Renalison Farias Pereira, Ms. Jiaying Wang, Ms. Jinning Liu, Ms. Sida Li, Ms. Zhuojia Qian, and Mr. Zhenyu Zhang for your friendship and help. It has been great sharing the lab with all of you in the past five years.

Thanks also go to all my friends in Amherst for making my life less stressful. I will always treasure our friendship.

I would like to express my gratitude to my loving family in China for being supportive. Last but not least, I would thank my wife, Hao Wang, for your understanding and for being such a great person that help me out when I am emotionally weak throughout my Ph.D. study.

ABSTRACT

EFFECT OF IVERMECTIN AND PERFLUOROBUTANESULFONIC ACID ON LIPID METABOLISM

September 2019

WEIPENG Qi

B.S., SICHUAN UNIVERSITY

Ph.D., UNIVERSITY OF MASSACHUSETTS AMHERST

Directed by: Professor Yeonhwa Park

Accumulating evidence has shown a link between environmental contaminants and altered lipid metabolism. There is currently, however, limited knowledge regarding the causal molecular mechanisms. Therefore, we investigated the molecular mechanisms of two environmental contaminants, ivermectin and perfluorobutanesulfonic acid (PFBS), on lipid metabolism in adipocytes and hepatocytes using cell culture models. We first studied the effects of ivermectin, an anti-parasitic agent, on the adipogenesis of 3T3-L1 preadipocytes. Our current results suggest that ivermectin inhibits adipogenesis in 3T3-L1 preadipocytes and the expression of adipogenic genes where these effects were found to be partially via PPARγ-dependent, but not FXR-dependent, pathway. Additionally, ivermectin also activates the expression of glycine receptor subunits, potentially related to the inhibitory effect on adipogenesis. PFBS is the replacement of perfluorooctanesulfonic acid, which has been reported to disrupt lipid metabolisms. There is no report, however, of the effect of PFBS on lipid metabolisms. We found that PFBS treatment extensively promoted the differentiation of 3T3-L1 preadipocytes, resulting in significantly increased TG levels. The effects of PFBS were found to target the early stage of differentiation, in particular via MEK/ERK-dependent pathway. The effects of PFBS on hepatic lipid metabolisms were also investigated by using HepG2 hepatocytes. The current results suggested that PFBS increased the hepatic TG accumulation when supplemented with fatty acid mixture. The effects were also found mediated by PPARγ-mediated pathways.

TABLE OF CONTENTS

LIST OF TABLES

Page

LIST OF FIGURES

CHAPTER 1

INTRODUCTION

Previous studies have revealed that environmental factors, other than diet, can be responsible for the development of metabolic syndromes, which is the clustering of abdominal obesity, hypertension, dyslipidemia, and type 2 diabetes. Among them, prolonged exposure to environmental contaminants has attracted more attention as one of the potential causes (Arciello et al., 2013; Armstrong and Guo, 2019; Patel et al., 2012; Wang et al., 2016). Significant progress has been made on determining the effect of different kinds of environmental contaminants on lipid metabolism. However, little is known about the molecular mechanisms by which environmental contaminants disturb lipid metabolism. Therefore, elucidating the potential role of environmental contaminants on lipid metabolism, and the underlying mechanisms behind should provide useful information in developing strategies to prevent and treat related diseases, such as obesity and type 2 diabetes.

Ivermectin typically consists of a mixture of avermectin B1a and B1b at a ratio of 80:20 and kills parasites and insects in and on animals and humans primary by interfering with the glutamate-gated chloride channels, inducing membrane hyperpolarization and paralysis of nerve and muscle cells (Turner and Schaeffer, 1989). PFBS, the replacement of PFOS since early 2000s, is a four-carbon fluorosurfactant widely used in a wide range of consumer products, including food packages, fabrics, non-stick products, paints, waxes, cleaners, as well as in some production facility, including electronics manufacturing, and oil recovery (Favreau et al., 2017; Herzke et al., 2012). In this proposal, we aimed to determine if ivermectin could alter the adipogenesis of preadipocytes and if PFBS could impair lipid metabolism in adipocytes and hepatocytes. The identification of underlying mechanisms of these environmental contaminants on lipid metabolism is expected to help understanding the role of environmental contaminants in the development of metabolic diseases associated with lipid metabolism.

CHAPTER 2

LITERATURE REVIEW

2.1 Introduction

Perfluoroalkyl and polyfluoroalkyl substances (PFAS) are a group of man-made chemicals that share an aliphatic carbon backbone in which hydrogen atoms have been replaced by fluorine. In perfluoroalkyl substances, carbon atoms are completely saturated by fluorine; while in polyfluoroalkyl substances, carbon atoms are mostly replaced by fluorine, and they contain at least one perfluoroalkyl moiety CnF2(n+1)-, but still contain some carbon-hydrogen bonds. In both perfluoroalkyl and polyfluoroalkyl substances, the structures are characterized by the high amount of carbon-fluorine bonds, the forth strongest chemical bond in general and the strongest bond in organic chemistry (O'Hagan, 2008). With increasing number of fluorine atoms on one carbon, the bonds become stronger (Lemal, 2004). Due to this structural attribute, PFAS are generally stable and chemically inert, being able to withstand heat, acids, bases, reducing agents, oxidants, etc. In addition, the fluorocarbon chain of PFAS is non-polar, and hence highly hydrophobic. At the same time, this chain is highly lipophobic due to the lower ability to form instantaneous dipoles that forms the basis of London dispersion force (Lemal, 2004). Additionally, the sulfate or carboxylate "head" group is hydrophilic, which make PFAS amphipathic and great materials for use as surfactants. Because of these traits, PFAS, as well as surfactants and polymers made with the aid of PFAS have been extensively manufactured and used in a wide range of consumer products, including food packages, fabrics, non-stick products, paints, waxes, firefighting foam, cleaners, makeup, as well as some production facility, including electronics manufacturing, and oil recovery since the 1940s (Favreau et al., 2017; Herzke et al., 2012).

As the result of extensive use, PFAS contaminated the environment through PFAS or fluoropolymer manufacturing (Emmett et al., 2006; Hoffman et al., 2011; Hu et al., 2016; Hurley

et al., 2016; Landsteiner et al., 2014; Shin et al., 2011), waste (Allred et al., 2015; Eriksson et al., 2017; Gallen et al., 2018; Hamid et al., 2018; Lang et al., 2017; Sindiku et al., 2013), aqueous Film-Forming Foam Concentrates (AFFF) used at airports, military bases and firefighter training sites (Houtz et al., 2013; Houtz et al., 2016a; Hu et al., 2016), and degradation from precursor chemicals (Butt et al., 2014; Hagen et al., 1981; Wang et al., 2015; Young and Mabury, 2010). Drinking water, especially localized with facilities using PFAS, is one of the primary exposure routes for PFAS. In fact, PFAS can be detected at relatively high concentrations in surface water all over the world (Post et al., 2012). As most PFAS are extremely stable and hence, relatively resistant to degradation, which exacerbates their contamination in the environment. Longer chain PFAS, such as C8 PFAS, have been reported to bioaccumulate in wildlife (Houde et al., 2011). The bioaccumulation in animal- and plant-based food, as well as the direct contamination from food packaging, makes food an important route of exposure (Trudel et al., 2008). Alternatively, air, dust, and direct contact with PFAS-treated products, can also potentiate the exposure of PFAS to human. In fact, PFAS, especially perfluorooctanesulfonic acid (PFOS) and perfluorooctanoic acid (PFOA), have been detected in the plasma of human worldwide (Post et al., 2012).

The exposure of PFAS has been extensively reported to induce adverse human health effects on reproduction (Bach et al., 2016), immune system (Chang et al., 2016), endocrine function (Kim et al., 2018), kidney function (Conway et al., 2018), cancer (Chang et al., 2014), metabolic diseases (Christensen et al., 2019), and adverse developmental effects in offspring, such as low birth weight, high diabetes and obesity risk (Heindel et al., 2017). The concern about potential adverse effects of PFAS on the environment, wildlife, and humans - especially the long-chain PFAS- led to the phase-out of perfluorooctanesulfonic acid (PFOS) and perfluorooctanoic acid (PFOA) in 2000s. Alternative shorter-chain PFAS have been developed to replace the long-chain PFAS. In this review, we summarize the chemistry and historical uses of PFAS and present a systematic review of the current epidemiology findings on associations between PFAS exposure and the

development of metabolic syndrome and related diseases including obesity, diabetes, and non-alcoholic fatty liver disease (NAFLD).

2.2 Classification of PFASs

Characterized by their functional groups, PFAS can be divided into numerous families. This section provides an overview of the common names, chemical structures, and some important properties and uses of most well-studied PFAS that have been detected in environment and in humans. The structures for selected PFAS was given in Figure 2.1.

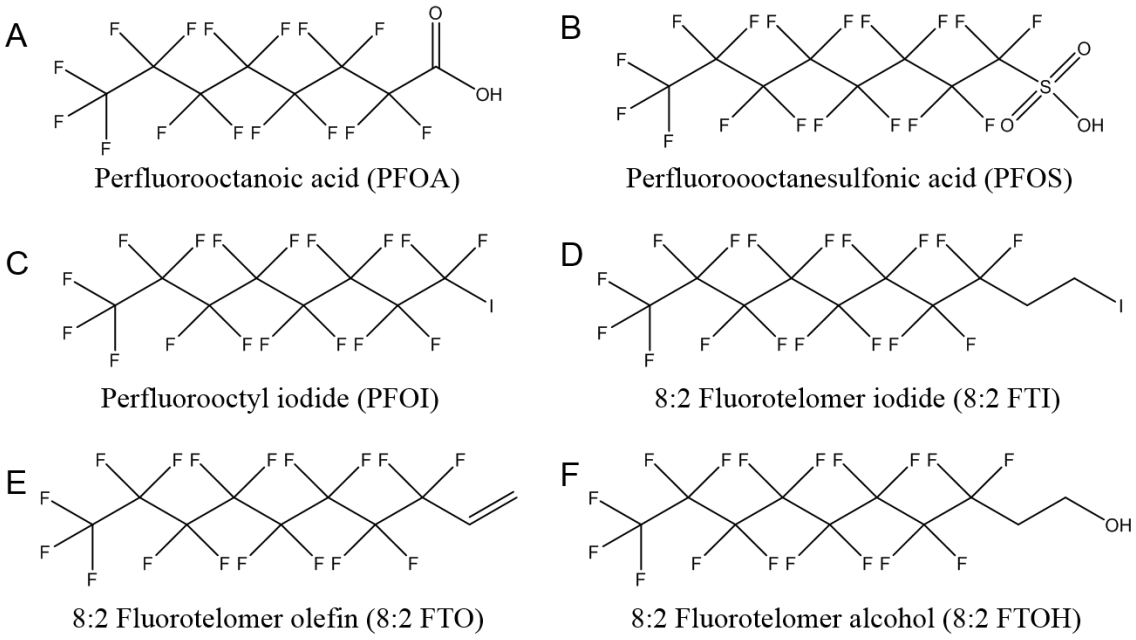

Figure 2.1 Structures of perfluoroalkyl and polyfluoroalkyl substances (PFAS).

2.2.1 Perfluoroalkyl acids

Perfluoroalkyl acids (PFAAs) are the most studied PFASs due to their extensive use in various industries and their high persistence in both the environment and animal bodies. PFAA family includes perfluoroalkyl carboxylic, sulfonic, sulfinic, phosphonic, and phosphinic acids.

Perfluoroalkyl carboxylic acids: Perfluoroalkyl carboxylic acids (PFCAs) are a group of compounds of the formula of $C_nF_{(2n+1)}COOH$. The chemical structures of these compounds consist of a hydrophilic carboxylate "head group" and a hydrophobic fluorocarbon chain. The

most studied PFCA is PFOA, $C_7F_{15}COOH$ (Figure 1A). PFOA can be synthesized by two major electrochemical fluorination (ECF) and telomerization. ECF is a technology replacing all the H atoms in an organic raw material with F atoms by electrolysis in HF (Karsa, 1995; Simons, 1949). In the early 2000s, a new method was introduced to produce higher percentages of linear products by oxidizing linear perfluorooctyl iodide (PFOI), $F(CF_2)_8I$ (Figure 1C), synthesized by telomerization into PFOA (Ameduri and Boutevin, 2004). PFOA, commonly used as its ammonium salt ammonium perfluorooctanoate (APFO) produced exclusively by ECF, has been used as surfactant to solubilize the fluoromonomers in the manufacture of fluoropolymers, for example polytetrafluoroethylene (PTFE), since 1940s (Ebnesajjad, 2013). Perfluorononanoic acid (PFNA), $C_8H_{17}COOH$, is another PFCA widely used as the ammonium form in the production of polyvinylidene fluoride (PVDF) (Schué, 1999). PFNA is produced mainly from the oxidation of fluorotelomer olefin (Buck et al., 2011).

In the recent decade, production of PFOA and its related precursors has been largely reduced. In 2006, eight leading manufacturers in PFAS were invited by EPA to join a global stewardship program aiming to achieve 95% reduction in both emission and product content levels of PFOA, related higher homologue chemicals and their precursor chemicals by 2010, and to eliminate these chemicals from emissions and products by 2015.

Besides their major use in fluoropolymer industry, PFCAs are also considered the final biodegradation product of some precursor PFAS, especially fluorotelomer-based products including fluorotelomer alcohol, fluorotelomer olefin, fluorotelomer iodides, etc. (Dinglasan et al., 2004; Frömel and Knepper, 2010; Hagen et al., 1981). It has been estimated, however, ~80% of PFCAs released to the environment are directly from the fluoropolymer production (Prevedouros et al., 2006).

Perfluoroalkyl sulfonic acids: Perfluoroalkyl sulfonic acids (PFSAs) are another group of major PFAAs. Among all the PFSAs, PFOS (Figure 1B), the 8 carbon PFSA, is the most used and well-studied. Since 1949, the 3M company started to synthesize PFOS by the degradation from

precursor perfluorooctane sulfonyl fluoride (POSF) produced by ECF, and it can also be produced by telomerization (Lehmler, 2005). However, PFOS was later detected globally in wildlife and human, and the biological half-life of PFOS was reported to be 5.4 years (Li et al., 2018; Olsen et al., 2007). Meanwhile, correlations were reported between serum levels of PFOS and the development of various diseases (Bach et al., 2016; Chang et al., 2014; Chang et al., 2016; Heindel et al., 2017; Kim et al., 2018). 3M announced the phase out of C8 based chemicals in early 2000s. In 2009, PFOS-based compounds were listed in Annex B of the Stockholm Convention on persistent organic pollutants. Perfluorohexanesulfonic acid (PFHxS), the 8 carbon PFSA and its salt are also used as a replacement of PFOS. However, the estimated half-life of PFHxS in human is equivalent to or even longer than PFOS (Li et al., 2018; Olsen et al., 2007). Thus, PFHxS was added to the candidate list of Substances of Very High Concern (SVHC) in 2007.

Since 2003, 3M started to use perfluorobutanesulfonic acid (PFBS) as a replacement of PFOS/PFHxS-based chemicals. PFBS is the 4 carbon PFSA, with a half-life in human of about a month (Olsen et al., 2009b), which is significantly shorter than PFOS and PFHxS. In the last decade, the levels of PFBS detected in the environment, wildlife and human serum have been increasing (Glynn et al., 2012; Hölzer et al., 2008; Lam et al., 2016; Ruan et al., 2015; Zhou et al., 2013b), which poses a concern about the potential adverse effect on public health.

Other perfluoroalkyl acids: Besides PFCAs and PFSAs, environmental occurrence and detections of perfluoroalkyl sulfinic acids (PFSIAs), perfluoroalkyl phosphonic acids (PFPAs) and perfluoroalkyl phosphinic acids (PFPIAs) has also been increasingly reported in human (Ahrens and Ebinghaus, 2010; D'Eon J et al., 2009; Lee and Mabury, 2011). PFSIAs are the biodegradation products of some precursors chemicals, including N-ethyl perfluorooctane sulfonamidoethanol (N-EtFOSE) (Boulanger et al., 2005; Rhoads et al., 2008), while PFPAs and PFPIAs are widely used surfactants in various industries (Howard and Muir, 2010).

.

2.2.2 Fluorotelomer-based chemicals

Fluorotelomers are a group of oligomers with multiple perfluoroalkyl moieties, synthesized by telomerization (Ameduri and Boutevin, 2004). Some of these compounds have recently become of interest as they are recognized as the environmental precursors of PFCAs (Butt et al., 2014; Dinglasan et al., 2004; Hagen et al., 1981; Young and Mabury, 2010), although the contribution of these precursors to total exposure to human was reported to be variable among different PFCAs.

Perfluoroalkyl iodides (PFAIs), also known as Telomer A, are major raw materials in the production of PFAS-based surfactants by telomerization, with common formula $C_nF_{2n+1}I$. They are usually obtained by the reaction between a short starting PFAI, the telogen, and tetrafluoroethylene ($CF_2=CF_2$), the taxogen. PFAIs are the most important precursors of fluorotelomer-based chemicals including fluorotelomer iodides, fluorotelomer alcohol and fluorotelomer olefin (Lehmler, 2005). By inserting ethylene in the structure, n:2 fluorotelomer iodides (n:2 FTIs), $C_nF_{2n+1}CH_2CH_2I$, is obtained. The n:2 FTIs serve as the intermediate products in the synthesis of the n:2 fluorotelomer alcohols (n:2 FTOHs), as well as certain PFAS. The n:2 fluorotelomer olefins (n:2 FTOs), $C_nF_{2n+1}CH=CH_2$, are synthesized by dehydrohalogenation of n:2 FTIs. As stated above, PFAS, for example PFNA, can be produced by the oxidation of the respective fluorotelomer olefin. FTOs are also the byproducts of the synthesis of several fluorotelomer-based chemicals from n:2 FTIs.The n:2 fluorotelomer alcohols (n:2 FTOH), $C_nF_{2n+1}CH_2CH_2OH$, are the precursors of their acrylic and methacrylic ester, which can be used to form fluorinated polymers providing water and oil repellency (Rao and Baker, 1994). These polymers can be used in textile, paper and leather industry. The phosphoric mono- and di-esters of FTOH, which are also produced from FTOH, have been used as oil-proof food packaging (Begley et al., 2008; Yuan et al., 2016). In human, n:2 FTOHs have been reported to be metabolized into PFCAs (Henderson and Smith, 2007; Martin et al., 2005), which could induce adverse effects.

2.3 Sources and pathways of human exposure

Exposure to PFAS can occur through a variety of sources and pathways, including but not limited to drinking water, food, indoor air and dust. Among them, water contamination is considered one of the major sources, especially those near certain locations including industrial sites, military fire training sites, and wastewater treatment plants (Egeghy and Lorber, 2010; Emmett et al., 2006; Hu et al., 2016; Vestergren and Cousins, 2009). In a US national research project to determine the contaminants in drinking water, 50% of samples were determined to contain more than two PFAS, and 72% of detections occurred in ground water samples (Guelfo and Adamson, 2018). In a US national spatial analysis of PFAS concentrations in drinking water from 2013-2015, water supplies for 6 million US residents exceed US EPA lifetime advisory levels for PFOS and PFOA, which is 70 ng/L (Hu et al., 2016). In the last decades, while the detection levels of long chain PFAS, including PFOS and PFOA, have been declining, alternative PFAS have been increasingly detected in the drinking water (Houtz et al., 2016; Ruan et al., 2015; Zhou et al., 2013b).

Dietary intake is another important source of PFAS exposure. According to modeling studies, PFAS contamination in food accounts for the majority of non-occupational exposure to PFAS among all the contributing factors (Gebbink et al., 2015; Papadopoulou et al., 2017). Considering PFAS exposure from all potential exposure routes, Fromme et al. (Fromme et al., 2009) suggested that food accounts for over 90% of PFOS/PFOA exposure. Recently, more individual-based daily PFAS intake studies further solidified the conclusion that food is the main contributor of PFAS in humans (Chen et al., 2018; Haug et al., 2011; Jain, 2018a; Tittlemier et al., 2006; Tittlemier et al., 2007; Vestergren et al., 2012). According to research comparing multiple dietary assessment methods, the most abundant individual PFAS in food are PFOA, PFOS and PFHxS. Among them, PFOS is the main contributor in solid food, while PFOA contributes the most in liquid food (Papadopoulou et al., 2017). Interestingly, the dietary

exposure of PFAS is correlated with high consumption of fats, oils, eggs, milk, as well as foods in paper containers (Tian et al., 2018).

Multiple causes can lead to the contamination of PFAS in food. As PFAS are bio-accumulative and persistent in environment, food derived from animals, in particular seafood, may contain PFAS due to the exposure of animals to the environment, especially water. Plant-based food can also be contaminated by being watered by PFAS contaminated water. Direct exposure to food packaging can be another possible cause of contamination, as a great number of PFAS are widely used in food packaging as oil and/or water repellent, especially in fast food packaging (Begley et al., 2005; Herzke et al., 2012; Martinez-Moral and Tena, 2012; Poothong et al., 2012; Tittlemier et al., 2006; Yuan et al., 2016). The migration of PFAS from food packaging to food has also been extensively reported (Begley et al., 2008; Begley et al., 2005). PFOA residue in PTFE-coated non-stick cookware could likewise be a potential source of PFAS exposure through food, although it is generally not considered significant (Schlummer et al., 2015). Besides these dietary sources, the accumulation of PFAS in human milk, which is the most important source of PFAS exposure for infants, has also been well-studied, and a growing body of literature has suggested a link between postnatal exposure to PFAS and health effects in childhood, adolescence and adulthood (Antignac et al., 2013; Kang et al., 2016; Lee et al., 2018; Macheka-Tendenguwo et al., 2018; Nyberg et al., 2018; Sundstrom et al., 2011).

In addition to drinking water and food, it has been reported that humans can also be exposed to PFAS by indoor air, indoor dust, and direct contact with PFAS-treated consumer products (Fraser et al., 2012; Harrad et al., 2010), which could account for up to 50% of PFAS exposure in certain individuals (Haug et al., 2011). It has also been suggested that the exposure of PFAS to pregnant women might also induce exposure of PFAS to embryos and fetus in placenta during gestation (Apelberg et al., 2007; Fei et al., 2007; Inoue et al., 2004; Midasch et al., 2007).

Along with the trend restricting long chain PFAS production and use in the past decade, the serum levels of long chain PFAS, including PFOS and PFOA, have been reported to be

reduced globally, especially in western countries and Japan (Jain, 2018b; Okada et al., 2013; Olsen et al., 2012; Shu et al., 2019; Tsai et al., 2018). However, the concentration of the replacements of these long chain PFAS, for example four-carbon PFBS, keep increasing in the same timeframe (Glynn et al., 2012), which calls for further investigation on their safety.

2.4 Epidemiological evidences

2.4.1 Overweight and obesity

Overall, of the 22 epidemiology studies we found, 15 studies reported positive associations between overweight or obesity and the exposure to at least one PFAS (Table 2.1). Among the ten studies that examine obesity/overweight in general populations, at least one PFAS was found to be associated with increased body mass index (BMI), waist circumference or weight gain in three cohort studies (Cardenas et al., 2018; Jaacks et al., 2016; Liu et al., 2018a) and three cross-sectional studies (Christensen et al., 2019; Tian et al., 2019; Yang et al., 2018b) conducted among general populations in China and US. In these studies, three suggested a positive association between serum PFOS and overweight or related symptoms (Jaacks et al., 2016; Liu et al., 2018a; Tian et al., 2019), although a negative association between PFOS and BMI was reported among German men (Hölzer et al., 2008). Similarly, PFOA was also reported to be positively associated with increased BMI (Yang et al., 2018b), waist circumference (Tian et al., 2019), as well as weight re-gain after diet induced weight loss potentially by reducing resting metabolic rate (Liu et al., 2018a). Positive associations were also reported on other commonly used PFAS, including PFNA (Christensen et al., 2019; Liu et al., 2018a; Tian et al., 2019; Yang et al., 2018b), PFHxS (Liu et al., 2018a), and PFDA (Liu et al., 2018a; Tian et al., 2019). Meanwhile, perfluoroundecanoic acid (PFUnDA), a less studied PFAS, was inversely associated with the risk of overweight (Christensen et al., 2019). However, four studies in US, Korea and Germany have shown null association (Blake et al., 2018; Hölzer et al., 2008; Nelson et al., 2010; Seo et al., 2018).

Prenatal exposure is another major focus of epidemiology study in overweight or obesity induction by PFAS. Although the *in-utero* exposure to PFAS was largely associated with low birth weight, cohort studies have reported the association between maternal PFAS exposure and overweight/obesity in childhood and adolescence. Girls born to mother with higher PFOS, PFOA and PFHxS weighed less when newborn. After 20 months, however, females in the higher quartile of maternal PFOS concentration were observed to be overweight compared to those in lower quartile, while no differences in weight were found in PFOA and PFHxS (Maisonet et al., 2012). Five prospective cohort studies have reported the association between maternal PFAS exposure and obesity or overweight in children at school age in Europe (Hartman et al., 2017; Høyer et al., 2015; Lauritzen et al., 2018) and US (Braun et al., 2016; Mora et al., 2016). Among these studies, two reported positive association limited to female offspring (Hartman et al., 2017; Mora et al., 2016). Similar results were found in a 20-year follow-up prospective cohort study, which provides more information for offspring up to young adulthood. The highest quartile of PFOA concentration in maternal cord blood showed increased risks in higher BMI and waist circumference in female offspring at age 20 (Halldorsson et al., 2012). However, such associations cannot be found in male offspring or with other PFAS, including PFOS, PFOSA, and PFNA (Halldorsson et al., 2012). Therefore, sex might be a potential contributing factor for PFAS-induced obesity. Despite the positive correlation listed above, several studies reported inconsistent results on the association between maternal PFAS exposure and obesity. One prospective study in Netherland reported a non-association between prenatal PFOS/PFOA and BMI of offspring at 12 months (de Cock et al., 2014). Anderson et al. observed inverse association between higher PFOS and PFOA maternal exposure and weight and BMI in the first year (Andersen et al., 2010), although this trend was then diminished when they were at the age of seven (Andersen et al., 2013).

Adiposity was also found to be associated with PFAS exposure during postnatal and early childhood. In a perspective birth cohort study in Faroe Islands, the child's BMI at age 18 months

and 5 years were associated with maternal postpartum serum concentration of PFOS and PFOA (Karlsen et al., 2017). However, they only observed weak correlations in PFHxS, PFNA and PFDA (Karlsen et al., 2017). In another large multicenter prospective cohort study, childhood exposure to PFOS, but not PFOA, at the age of nine was associated with increase adiposity markers, including elevated BMI, skinfold thickness and waist circumference, in adolescence and young adulthood (Domazet et al., 2016).

To summarize, obesity and overweight have been connected to PFAS exposure to general populations, as well as maternal exposure and childhood exposure. Although null association was reported in some of these studies, and three studies reported negative associations (Andersen et al., 2010; Christensen et al., 2019; Hölzer et al., 2008), from the epidemiology data, it may be sufficient to conclude the positive associations between PFAS exposure and overweight or obesity.

Table 2.1 Summary of epidemiology studies of perfluoroalkyl and polyfluoroalkyl substances (PFASs) on risk of obesity or overweight in human.

Study design	**Demographics**	**N**	**Summary of results**	**Ref**
Cross-sectional	German men, mother and child	345	Negative association between serum PFOS and BMI in men	(Hölzer et al., 2008)
Cohort	Danish mother-child pairs	1010	Negative association between maternal PFOS/PFOA and weight at 12 months	(Andersen et al., 2010)
Cross-sectional	US aged 12-80	2094	No association between serum PFOS/PFOA/PFHxS/PFNA and BMI	(Nelson et al., 2010)
Cohort	Danish mother-child pairs	665	Positive association between maternal PFOA and increased BMI and waist circumference of female offspring at 20 years of age; No association in male offspring	(Halldorsson et al., 2012)
Cohort	British mother-daughter pairs	447	Association between maternal PFOS and PFOA levels and low birth weight; Positive association between prenatal PFOA and body weight of female offspring at 20 months	(Maisonet et al., 2012)
Cohort	Danish mother-child pairs	811	No association between maternal PFOS/PFOA and overweight at 7 years of age	(Andersen et al., 2013)
Cohort	Dutch mother-child pairs	148	No association between maternal PFOS/PFOA and weight at 12 months	(de Cock et al., 2014)
Cohort	Greenlandic and Ukrainian mother-child pairs	1022	No association between PFOS/PFOA and overweight; Significant increase in relative risks of having waist-to-height ratio>0.5 at 5 to 9 years	(Høyer et al., 2015)
Cohort	US mother-child pairs	204	Positive association between maternal PFOA concentration and offspring adiposity at 8 years of age, and BMI gain from age 2-8	(Braun et al., 2016)
Cohort	Danish children	201/202	Positive association between serum PFOS at 9 and overweight at 15 and 21	(Domazet et al., 2016)
Cohort	US pregnant women with BMI< 25 kg/m^2	218	Positive association between pre-pregnant serum PFOS and gestational weight gain	(Jaacks et al., 2016)
Cohort	US mother-child pairs	1006 + 876	Positive association between maternal PFOS, PFOA, PFNA, and PFHxS and mid-childhood (median, 7.7 years) overweight in female offspring; No association in male or early childhood (median, 3.2 years)	(Mora et al., 2016)
Cohort	UK mother-daughter pairs	359	Positive association between PFOA and body fat percentage of female offspring of mothers at middle education level, and negative association for highest education group; No overall association between maternal PFOS, PFOA, PFHxS or PFNA and body fat percentage at 9 years of age	(Hartman et al., 2017)

Cohort	Faroese mother-child pairs	444	Positive association between postpartum maternal PFOS/PFOA and overweight in offspring at 5 years of age; No association in PFHxS, PFNA, and PFDA	(Karlsen et al., 2017)
Cohort	US adults	210	No association between serum levels of 8 PFASs and BMI	(Blake et al., 2018)
Cohort	US adults	957	Positive association between serum PFASs and weight and hip girth	(Cardenas et al., 2018)
Cohort	Norwegian and Swedish mother-child pairs	412	Positive association between maternal PFOS concentration and increased odds of child overweight/obesity at 5 years of age	(Lauritzen et al., 2018)
Cohort	US overweight adults	621	Positive association between baseline PFOS, PFOA, PFHxS, PFNA and PFDA and a greater weight re-gain in a diet-induced weight loss setting, primarily in women	(Liu et al., 2018a)
Cross-sectional	Korean adults	786	No association between serum levels of 13 PFASs and BMI	(Seo et al., 2018)
Cross-sectional	Chinese male adults	148	Positive association between serum PFOA/PFNA and increased BMI	(Yang et al., 2018b)
Cross-sectional	US adults	2975	Positive association between serum PFNA and increased waist circumference; Negative association between serum PFUnDA and waist circumference	(Christensen et al., 2019)
Cross-sectional	Chinese adults	1612	Positive association between serum PFOS, PFOA, PFNA and PFDA and overweight and waist circumference	(Tian et al., 2019)

PFOS, perfluorooctanesulfonic acid; PFOA, perfluorooctanoic acid; PFNA, perfluorononanoic acid; PFHxS, perfluorohexanesulfonic acid; PFUnDA, perfluoroundecanoic acid; PFDA, perfluorodecanoic acid

2.4.2 Diabetes

Among 32 studies we found, 21 reported positive association between PFAS exposure and prevalence of diabetes (type 2, type 2, and gestational diabetes) or related markers (Table 2.2). Initially, increased standardized mortality rate of diabetes was reported to increase among workers in polymer production plants, where workers could be exposed to PFOA and APFO (Leonard et al., 2008). Two reports also observed positive associations with the increase mortality rate or onset of diabetes (Lundin et al., 2009; Steenland et al., 2015). Ten reports have suggested that environmental exposure to PFAS was associated with the elevated prevalence of type 2 diabetes (Christensen et al., 2016; He et al., 2018; Lind et al., 2014; Mancini et al., 2018; Su et al., 2016; Sun et al., 2018), or related biomarkers including area under the curve (AUC) in oral glucose tolerance test (OGTT), homeostatic model assessment for insulin resistance (HOMA-IR) index, and fasting glucose (Alderete et al., 2019; Cardenas et al., 2017; Kim et al., 2016b; Timmermann et al., 2014). However, few studies have found null to inverse relationships; five reported null associations among US and Canadian adults and children (Fisher et al., 2013; Karnes et al., 2014; Khalil et al., 2018; MacNeil et al., 2009; Nelson et al., 2010), while inverse associations were reported by four studies among Taiwanese adults (Su et al., 2016), Swedish adults (Donat-Vargas et al., 2019), US adults, adolescence and children (Conway et al., 2016; Koshy et al., 2017), as well as mother and child pairs (Fleisch et al., 2017).

A positive association has also been reported between PFAS exposures and type 1 diabetes. In a case-control study with 44 children and adolescents in Italy, the serum concentrations of PFOS were significantly higher in patients with type 1 diabetes than in healthy controls (Predieri et al., 2015), although the significance of this result is limited by its small sample size. In a larger case-control study among 66,899 participants in C8 Health Project, however, serum levels of PFOS, PFOA and PFNA were all negatively associated with type 1 diabetes (Conway et al., 2016). Consistent with the finding that PFAS might have protective

association with type 1 diabetes, PFOS and PFOA exposure have been reported to be positively associated with improved beta cell function in three different studies in US adults (Cardenas et al., 2017; Lin et al., 2009; Liu et al., 2018b), although PFNA level was negatively associated with beta cell function in adolescent (Lin et al., 2009).

PFOS and PFOA exposure was found to be positively associated with gestational diabetes according to three cohort studies conducted in US, Spain Denmark, and China (Jensen et al., 2018; Matilla-Santander et al., 2017; Rahman et al., 2019; Wang et al., 2018; Zhang et al., 2015). Interestingly, in a case control study among Chinese pregnant women, serum levels of total short chain PFCAs (C4-C7) were positively associated with gestational diabetes (Liu et al., 2019).

Overall, the epidemiology findings in diabetes are relatively controversial. However, according to a review summarizing the dose response curves of PFOA in several outcomes, non-monotonic dose-response curves, even U-shaped dose response curves, were observed in many studies (Post et al., 2012). Consistently, non-linear relationship can be found in two different studies in diabetes (Lind et al., 2014; Mancini et al., 2018). Inverse U-shaped relationship between dietary exposure to PFOA and the risk of developing type 2 diabetes: increasing type 2 diabetes risk at low serum PFOA levels and decreasing risk at high serum PFOA levels (Mancini et al., 2018). Therefore, the inconsistency might be due to the different exposure levels in different geological areas in the respective studies, as different PFOA levels might show different dose responses on diabetes. From the current evidences, PFAS may be positively associated with type 2 diabetes and gestational diabetes. However, the effects of PFAS on type1 diabetes are not conclusive, as few epidemiological studies on beta cell function have found a positive association between PFAS and improved beta cell function.

Table 2.2 Summary of epidemiology studies of perfluoroalkyl and polyfluoroalkyl substances (PFASs) on risk of altered glucose metabolism in human.

Study design	**Demographics**	**N**	**Summary of results**	**Ref**
Cohort	US Dupont workers	6027	Mortality associated with diabetes significantly increases in workers in polymer production plan	(Leonard et al., 2008)
Cross-sectional	US adolescents and adults	474+969	Negative association between serum PFNA and beta cell function in adolescents; Positive association between serum PFOS/PFOA and beta cell function in adults	(Lin et al., 2009)
Cohort	US 3M workers	3993	Mortality associated with diabetes significantly increases in workers in polymer production plan	(Lundin et al., 2009)
Cross-sectional	US adults	13922	No association between serum PFOA and type 2 diabetes prevalence and fasting glucose	(MacNeil et al., 2009)
Cross-sectional	US aged 12-80	2094	No association between serum PFOS/PFOA/PFHxS/PFNA and HOMA-IR	(Nelson et al., 2010)
Cross-sectional	Canadian adults	3496	No association between serum PFOS/PFOA/PFHxS and blood insulin, glucose and HOMA-IR	(Fisher et al., 2013)
Cross-sectional	US adults	32254	No association between serum PFOA and type 2 diabetes prevalence	(Karnes et al., 2014)
Cross-sectional	Swedish elderly aged 70	1016	Non-linear relationship between serum PFNA and type 2 diabetes prevalence; No association between PFASs and HOMA-IR	(Lind et al., 2014)
Cohort	Overweight Danish children aged 8-10	499	Positive association between serum PFOS and blood insulin	(Timmermann et al., 2014)
Cross-sectional	Italian children aged 2-14	44	Positive association between serum PFOS and type 1 diabetes prevalence	(Predieri et al., 2015)
Cohort	US Dupont workers	3713	Significant positive trend for diabetes onset	(Steenland et al., 2015)
Cohort	US pregnant women	258	Positive association between serum PFOA and gestational diabetes prevalence	(Zhang et al., 2015)
Cross-sectional	US male adults aged > 50	154	Positive association between serum PFNA/PFUnDA/PFDA and the prevalence of prediabetes or diabetes	(Christensen et al., 2016)
Cross-sectional	US adults and children aged > 13	66899	Negative association between serum PFOS/PFOA/PFHxS/PFNA and type 1 and type 2 diabetes	(Conway et al., 2016)

Cohort	Danish children	201	Negative association between serum PFOS at 9 and beta cell function at 15	(Domazet et al., 2016)
Double-blind trial	Korean elderly aged > 60	141	Positive association between serum PFOS/PFDoDA and HOMA-IR index	(Kim et al., 2016b)
Cross-sectional	Taiwanese adults	571	Positive association between serum PFOS and diabetes prevalence; Negative association between PFOA/PFNA/PFUnDA and diabetes prevalence	(Su et al., 2016)
Cross-sectional	US adults with high diabetes risk	975	Positive association between serum PFOS/PFOA and beta cell function; Positive association between PFOS/PFOA and HOMA-IR	(Cardenas et al., 2017)
Cohort	US mother-child pairs	665	Negative association between serum PFOA and HOMA-IR	(Fleisch et al., 2017)
Cross-sectional	US adolescents	402	Negative association between serum PFHxS and HOMA-IR	(Koshy et al., 2017)
Cohort	Spanish pregnant women	1204	Positive association between serum PFOA/PFHxS and gestational diabetes prevalence	(Matilla-Santander et al., 2017)
Cross-sectional	US adults	7904	Positive association between serum PFOA and diabetes prevalence in male but not in female	(He et al., 2018)
Cohort	Danish pregnant women	318	Positive association between PFHxS and fasting insulin, fasting glucose and HOMA-IR in women with high GDM risk; positive association between PFNA and fasting insulin and HOMA-β in women with high GDM risk	(Jensen et al., 2018)
Cross-sectional	US obese children aged 8-12	48	No association between serum PFOS/PFOA/PFHxS/PFNA and fasting glucose, insulin and HOMA-IR	(Khalil et al., 2018)
Cross-sectional	US adults in NHANES	1871	Positive association between serum linear PFOA and branched PFOS and beta cell function	(Liu et al., 2018b)
Cohort	French women	71270	Non-linear relationship between dietary PFOS/PFOA and type 2 diabetes prevalence	(Mancini et al., 2018)
Case control	US women	29611	Positive association between plasma PFOS/PFOA and type 2 diabetes prevalence	(Sun et al., 2018)
Cohort	Chinese pregnant women	560	Positive association between serum PFOA and HOMA-IR and blood glucose; Negative association between PFOS and blood glucose	(Wang et al., 2018)
Cohort	US overweight Hispanic youth aged 8-14	40	Positive association between serum PFOS/PFOA and fasting glucose; Positive association between PFHxS and AUC in oral glucose tolerance test (OGTT)	(Alderete et al., 2019)

Case control	Swedish adults	248	Negative association between serum PFDA/PFUnDA and HOMA-IR	(Donat-Vargas et al., 2019)
Case control	Chinese pregnant women	439	Positive association between serum short chain PFCAs and gestational diabetes	(Liu et al., 2019)
Cohort	US pregnant women	2334	Positive association between serum PFOA/PFNA /PFHpA/PFDoDA and gestational diabetes prevalence	(Rahman et al., 2019)

PFOS, perfluorooctanesulfonic acid; PFOA, perfluorooctanoic acid; PFNA, perfluorononanoic acid; PFHxS, perfluorohexanesulfonic acid; PFUnDA, perfluoroundecanoic acid; PFDA, perfluorodecanoic acid; PFDoDA, perfluorododecanoic acid; PFHpA, perfluoroheptanoic acid.

2.4.3 Non-alcoholic fatty liver disease

In animals, PFAS have been extensively reported to disrupt hepatic lipid metabolism and induce non-alcoholic fatty liver disease (NAFLD), which can more specifically be referred to as Toxicant Associated Fatty Liver Disease (TAFLD) (Wahlang et al., 2012). Proposed mechanisms include the inhibition of fatty acid beta oxidation, increased fatty acid uptake (Cheng et al., 2016; Wan et al., 2012), and the induction of oxidative stress (Khansari et al., 2017). In addition, PFAS exposure is positively associated with increased serum liver enzyme levels of alanine transaminase (ALT), alkaline phosphatase (ALP) and, γ-glutamyltransferase (GGT) (Darrow et al., 2016; Gallo et al., 2012; Gleason et al., 2015; Nian et al., 2019; Salihovic et al., 2018; Yamaguchi et al., 2013), which indicates potential liver damage and leads to steatosis. Consistently, positive associations were observed between PFHxS/PFOA/PFNA and hepatocyte apoptosis markers in a report involving 200 adults in Ohio (Bassler et al., 2019), including Cytokeratin-18 which is also a fatty liver biomarker (Feldstein et al., 2009; He et al., 2017). However, epidemiology findings on the relationship between PFAS and NAFLD is scarce. The only report was found in a case control study among an Ohio Valley community, with an elevated hazard ratio for exposure at a 10-year lag (Darrow et al., 2016). However, this positive association was based on 36 self-reported cases (Darrow et al., 2016). Two other occupational studies reported positive trend on non-hepatitis liver disease, but not on NAFLD (Steenland et al., 2015; Winquist et al., 2013). No direct association between PFAS and NAFLD incidence was reported. PFAS exposure has been consistently reported to be associated with altered lipid profile in blood, including increased triglyceride, cholesterol, low density lipoprotein, and reduced high density lipoprotein (Christensen et al., 2019; Fitz-Simon et al., 2013; Fletcher et al., 2013; Maisonet et al., 2012). According to a cross-sectional study using NHANES data, participants with obesity tend to be more susceptible to PFAS-induced dyslipidemia. As NAFLD is well

associated with obesity, the author suggested that NAFLD might play a role in PFAS-induced dyslipidemia (Jain and Ducatman, 2019).

In general, epidemiology data on the relationship between PFAS exposure and NAFLD are largely limited due to the low validation rate of the disease. More well-designed epidemiology studies are needed to confirm the results from animal studies.

2.5 Conclusion

Accumulating evidences have illustrate the association between PFAS, especially PFCAs and PFSAs, and the onset or development of metabolic diseases, including obesity, diabetes and NAFLD. However, inconsistent results can be found in many cases. Therefore, more clinical or epidemiology studies, especially prospective cohort studies, are needed to confirm the results. It is also of great significance to investigate the potential mechanism behind these effects using *in vitro* and *in vivo* models, especially for the shorter chain PFAS that have not been well-studied.

CHAPTER 3

OBJECTIVES OF THE PROJECT

Our long-term goal is to illustrate the causes of the development of obesity and NAFLD, and to develop prevention and/or treatment strategies. In this proposal, the specific objective is to clarify the mechanisms of altered lipid metabolism in adipocytes and hepatocytes induced by environmental contaminants (ivermectin and PFBS). The central hypothesis is that ivermectin can inhibit adipogenesis of 3T3-L1 preadipocytes; exposure to PFBS can impair lipid metabolism in adipocytes and hepatocytes, inducing potentiated adipogenesis in adipocytes and fat accumulation in hepatocytes. The rationale of this proposed research is: by understanding molecular mechanisms by which exposure to environmental contaminants may induce or prevent the development of obesity and type 2 diabetes, we will be able to direct more efficient prevention and/or treatment strategies for these and related pathologies in the future.

Specific Aim 1: Determine the effects and the underlying mechanisms of ivermectin on adipogenesis in 3T3-L1 adipocytes. The working hypothesis is that ivermectin treatment can inhibit the differentiation of preadipocytes via PPARγ mediated pathway.

Specific Aim 2: Determine the effects and the underlying mechanisms of PFBS on adipogenesis in 3T3-L1 adipocytes. The working hypothesis is that PFBS treatment can induce the differentiation of preadipocytes via MEK/ERK pathway.

Specific Aim 3: Determine the effects and the underlying mechanisms of PFBS on fat accumulation in HepG2 hepatocytes. The working hypothesis is that PFBS treatment can induce excessive fat accumulation in HepG2 cells via PPARγ-mediated pathway.

CHAPTER 4

IVERMECTIN INHIBITS DIFFERENTIATION OF 3T3-L1 PREADIPOCYTES

4.1 Introduction

In the 1970s, a series of 16-membered macrocyclic lactone derivatives, known as avermectins, were discovered as anti-parasitic agents from the fermentation broth of a soil actinomycete, *Streptomyces avermitilis* (Campbell et al., 1983). After its introduction to the market in 1981, ivermectin, one of the avermectins, soon became the bestselling anti-parasitic drug, generating annual sales exceeding 1 billion USD worldwide. Currently, ivermectin is still one of the most widely used anti-parasitic agents against internal and external parasites and insects, including those that cause onchocerciasis, strongyloidiasis and scabies in humans, and also for animals, including animals for human consumption.

Ivermectin, typically consists of a mixture of avermectin B1a and B1b at a ratio of 80:20 and kills parasites and insects primary by interfering with the glutamate-gated chloride channels, inducing membrane hyperpolarization and paralysis of nerve and muscle cells (Turner and Schaeffer, 1989). Additional ligand-gated chloride channels in mammals (e.g., glycine receptors (GlyR), gamma aminobutyric acid$_A$ ($GABA_A$) receptors) can also be activated by ivermectin, however, only at substantially higher doses (Adelsberger et al., 2000; Lynagh and Lynch, 2010; Shan et al., 2001). Ivermectin is believed to be relatively safe to mammals because of the low effective dose used to control invertebrate pests and the lack of glutamate-gated chloride channels in mammals. Additionally, ivermectin cannot cross the blood brain barrier due to the efflux by ABC transporter, which further lower its potential harm to human. In fact, ivermectin is generally well tolerated at relatively high doses and more frequent regimens in human (Guzzo et al., 2002) and has displayed a potential in treating non-alcoholic fatty liver disease (NAFLD) and insulin resistance (Jin et al., 2015). Nevertheless, the potential effects of ivermectin on non-target tissues, in particular adipose tissue, are often overlooked. Ivermectin is highly hydrophobic with

an octanol/water coefficient (K_{ow}), an indicator of lipophilicity, of 1,651, suggesting that ivermectin is a lipophilic, water-insoluble compound (Bloom and Matheson III, 1993). Consistently, it has been shown that adipose tissue has the highest and the most persistent level of ivermectin in humans, cattle, goats, etc. (Baraka et al., 1996; Canga et al., 2008; Lanusse et al., 1997; Lespine et al., 2005). Although ivermectin has 35-day slaughter withdrawal time for cattle and an 18-day for swine, trace amount of ivermectin have been shown to remain in derived foods (Crooks et al., 2000; Crooks et al., 1998; Toutain et al., 1988), not to mention problems associated with the intentional or unintentional misuse of ivermectin (Chicoine et al., 2007). It is likely that humans have repeated and/or prolonged exposures to ivermectin due to ingestion, inhalation, and dermal absorption during its administration to animals as well as animal-derived foods from animals treated with ivermectin, especially in milk and fat (Chicoine et al., 2007; Toutain et al., 1988). There is a growing body of information reporting a positive correlation between prolonged exposure to membrane-depolarizing insecticides and altered adipogenesis (Kim et al., 2016a; Park et al., 2012; Xiao et al., 2017b); (Sun et al., 2017; Sun et al., 2016b; Xiao et al., 2017a; Xiao et al., 2018). Thus, there is a critical need to understand the role of ivermectin on human health, especially in adipogenesis. The aim of the present work was therefore to determine the role of ivermectin in adipogenesis using 3T3-L1 preadipocytes, a cell model most commonly used for this purpose.

4.2 Materials and Methods

4.2.1 Materials

3T3-L1 preadipocytes were obtained from American Type Culture Collection (Manassas, VA). Fetal bovine serum (FBS), Dulbecco's modified Eagle's medium (DMEM), methylisobutylxanthin, human recombinant insulin, dexamethasone (>98% purity), and dimethyl sulfoxide (DMSO) were purchased from Sigma Aldrich Co. (St. Louis, MO). Ivermectin (>98% purity, a mixture of 80% 22,23-dihydroavermectin B1a and 20% 22,23-dihydroavermectin B1b)

was purchased from Alfa Aesar Co. (Ward Hill, MA). Rosiglitazone (>98% purity) was purchased from Cayman Chemical (Ann Arbor, MI). Z-Guggulsterone (single spot by TLC, >98% purity) was purchased from Millipore (Bedford, MA). Permethrin (> 98.1% purity, 3-phenoxybenzyl (1RS)-cis, trans-3-(2,2-dichlorovinyl) -2,2-dimethylcyclopropanecarboxylate, a mixture of 38.7% *cis* and 59.4% *trans* isomers) and fipronil (> 95% purity, 5-amino-1-(2,6-dichloro-alpha,alpha,alpha-trifluoro-p-tolyl)-4-trifluoromethylsulfinylpyrazole-3-carbonitile) were purchased from Sigma-Aldrich Co. (St. Louis, MO). The amounts of triglyceride and protein were quantified using Infinity Triglycerides Kit and Pierce BCA Protein Assay Kit, respectively, both from Thermo Fisher Scientific (Middletown, VA). Trizol and High-Capacity cDNA Reverse Transcription Kit were purchased from Life Technologies (Carlsbad, CA). Taqman Universal Master Mix II was obtained from Applied Biosystems (Carlsbad, CA). Radioimmunoprecipitation assay (RIPA) buffer supplemented with 1% protease inhibitor was purchased from Boston Bioproducts Inc. (Ashland, MA). Rabbit antibodies against mouse CCAAT/enhancer-binding protein alpha (C/ EBPα), peroxisome proliferator-activated receptor gamma (PPAR γ), acetyl-CoA carboxylase (ACC), phospho-extracellular signal-regulated kinases (pERK), and extracellular signal-regulated kinases (ERK) were purchased from Cell Signaling Technology (Beverly, MA). Mouse antibodies against mouse β-actin was from Santa Cruz Biotechnology (Dallas, TX). Goat anti-rabbit and anti-mouse horseradish peroxidase conjugated secondary antibodies were purchased from Invitrogen (Carlsbad, CA). The Clarity™ Western ECL Substrate Kit was obtained from Bio-Rad Co. (Hercules, CA).

4.2.2 Cell culture

3T3-L1 preadipocytes were maintained in DMEM supplemented with 10% (v/v) FBS. Two days after confluence (day 0), preadipocytes were induced for differentiation with DMEM containing 10% FBS and a mixture of methylisobutylxanthine (0.5 mM), dexamethasone (1 mM), and insulin (1 μg/mL) as described previously (Qi et al., 2018a). At day 2, the medium was switched

to DMEM with 10% FBS and insulin only. From day 4, insulin was removed from the medium and cells maintained in DMEM with 10% FBS, changing medium every two days. During differentiation, cells were treated with ivermectin or with vehicle (DMSO). All treatments included DMSO at a final concentration of 0.1%.

4.2.3 Measurement of cell viability

Cell viability was determined by 3-(4,5-dimethylthiazol-2-yl)-2,5-diphenyltetrazolium bromide (MTT)-based assay (Gerlier and Thomasset, 1986). 3T3-L1 preadipocytes were seeded in a 96-well plate at a density of 5×10^3 cells per well. 2 days after confluence, cells were differentiated with or without ivermectin at various concentrations for 8 days. The cells were then treated with 5 mg/ml MTT at 37 °C for 4 h. Cell viability was then assessed by the formation of formazan from MTT. The purple formazan was dissolved in DMSO and the absorbance at 540 nm was determined using a SpectraMax i3 microplate reader (Molecular Devices, Sunnyvale, CA).

4.2.4 Triglyceride quantification

Triglyceride levels were determined using a commercial kit (Infinity™ Triglycerides Reagent; Thermo Scientific). Briefly, at day 8, cells were washed twice with phosphate-buffered saline (PBS) and harvested by scraping the cells from the culture plate in PBS containing 1% Triton-X. Cell homogenates were obtained by sonication using Fisherbrand™ Model 50 Sonic Dismembrator (Fisher Scientific), and TG concentrations were determined according to the manufacturer's instructions. Protein concentrations were measured using Pierce BCA Protein Assay Kit (Thermo Scientific) and used for normalization of samples.

4.2.5 Reverse transcriptase quantitative PCR (RT-qPCR) analysis

Total RNA was isolated from cells using TRIzol Reagent (Life Technologies, Carlsbad, CA) according to manufacturer's instruction. Conversion of total RNA to single stranded cDNA was performed using the High-Capacity cDNA Reverse Transcription Kit (Life Technologies, Carlsbad, CA). Gene expression assays for CCAAT/enhancer-binding protein alpha (C/ EBPα,

Mm00514283_s1), peroxisome proliferator-activated receptor gamma (PPARγ, Mm00440940_m1), acetyl-CoA carboxylase (ACC, Mm01304257_m1), fatty acid synthase (FAS, Mm00662319_m1), fatty acid binding protein 4 (FABP4, Mm00445878_m1), fatty acid translocase (FAT/CD36, Mm00432403_m1), carnitine palmitoyltransferase 1 alpha (CPT1α, Mm01231183_m1), glucose transporter 4 (GLUT4, Mm00436615_m1), farnesoid X receptor (FXR, Mm01240553_m1), CAATT element binding protein beta (C/EBPβ, Mm00843434_s1), C/EBP homologous protein (CHOP10, Mm00492097_m1), glycine receptor alpha 1 (GlyRα1, Mm00445061_m1), glycine receptor alpha 2 (GlyRα2, Mm01168376_m1), glycine receptor alpha 3 (GlyRα3, Mm00475507_m1), glycine receptor alpha 4 (GlyRα4, Mm00501674_m1), and glycine receptor beta (GlyRβ, Mm00439140_m1), were performed with Taqman Universal Master Mix II (Applied Biosystems, Carlsbad, CA) on a StepOne Plus Real Time PCR System (Applied Biosystems, Carlsbad, CA). The results of target gene expression levels were normalized to the expression level of the eukaryotic18S rRNA gene (Hs99999901_s1) using the $2^{-\Delta\Delta Ct}$ method (Livak and Schmittgen, 2001).

4.2.6 Immunoblotting

Cells were lysed with RIPA buffer supplemented with Protease & Phosphatase Inhibitor Cocktail (100X, Thermo Scientific, Rockford, IL). Proteins in the cell lysates were separated by electrophoresis using a 10% sodium dodecyl sulfate polyacrylamide gel (SDS-PAGE). Electrophoresed proteins were transferred to an Immobilon-P polyvinylidene difluoride membrane (Millipore, Bedford, MA). After blocking with 5% skim milk for two hours, the membrane was incubated overnight at 4 °C with primary antibodies at appropriate dilutions. Horseradish peroxidase conjugated to goat anti-rabbit or anti-mouse IgG was used as the secondary antibody. Specific proteins were detected using an image Station 4000 MM (Carestream Health, New Haven, CT) using the Clarity™ Western ECL Substrate Kit (Bio-Rad

Co., Hercules, CA). β-actin was used as an internal control. Image and results were quantified with Image J software (NIH).

4.2.7 Data Analysis

Data in Figures 1-5 were analyzed with one-way ANOVA using the Statistical Analysis System 9.3 (SAS Institute, Cary, NC). Data in Figures 6-8 were analyzed with two-way ANOVA. All data are expressed as the mean ± standard error of the mean (S.E.). Multiple comparisons among groups were performed using Tukey's test. *P* values less than 0.05 are reported as statistically significant. N is defined as the number of replicates in each experiment.

4.3 Results

4.3.1 Ivermectin inhibited the differentiation of 3T3-L1 preadipocytes

The cytotoxicity of ivermectin on 3T3-L1 preadipocytes was first determined. Cell viability was not affected by an 8-day exposure to ivermectin at concentrations up to 5 μM (Figure 4.1). At 10 μM ivermectin, however, significantly reduced cell viability (23% reduction) was observed when compared to the control ($P<0.0001$). Based on these results, we used concentrations at or lower than 5 μM for the following experiments.

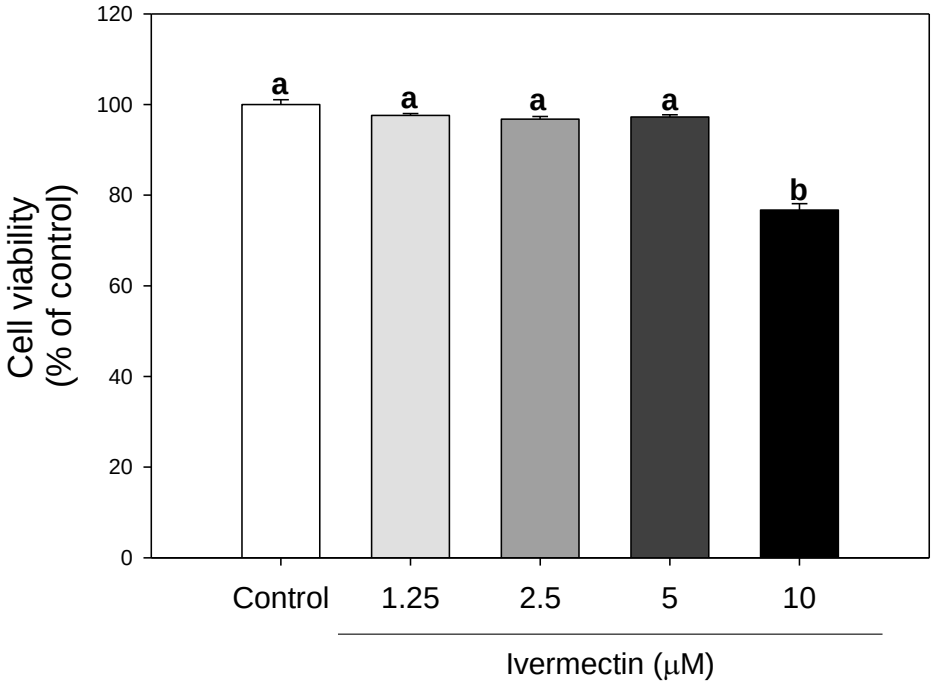

Figure 4.1 Cytotoxicity of ivermectin in 3T3-L1 adipocytes. 3T3-L1 cells in 96-well culture plates were treated with ivermectin (1.25, 2.5, 5 and 10 μM) for 8 days during differentiation. On day 8, cell viability was determined by MTT assay. Numbers are mean ± S.E. (n= 10). Means with different letters are significantly different at $P< 0.05$.

Next, the effect of ivermectin on triglyceride content was determined. Triglyceride accumulation was inhibited by ivermectin treatment in a concentration-dependent manner (Figure 4.2). Treatment with either 2.5 μM or 5 μM ivermectin exhibited 58% and 74% reduction in triglyceride content compared to the control, respectively ($P<0.0001$).

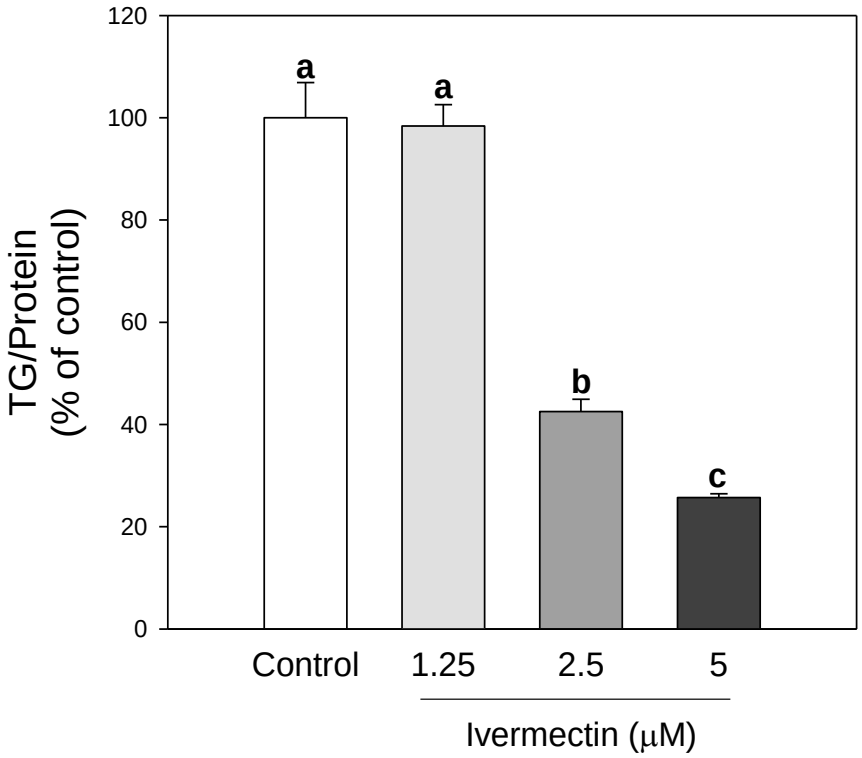

Figure 4.2 Ivermectin inhibits triglyceride accumulation in 3T3-L1 cells. After treatment for 8 days, adipocytes were harvested and measured for triglyceride content that were normalized by protein. Numbers are mean ± S.E. (n=4). Means with different letters are significantly different at $P< 0.05$.

4.3.2 Ivermectin inhibited the protein levels of key adipogenic regulators

We further investigated the protein expression levels of key regulators in adipogenesis and lipogenesis during differentiation period (Figure 4.3). Compared to the control, 5 μM ivermectin treatment markedly decreased the protein expression of key regulators in adipogenesis and lipogenesis on day 6 and day 8: peroxisome-proliferator activated receptor gamma (PPARγ, day 6 - 39% reduction, P=0.0022; day 8 - 45% reduction, P=0.039); CCAAT/enhancer-binding protein alpha (C/EBPα, day 6- 39% reduction, P=0.018; day 8- 75% reduction, P=0.0036) and acetyl-CoA carboxylase (ACC, day 6- 35% reduction, P=0.032; day 8- 29% reduction, P=0.0021).

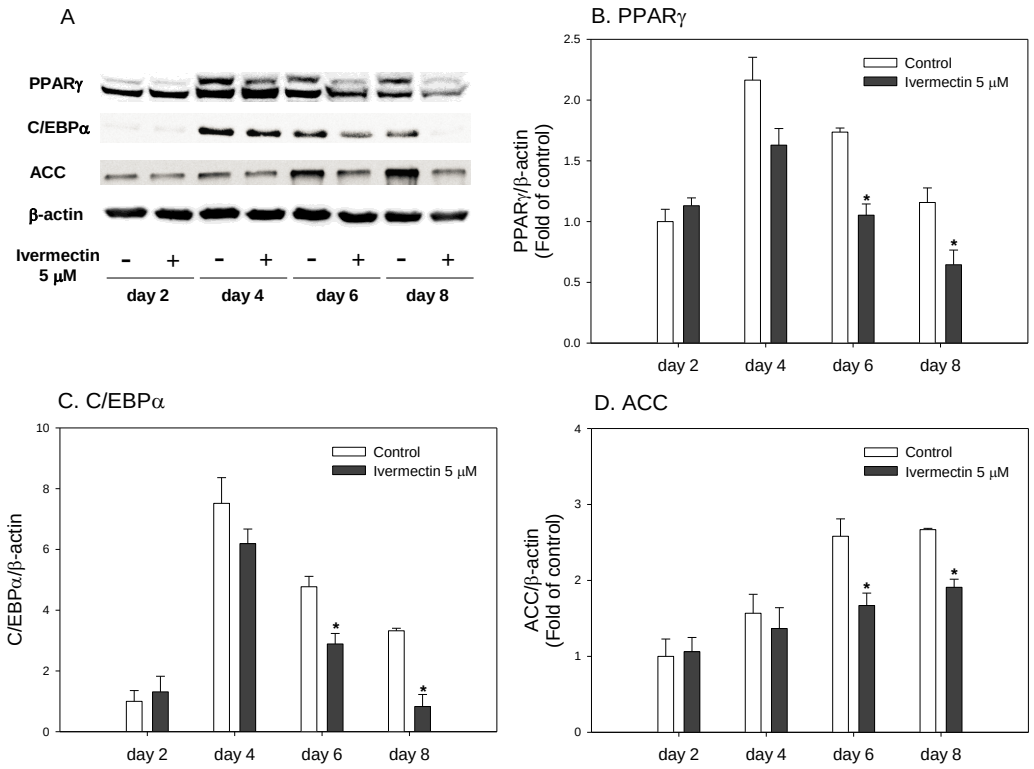

Figure 4.3 Effects of ivermectin on protein levels of key molecular mediators of adipogenesis. Cells were induced to differentiation for 2, 4, 6 and 8 days with or without ivermectin (5 μM) before harvesting for analysis at day 8. Protein levels of indicated genes were quantified by western blot analysis. A. Representative results; B. PPARγ, Peroxisome proliferator-activated receptor gamma; C. C/EBPα, CAATT element binding protein alpha; D. ACC, Acetyl-CoA carboxylase. Numbers represent mean ± S.E. (n=4). * indicates a significant difference against the respective control ($P< 0.05$).

4.3.3 Ivermectin altered the expression of adipogenic genes

Next, we assessed if ivermectin inhibited adipogenesis through the modulation of genes regulating adipogenic differentiation and lipid metabolism. Figure 4.4A shows the influence of sustained ivermectin exposure for 8 days on the gene expression levels. Treatment with 5 μM ivermectin significantly reduced the mRNA levels of the gene encoding the master regulator of adipogenic differentiation; PPARγ (80% reduction, P=0.0029) as well as its target genes, C/EBPα (72% reduction, P=0.0004), fatty acid binding protein 4 (FABP4 reduction, 73% reduction, P=0.0036), and fatty acid translocase (FAT/CD36, 45% reduction, P=0.033) compared to their respective controls. Consistently, the mRNA expression levels of a key enzymes in *de novo* fatty

acid synthesis; fatty acid synthase (FAS, 56% reduction, *P*=0.0008) and ACC (35% reduction, *P*=0.0031) were also suppressed compared to their respective controls. In addition, ivermectin activated the expression of carnitine palmitoyltransferase 1 alpha (CPT1α, 64% increase, *P*=0.050) compared to the control, which is the key enzyme in fatty acid β-oxidation. Expression of glucose transporter 4 (GLUT4, 69% reduction, *P*=0.0023), a membrane protein that play a crucial role in insulin mediated glucose uptake, was also suppressed by ivermectin treatment (5 μM) over the control. However, the expression of FXR, which was also known to regulate adipogenesis, remained unchanged by ivermectin treatment (*P*=0.8932).

We further determined if ivermectin influence the expression of key adipogenic genes in the earlier stage of the adipogenesis. C/EBPβ, expresses upon initiation of differentiation and promotes the expressions of PPARγ and C/EBPα at day 2, was not affected following a 48-hour treatment with ivermectin (Fig. 4.4B, *P*=0.5306). However, ivermectin significantly up-regulated the expression of CHOP10 compared to the control (Figure 4.4B, 168% increase, *P*=0.0001), which may lead to suppressed DNA-binding activity of C/EBPβ (Tang and Lane, 2000).

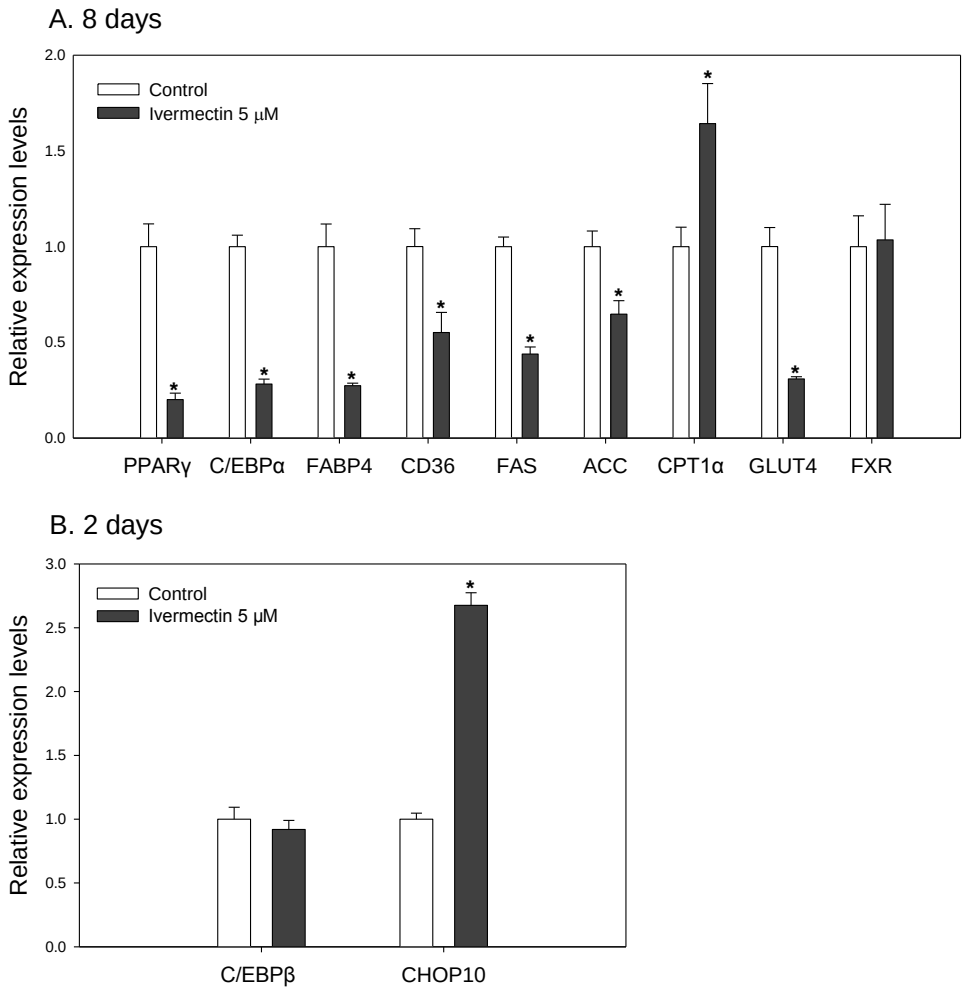

Figure 4.4 Effects of ivermectin on adipogenic gene expression levels. Cells were induced to differentiation for 8 days (A) or 2 days (B) with or without ivermectin (5 μM). mRNA levels of indicated genes were quantified by RT-qPCR and the ΔΔCt was determined using eukaryotic 18S rRNA as a housekeeping gene. A. PPARγ, Peroxisome proliferator-activated receptor gamma; C/EBPα, CAATT element binding protein alpha; FABP4, Fatty acid binding protein 4; CD36, fatty acid translocase; FAS, Fatty acid synthase; ACC, Acetyl-CoA carboxylase; CPT1α, carnitine palmitoyltransferase 1 alpha; GLUT4, glucose transporter 4, and FXR, farnesoid X receptor. B. C/EBPβ, CAATT element binding protein beta; and CHOP10, C/EBP homologous protein. Numbers are mean ± S.E. (n=3). * indicates a significant difference against the respective control ($P< 0.05$).

4.3.4 Ivermectin inhibited fat accumulation by suppressing the middle to late phases of adipogenesis

To determine the specific adipogenic stages involved in the inhibitory effect of ivermectin, different exposure periods were evaluated (Figure 4.5). The treatment of ivermectin during day 2-4, day 0-4, and day 4-8 produced significant reduction in TG content compared to

the control (day 2-4, 34% reduction, P=0.0003; day 0-4, 37% reduction, P=0.0012; day 4-8, 44% reduction, P<0.0001). However, treating ivermectin during the first 2 days resulted in no difference of TG levels compared to the control (Fig. 5, P=0.2808). These results suggest that ivermectin regulated adipogenic differentiation primarily through suppressing the middle to late adipogenic stages.

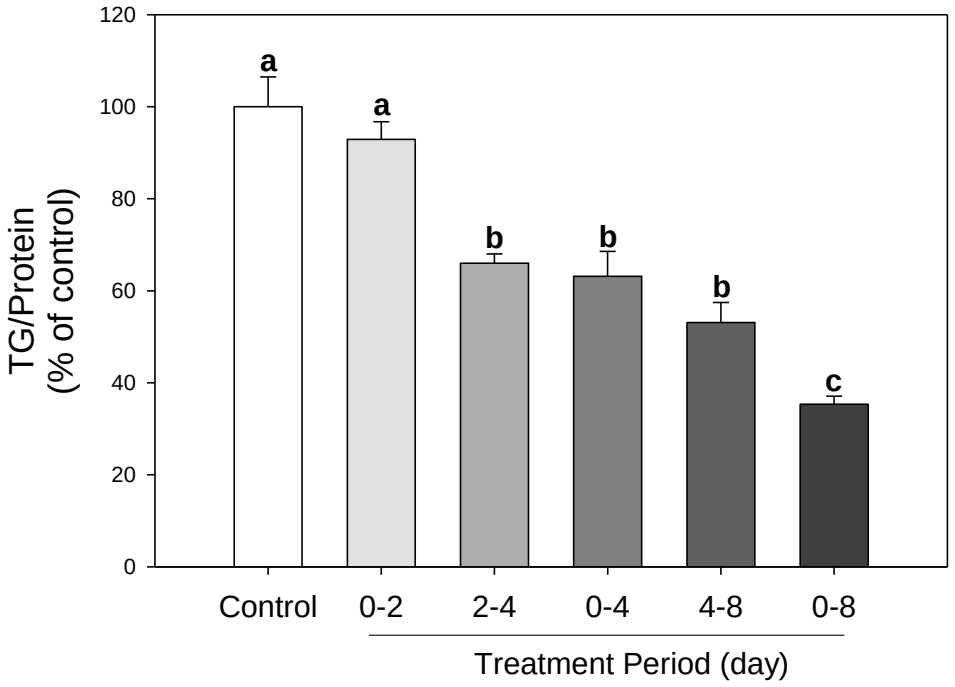

Figure 4.5 Effects of ivermectin on triglyceride accumulation following different treatment periods. Cells were exposed to ivermectin (5 μM) during indicated time period and harvested at day 8. Numbers are mean ± S.E. (n=4). Means with different letters are significantly different at P<0.05.

4.3.5 Ivermectin inhibits adipogenesis partially by way of a PPARγ-dependent pathway

Based on the observation that ivermectin inhibited adipogenesis likely during the middle to late stages, we further investigated whether the suppressed adipogenesis caused by ivermectin is mediated by the inhibition of PPARγ, since PPARγ is one of the most important regulators in the middle to late adipogenic stage (Chawla et al., 1994; Tontonoz et al., 1995). To determine whether the effect of ivermectin is PPARγ-mediated, rosiglitazone (an agonist of PPARγ) was

used to determine if the activation of PPARγ could reverse the inhibition of adipogenesis induced by ivermectin. Differentiation was induced under the combination treatment of 5 μM ivermectin and 5 μM rosiglitazone, a potent PPARγ agonist (Hwang et al., 2011; Zebisch et al., 2012). As shown in Figure 4.6A, there was significant interaction between ivermectin and rosiglitazone treatment (P=0.0083). As expected, treatment of rosiglitazone alone increased the fat accumulation by 27% (P=0.0027) and ivermectin significantly reduced the fat accumulation by 70% (P<0.0001) when compared to their respective controls. The fat content of cells treated with both ivermectin and rosiglitazone, however, were not different from the control but increased significantly compared to cells treated with ivermectin only (226% increase, P<0.0001), although still significantly less than rosiglitazone alone (23% reduction with P=0.0011). These results suggested that ivermectin suppressed fat accumulation, in part, by way of a PPARγ-dependent pathway.

Figures 4.6B-D shows mRNA expression of regulators of adipogenesis under the co-treatment of ivermectin and rosiglitazone. Interaction can be observed between ivermectin and rosiglitazone in the expression of PPARγ (P=0.0264), C/EBPα (P=0.0081) and FABP4 (P=0.0038). As expected, rosiglitazone alone significantly increased the expression of PPARγ (69% increase, P=0.0054), C/EBPα (94% increase, P=0.0037) and FABP4 (94% increase, P<0.0001) compared to their respective controls. Ivermectin, consistent with the previous data, significantly inhibited the expression of PPARγ (65% reduction, P=0.0076), C/EBPα (68% reduction, P=0.028) and, FABP4 (68% reduction, P=0.0006) when compared to the control. The reduction in gene expression levels induced by ivermectin, however, were abolished by the co-treatment with rosiglitazone (Figures 4.6B-D). These results suggest that PPARγ activation attenuated the inhibited adipogenesis induced by ivermectin.

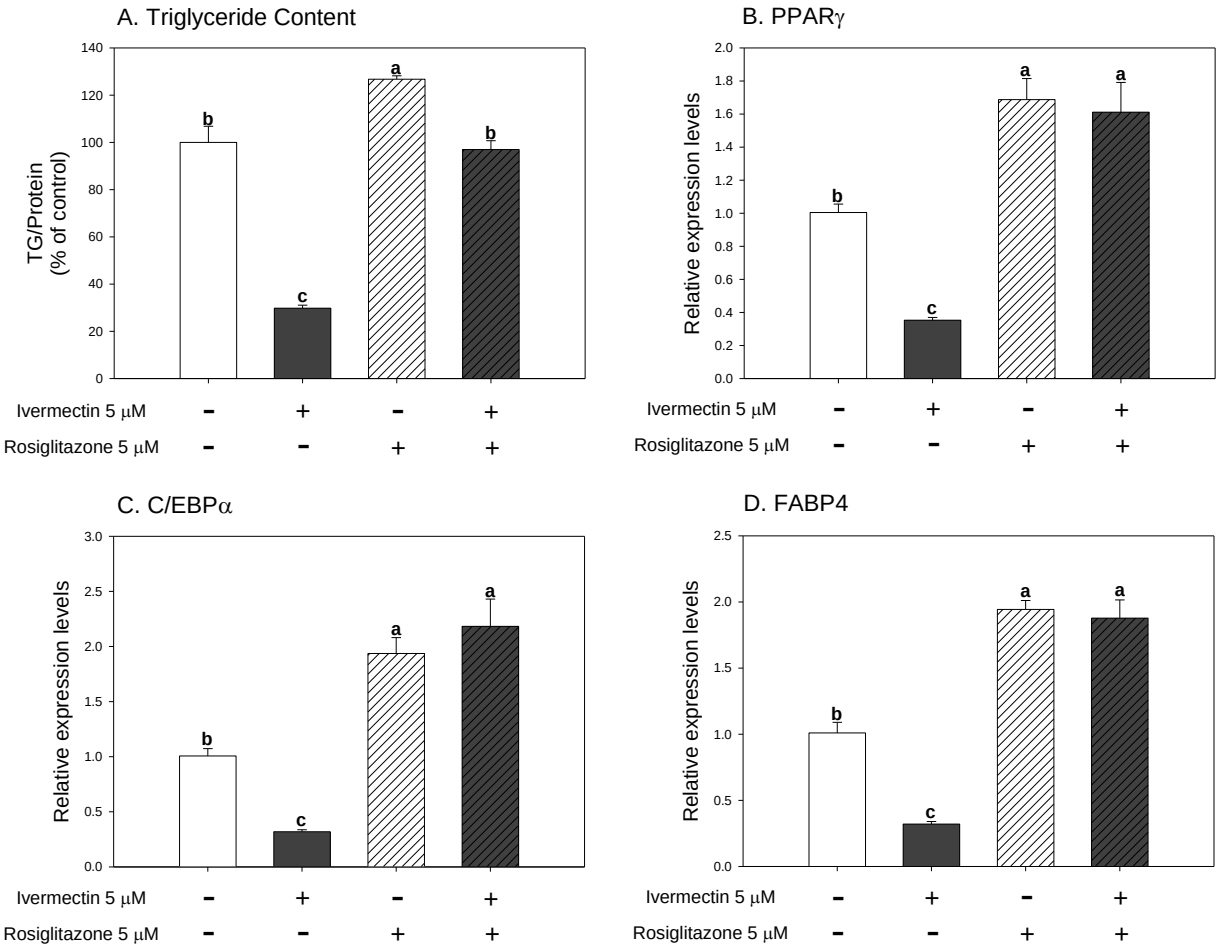

Figure 4.6 Inhibition of triglyceride accumulation and adipogenic gene expression levels caused by ivermectin were abolished by rosiglitazone. During differentiation, the cells were treated with ivermectin (5 μM) and rosiglitazone (5 μM). On day 8, (A) triglyceride contents were measured; (B) gene expression levels were quantified by RT-qPCR and the ΔΔCt was determined using eukaryotic 18S rRNA as a housekeeping gene. Numbers are mean ± S.E. (n=4). Means with different letters are significantly different at $P< 0.05$.

4.3.6 Ivermectin enhances the expression of glycine receptor subunits

Ivermectin is a known activator of glycine receptor chloride channel (Shan et al., 2001). Meanwhile, the influx of chloride could cause hyperpolarization (Sharmeen et al., 2010), which potentially results in altered calcium signals (McCarty et al., 2009) and therefore the inhibition in the differentiation of adipocytes (Neal and Clipstone, 2002). Thus, here we next investigated the effects of ivermectin on the expression of the subunits of glycine receptor, which is known to express in adipocytes (Lopez et al., 2016). As shown in Figure 4.7, ivermectin significantly

enhanced the expressions of GlyRα3 (123% increase, *P*=0.0229) and GlyRβ (57% increase, *P*=0.021). Therefore, ivermectin activates the expressions of certain subunits of glycine receptor in 3T3-L1 cells.

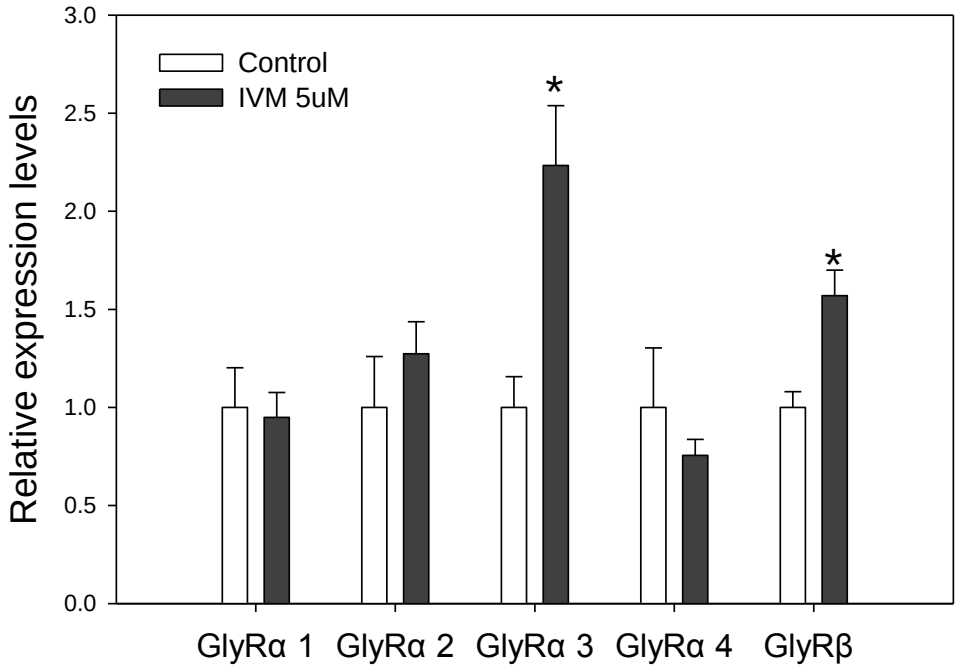

Figure 4.7 Effects of ivermectin on gene expression of glycine receptor subunits. Cells were induced to differentiation for 8 days with or without ivermectin (5 μM). mRNA levels of indicated genes were quantified by RT-qPCR and the ΔΔCt was determined using eukaryotic 18S rRNA as a housekeeping gene. GlyRα1, glycine receptor alpha 1; GlyRα2, glycine receptor alpha 2; GlyRα3, glycine receptor alpha 3; GlyRα4, glycine receptor alpha 4; GlyRβ, glycine receptor beta. Numbers are mean ± S.E. (n=3). * indicates a significant difference against the respective control (*P*< 0.05).

4.3.7 The inhibitory effect of ivermectin on adipogenesis is FXR-independent

Ivermectin was previously identified as a ligand of FXR in the liver where it downregulated serum glucose and cholesterol levels by directly targeting FXR (Jin et al., 2013). In addition, previous *in vitro* and *in vivo* studies reported that FXR upregulated adipogenic genes partially via PPARγ (Abdelkarim et al., 2010; Rizzo et al., 2006). Therefore, we next examined whether ivermectin influences adipogenesis is FXR-dependent, even though the expression of FXR was not affected by ivermectin treatment (Figure 4.4A). As shown in Figure 4.8, there was

interaction between ivermectin and Z-guggulsterone (P=0.0014). Z-gugglesterone, a selective antagonist of FXR (Urizar et al., 2002), significantly inhibited the triglyceride accumulation compared to the control (48% reduction, P<0.0001). Ivermectin treatment alone also significantly reduced triglyceride accumulation (54% reduction, P<0.0001), while the co-treatment of Z-guggulsterone and ivermectin further reduced fat content, a 75% reduction compared to Z-guggulsterone treated group (P<0.0001). Therefore, combined with the observation that FXR gene expression was not influenced by ivermectin treatment (Figure 4.4A), we concluded that FXR is not likely to be involved in the effect of ivermectin on adipogenesis in 3T3-L1.

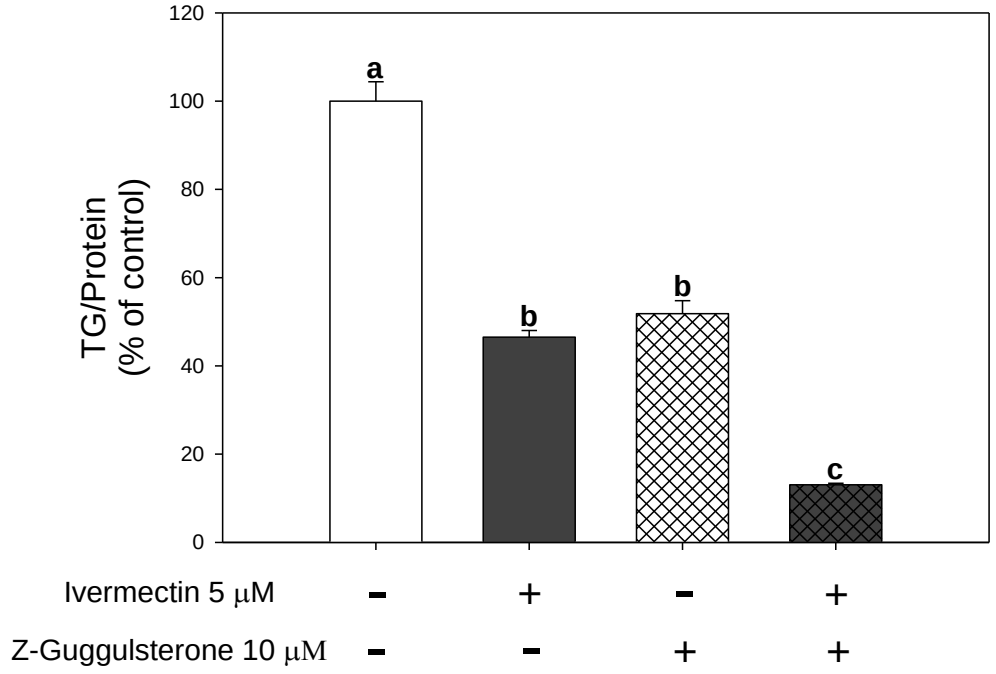

Figure 4.8 Inhibition of triglyceride accumulation caused by ivermectin was unaffected by FXR antagonist Z-guggulsterone. During differentiation, the cells were treated with ivermectin (5 μM) and Z-guggulsterone (10 μM). On day 8, triglyceride contents were measured. Numbers are mean ± S.E. (n=4). Means with different letters are significantly different at P< 0.05.

4.3.8 Ivermectin prevents permethrin- and fipronil-induced adipogenesis

Previously, several membrane depolarizing insecticides, including permethrin and fipronil, were reported to induce adipogenesis (Kim et al., 2014; Kim et al., 2016a; Park et al.,

2012; Sun et al., 2016a). Thus, we determined whether the treatment of ivermectin could revert the adipogenesis induced by these insecticides. From Figure 4.9, permethrin and fipronil significantly increase the fat content by 54% (P=0.0021) and 21% (P=0.020), respectively, compared to the control, while ivermectin alone reduced the fat content by 57% (P=0.0005). The co-treatment of ivermectin with either permethrin or fipronil prevented the increased fat accumulation caused by these insecticides when administered alone. The co-treatment of ivermectin with permethrin reduced fat content by 51% compared to permethrin alone (P=0.0006) and the co-treatment of ivermectin with fipronil reduced fat content by 77% compared to fipronil alone (P<0.0001).

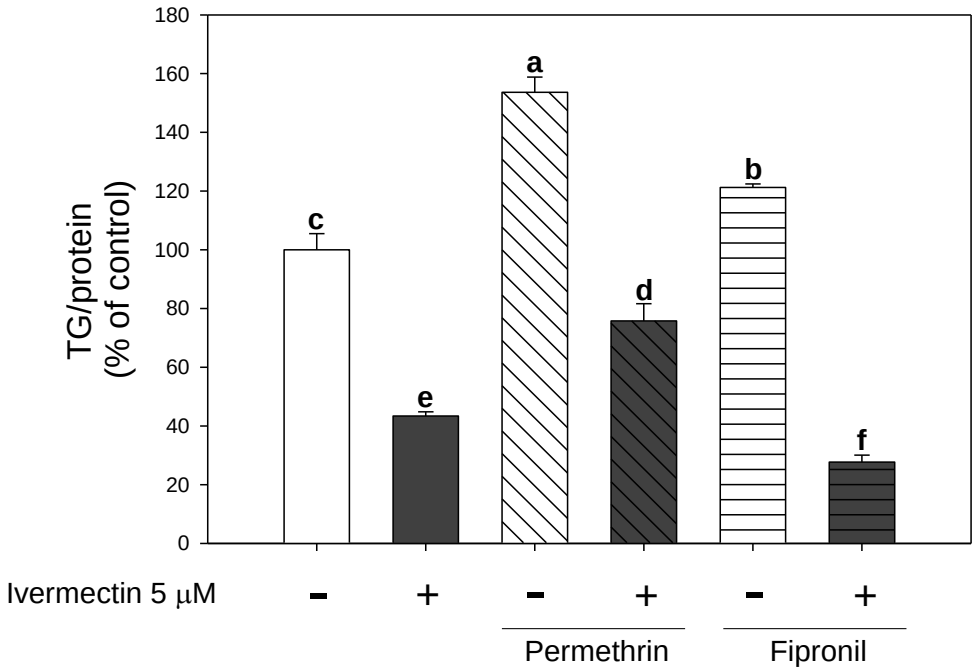

Figure 4.9 Treatment of ivermectin significantly reduced fat accumulation induced by permethrin and fipronil. During differentiation, the cells were treated with ivermectin (5 μM) with or without permethrin or fipronil (both at 10 μM). On day 8, triglyceride contents were measured. Numbers are mean ± S.E. (n=3). Means with different letters are significantly different at P< 0.05.

4.4 Discussion

In the current study, we demonstrated that ivermectin treatment inhibited the adipogenesis of 3T3-L1 preadipocytes. To our knowledge, this is the first report on the correlation between

ivermectin exposure and adipogenesis. We further illustrated that ivermectin targeted events in mid- to later stage of adipogenesis, in part, by the down-regulation of PPARγ, which is required for the maturation of adipocytes (Rosen and MacDougald, 2006).

As most genes that are induced in adipogenesis possess a PPARγ binding site (Siersbæk et al., 2010), PPARγ is one of the most important transcription factors in the development and the function of adipocytes. Indeed, the occurrence of high fat diet-induced obesity and insulin resistance are reduced by the deletion of PPARγ in adipose tissue (Jones et al., 2005) and in PPARγ-deficient mice (Kadowaki et al., 2002). According to the current results, the effect of ivermectin on adipogenesis likely occurred in the middle to late stages (day 2-8) of the differentiation when PPARγ is the key regulator. Treatment with ivermectin during early stage did not influence the fat content, which further supports a potential key role of PPARγ in the effect of ivermectin on adipogenesis. Nevertheless, it still remains unclear how ivermectin suppresses PPARγ and therefore adipogenesis. Previously, it was reported that ivermectin does not influence the transcriptional activity of PPARγ in COS-7 kidney cells (Jin et al., 2013). However, it is still possible that ivermectin negatively regulates PPARγ in adipocytes.

C/EBPβ is one of the most well-known upstream regulators of PPARγ (Wu et al., 1995). C/EBPβ, which is expressed upon the induction of adipocyte differentiation, induces the expression of PPARγ by binding to its promoter. However, the activation of PPARγ by C/EBPβ does not occur until 36 hours after induction, as CHOP10 associates with C/EBPβ and fully suppresses its transcription activity (Tang and Lane, 2000; Tang et al., 2004). At the end of mitotic clonal expansion (MCE, the two-rounds of cell division in the early stage that is required for adipogenesis), the expression of CHOP10 declines, completely releasing C/EBPβ from the CHOP10-dependent constraint, allowing the subsequent transcription of PPARγ and C/EBPα (Tang and Lane, 1999). In fact, inhibition of C/EBPβ transcriptional activity is essential for the process of MCE, as the premature expression of PPARγ and C/EBPα prevents MCE (Altiok et al., 1997; Timchenko et al., 1996; Wang et al., 2001). Although the expression of C/EBPβ was

reported to be essential for MCE, the CHOP10-induced inhibition of C/EBPβ activity is independent of MCE (Tang et al., 2003a). In this study, the expression of C/EBPβ was not affected by the treatment of ivermectin, therefore MCE is likely not involved in the effect of ivermectin. However, CHOP10 expression was significantly enhanced (Figure 4.4B). Therefore, it is possible that ivermectin treatment could potentially prevent or delay the downregulation of CHOP10 without affecting MCE, resulted in inhibited the transcriptional activity of C/EBPβ, subsequently suppressed the expression of PPARγ and C/EBPα. This possibility is further supported by the fact that the treatment of ivermectin during early adipogenesis (day 0-2) did not affect the fat accumulation. Consistently, cell number after 48-hour ivermectin treatment was not significantly different from control (data not shown). It remains inconclusive, however, whether ivermectin inhibits the expression of PPARγ via CHOP10 or ivermectin directly affects the expression of PPARγ.

Ivermectin acts as an activator at mammalian ligand-gated chloride channels (Adelsberger et al., 2000; Shan et al., 2001). Consistently, with the current data, ivermectin enhanced the expression of the subunits of glycine receptor chloride channel (Figure 4.7). The influx of chloride into the cytosol induced by the activation of chloride channels could result in plasma membrane hyperpolarization (Sharmeen et al., 2010). Hyperpolarization can lead to a voltage-gated calcium channel-independent calcium influx from media to the cytosol (Konig et al., 2006; McCarty et al., 2009), which could potentially be associated with ORAI channels (Trebak and Jr., 2017), and ivermectin has been shown to increase intracellular calcium in leukemia cells (Sharmeen et al., 2010). The regulation of intracellular calcium levels is essential for the adipogenesis and lipid metabolism in adipocytes (Shi et al., 2000). The activation of calcineurin, a calcium-dependent serine/threonine phosphatase, inhibits adipogenesis by preventing the expression of PPARγ and C/EBPα, but not C/EBPβ (Neal and Clipstone, 2002), which is in consistent to the current results (Figure 4.4). Indeed, the treatment of glycine receptor ligand has been reported to decrease high-sucrose-diet induced adiposity in rats (Lopez et al.,

2016). Interestingly, fipronil, a membrane depolarizing insecticide that blocks GABA-gated chloride channel and glycine receptor chloride channel, was previously reported to potentiate the adipogenesis of 3T3-L1 cells (Sun et al., 2016a). Therefore, it is possible that ivermectin could increase intracellular calcium levels by inducing hyperpolarization, and subsequently activated calcineurin, which inhibits adipogenesis. Besides CHOP10-mediated and calcineurin-mediated pathways, PPARγ expression can also be modulated by multiple factors including Early B-cell factors (EBFs) (Jimenez et al., 2007), Krüppel-like factors (KLFs) (Banerjee et al., 2003; Birsoy et al., 2008; Mori et al., 2005; Oishi et al., 2005; Pei et al., 2011), sterol regulatory element-binding protein-1 (SREBP1) (Fajas et al., 1999), zinc finger protein 423 (ZFP423) (Gupta et al., 2010), nuclear factor I (NFI) (Waki et al., 2011), and GATA-binding factors (Tong et al., 2000). Further mechanistic study is needed to determine the exact mechanism by which ivermectin inhibits adipogenesis.

Ivermectin is a known agonist of FXR in the liver and it has been suggested to suppress hepatic lipogenesis and improve insulin resistance in mice in an FXR-dependent manner (Jin et al., 2013; Jin et al., 2015; Yang et al., 2019b). Therefore, ivermectin has the potential to be used to treat non-alcoholic fatty liver disease (Cariou, 2008; Carr and Reid, 2015). The activation of FXR, however, promotes adipogenic gene expression both *in vitro* and *in vivo* in adipose tissue (Rizzo et al., 2006). Moreover, adipose tissue mass was reduced in FXR-deficient mice, and mouse embryonic fibroblasts, which were derived from FXR-deficient mice, displayed impaired adipocyte differentiation, with inhibited expression of PPARγ, C/EBPα and FABP4, as well as suppressed *de novo* lipogenesis (Abdelkarim et al., 2010; Cariou et al., 2006). Consistently, Z-guggulsterone, an FXR antagonist, inhibited the adipogenesis of 3T3-L1 cells (Yang et al., 2008), while 6-ethyl-chenodeoxycholic acid, an FXR agonist, promoted adipocyte differentiation in 3T3-L1 cells and induced the expression of adipogenic genes in adipose tissue of mice (Rizzo et al., 2006), although it had no effect on epididymal fat mass (Cipriani et al., 2010). In the current study, ivermectin, a known agonist of FXR, inhibited the adipogenesis of 3T3-L1 cells. The

current results also showed that the expression of FXR was not induced by ivermectin in adipocytes (Figure 4.4A). The discrepancy on the effects of ivermectin on FXR in liver and adipocytes might be due to the difference in the expression levels of FXR. FXR is expressed at a relatively low level in adipocytes (~50 folds lower than in liver) (Cariou et al., 2006). Moreover, there might be distinctive tissue specific effects of ivermectin on FXR. With the current data, it remains inconclusive whether ivermectin influences FXR-induced adipogenesis. However, because an antagonist of FXR failed to reverse the effect of ivermectin on adipogenesis in 3T3-L1 cells, we can conclude that the known role of ivermectin as an agonist of FXR did not play a role in inhibitory effect of ivermectin in adipogenesis. Because the effect of FXR on adipogenesis is, in part, dependent on PPARγ (Abdelkarim et al., 2010; Rizzo et al., 2006), the inhibition of PPARγ by ivermectin might potentially mask the effect of ivermectin-induced FXR activation on adipogenesis.

The current clinical doses of ivermectin for human parasitic diseases range from 150 to 200 μg/kg body weight (Dourmishev et al., 1998; Youssef et al., 1995). To understand the absorption, distribution, metabolism and excretion of ivermectin when given at the optimal doses for human parasitic diseases, a few studies have studied the pharmacokinetic profile of ivermectin in human. The administration of three subcutaneous doses (200 μg/kg), injected every 2 days after an oral dose of 200 μg/kg, increased plasma ivermectin levels to 7.9 ng/ml (~9 nM) at 1 week after the last dose (Marty et al., 2005). In 22 patients and 44 healthy volunteers treated with a single oral dose of 150 μg/kg, the maximal plasma concentration of ivermectin was 52 ng/ml (~60 nM) (Baraka et al., 1996). Following an oral administration of 12 mg ivermectin-containing alcoholic solution, the plasma concentration was reported to be 81 ng/ml (~92 nM) (Edwards et al., 1988). Due to the high hydrophobicity of ivermectin, this compound is widely distributed within the body, with fat showing the highest and most persistent concentration of 141 ng/g tissue (~149 nM) after a single oral dose of 150 μg/kg (Baraka et al., 1996). Given this limited data set, the concentrations used in the current study may not be achievable under these dosing regimens.

Nonetheless, ivermectin has a broad range of effects and has been used in the treatment of other human diseases at higher doses. Ivermectin at 10 mg/kg (approximately 11 μM) was reported to inhibit Wnt-TCF-dependent of human colon cancer (Melotti et al., 2014). Similarly, ivermectin at 3 mg/kg (approximately 3.4 μM) was effective on slowing tumor growth in mice (Sharmeen et al., 2010). Additionally, ivermectin up to 1.6 mg/kg (approximately 1.8 μM) was previously used successfully for symptomatic treatment of severe muscle spasticity in human (Costa and Diazgranados, 1994). Thus, it is possible that repeated exposures to ivermectin may result in its accumulation in adipose tissue to levels similar to those achieved using the concentrations applied in the current study, and the significance of the concentrations used in the current study may need to be carefully evaluated.

4.5 Conclusion

In conclusion, our current study demonstrated the inhibitory effect of ivermectin on adipogenesis. These results elucidated a potential link between ivermectin exposure and altered lipid metabolism and adipogenesis. Considering ivermectin is approved for human use and its safety has been verified by decades of uses, ivermectin can provide a critical insight for the design of drugs with therapeutic potential against obesity. The current results, however, are limited to an in vitro model using relatively high concentrations of ivermectin. Further studies in animals, as well as epidemiology studies, are needed to further evaluate the significance of the current observations.

CHAPTER 5

PERFLUOROBUTANESULFONIC ACID (PFBS) POTENTIATES ADIPOGENESIS OF 3T3-L1 ADIPOCYTES

5.1 Introduction

Per- and polyfluoroalkyl substances (PFASs) are a large group of surface-active compounds. PFASs, such as perfluorooctanesulfonic acid (PFOS), were extensively used as water, oil, and stain repellents in food packaging, non-stick cookware, and textiles, for over 50 years. These ubiquitous environmental contaminants are highly persistent in the environment, and bioaccumulate in living organisms, posing a growing concern for potential adverse effects on human health (Joensen et al., 2009; Lau et al., 2004; Pérez et al., 2013). Accumulating evidence reveals a strong correlation between exposure to PFASs and the increased risks for metabolic syndromes, including obesity (Braun et al., 2016; Halldorsson et al., 2012; Liu et al., 2018a; Maisonet et al., 2012; Mora et al., 2016).

As a replacement for PFOS, its four-carbon cognate, perfluorobutanesulfonic acid (PFBS), is widely used due to its shorter biological half-life in humans of ~1 month compared to that of 5 years for PFOS (Olsen et al., 2007; Olsen et al., 2009a). PFBS is also generated as the final degradation product from some of the perfluorobutanesulfonyl fluoride-based chemicals (D'eon et al., 2006). After production and usage for over 15 years, PFBS has become one of the major perfluorinated environmental contaminants (Skutlarek et al., 2006; Zhou et al., 2013a). PFBS has been detected in human populations, with increasing concentrations seen in humans from 2006 to 2010 (Glynn et al., 2012). Similar to PFOS, PFBS was found to distribute to fat tissue, although the potential adverse effects are largely unknown and understudied (Bogdanska et al., 2014).

Previously, PFASs, particularly PFOS and perfluorooctanoic acid (PFOA), were reported to promote adipogenesis in 3T3-L1 adipocytes with increased expression of adipogenic genes,

including CCAAT/enhancer-binding protein alpha (C/EBPα), peroxisome proliferator-activated receptor gamma (PPARγ), fatty acid binding protein 4 (FABP4) and lipoprotein lipase (LPL) (Watkins et al., 2015; Yamamoto et al., 2015). Further, evidence from an animal study revealed that PFOS administration to mice induced adipogenic gene expression and activated nuclear factor erythroid 2-related factor 2 (Nrf2) signaling in epididymal white adipose tissue (Xu et al., 2016). PFASs have also been reported to activate the peroxisome proliferator-activated receptors (PPARs), PPARα and PPARγ, both in hepatocytes and adipocytes, which play key roles in lipid metabolism (Rosen et al., 2008; Vanden Heuvel et al., 2006; Zhang et al., 2014). Moreover, higher plasma concentration of PFASs was associated with the risk of weight gain in human (Liu et al., 2018a). The effects of PFBS on adipogenesis, however, have not been investigated. Therefore, we aimed to examine the effects of PFBS exposure on adipogenesis using 3T3-L1 adipocytes.

5.2 Materials and Methods

5.2.1 Materials

3T3-L1 preadipocytes were obtained from American Type Culture Collection (Manassas, VA). Fetal bovine serum (FBS), Dulbecco's modified Eagle's medium (DMEM), methylisobutylxanthin, human recombinant insulin, dexamethasone, dimethyl sulfoxide (DMSO), and Perfluorobutanesulfonic Acid (PFBS, 97%) were purchased from Sigma Aldrich Co. (St. Louis, MO). The amounts of triglyceride and protein were quantified using Infinity triglycerides kit and Pierce BCA protein assay kit, respectively, both from Thermo Fisher Scientifics (Middletown, VA). Trizol and High-Capacity cDNA Reverse Transcription Kit were purchased from Life Technologies (Carlsbad, CA). Taqman Universal Master Mix II was obtained from Applied Biosystems (Carlsbad, CA). Radioimmunoprecipitation assay (RIPA) buffer supplemented with 1% protease inhibitor was purchased from Boston Bioproducts Inc. (Ashland, MA). Rabbit anti-CCAAT/enhancer-binding protein alpha (C/ EBPα), anti-peroxisome

proliferator-activated receptor gamma (PPAR γ), anti-acetyl-CoA carboxylase (ACC), anti-phosphor-p42/p44 (pERK), and anti-p42/p44 (ERK) were purchased from Cell Signaling Technology (Beverly, MA). Mouse anti-β-actin was from Santa Cruz Biotechnology (Dallas, TX). Goat anti-rabbit and anti-mouse horseradish peroxidase conjugated secondary antibodies were purchased from Invitrogen (Carlsbad, CA). The Clarity™ Western ECL Substrate Kit was obtained from Bio-Rad Co. (Hercules, CA).

5.2.2 Cell culture

3T3-L1 preadipocytes were maintained in DMEM supplemented with 10% (v/v) FBS. Two days after confluence (day 0), preadipocytes were induced for differentiation with DMEM containing 10% FBS and a mixture of methylisobutylxanthin (0.5 mM), dexamethasone (1 mM), and insulin (1 μg/mL), as described previously (Sun et al., 2016a). At day 2, the medium was switched to DMEM with 10% FBS and insulin only. From day 4, insulin was removed from the medium and cells maintained in DMEM with 10% FBS, changing medium every two days. During differentiation, cells were treated with PFBS at increasing concentrations or with vehicle (dimethylsulfoxide, DMSO). All treatments included DMSO at a final concentration of 0.1%.

5.2.3 Measurement of cell viability

Cell viability was determined by 3-(4,5-dimethylthiazol-2-yl)-2,5-diphenyltetrazolium bromide (MTT)-based assay (Gerlier and Thomasset, 1986). 3T3-L1 preadipocytes were seeded in a 96-well plate at a density of 5×10^3 cells per well. 2 days after confluence, cells were exposed to PFBS for 6 days. The cells were then treated with 5 mg/ml MTT at 37 °C for 4 h. After incubation, MTT-formazan was dissolved in DMSO and the absorbance at 540 nm was determined using a SpectraMax i3 microplate reader (Molecular Devices, Sunnyvale, CA).

5.2.4 Triglyceride quantification

Triglyceride (TG) levels were determined using a commercial kit (Infinity™ Triglycerides Reagent; Thermo Scientific). Briefly, at day 6 cells were washed twice with phosphate-buffered

saline (PBS) and harvested by scraping the cells from the culture plate in PBS containing 1% Triton-X. Cell homogenates were obtained by sonication and TG concentrations were determined uisng the commercial kit according to the manufacturer's instructions. Protein concentrations were measured using Pierce BCA protein assay kit (Thermo Scientific) and used for normalization of samples.

5.2.5 Reverse Transcriptase quantitative PCR (RT-q-PCR) analysis

Total RNA was isolated from cells using TRIzol Reagent (Life technologies, Carlsbad, CA) according to manufacturer's instruction. Conversion of total RNA to single stranded cDNA was performed using the High-Capacity cDNA Reverse Transcription Kit (Life Technologies, Carlsbad, CA). Gene expression assays for CCAAT/enhancer-binding protein a (C/ EBPα, Mm00514283_s1), peroxisome proliferator-activated receptor gamma (PPARγ, Mm00440940_m1), acetyl-CoA carboxylase (ACC, Mm01304257_m1), fatty acid synthase (FAS, Mm00662319_m1), and fatty acid binding protein 4 (FABP4, Mm00445878_m1) were performed with Taqman Universal Master Mix II (Applied Biosystems, Carlsbad, CA) on a StepOne Plus real time PCR instrument (Applied Biosystems, Carlsbad, CA). The results of target gene expression levels were normalized to the expression level of the18S rRNA gene(Hs99999901_s1) using the $2^{-\Delta\Delta Ct}$ method (Livak and Schmittgen, 2001).

5.2.6 Immunoblotting

Cells were lysed with RIPA buffer supplemented with Protease & Phosphatase Inhibitor Cocktail (100X, Thermo Scientific, Rockford, IL). Proteins in the cell lysates were separated by electrophoresis using a 10% sodium dodecyl sulfate polyacrylamide gel (SDS-PAGE). Electrophoresed proteins were transferred to an Immobilon-P polyvinylidene difluoride membrane (Millipore, Bedford, MA). After blocking with 5% skim milk for two hours, the membrane was incubated overnight under 4 °C with primary antibodies at appropriate dilutions. Horseradish peroxidase conjugated goat anti-rabbit or anti-mouse IgG was used as the secondary

antibody. Specific proteins were detected using an image Station 4000 MM (Carestream Health, New Haven, CT) using the Clarity™ Western ECL Substrate Kit (Bio-Rad Co., Hercules, CA). GAPDH or β-actin was used as an internal control. Image and results were quantified with Image J software (NIH).

5.2.7 Cell counting

After exposure to PFBS (0, 10, 50, 100 μM) for 48 hours, cells were trypsinized and collected by centrifugation at 1000g for 5 minutes. Cell suspension was then subjected to cell counting with hemocytometer (Fisher Scientific, Horsham, PA).

5.2.8 Data Analysis

Data in figure 1-6 were analyzed with one-way ANOVA using the Statistical Analysis System (SAS Institute, Cary, NC). Data in figure 7 were analyzed with two-way ANOVA. All data are expressed as the mean ± standard error of the mean (S.E.). Multiple comparisons among groups were performed using Tukey's test. *P* values less than 0.05 are reported as statistically significant. N is defined as the number of replicates in each experiment.

5.3 Results

5.3.1 PFBS enhances fat accumulation in 3T3-L1 cells

PFBS had no effect on cell viability at concentrations up to 200 μM after a 6-day exposure (Figure 5.1). PFBS treatment during adipogenic differentiation significantly promoted lipid accumulation in a dose dependent manner compared with the DMSO control (Figure 5.2). Cells treated with 200 μM PFBS showed a 35% increase in triglyceride content compared to the control ($P<0.0001$). Treatments of 50 μM and 100 μM PFBS also significantly elevated TG levels above the control (21% and 25% increases, respectively). From these results, it was decided to use PFBS concentrations up to 100 μM for the following experiments.

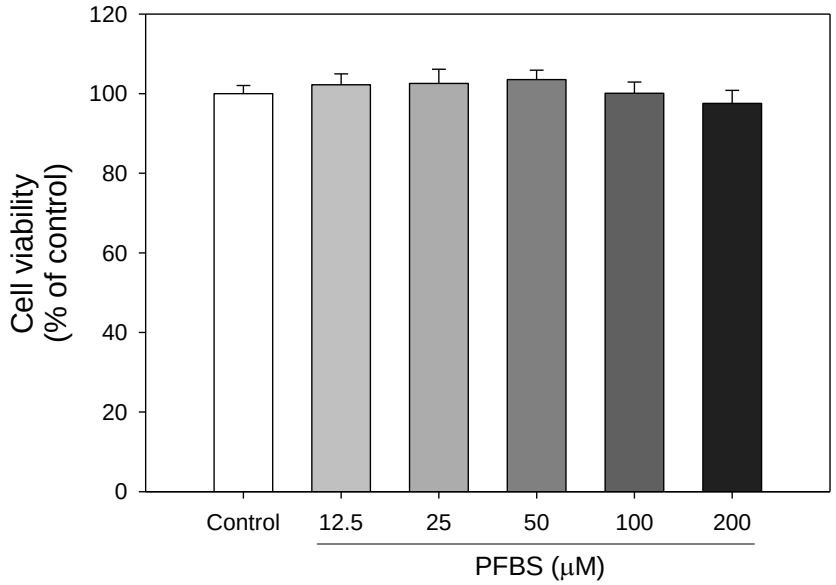

Figure 5.1 Cytotoxicity of PFBS in 3T3-L1 adipocytes. 3T3-L1 cells in 96-well culture plates were treated with PFBS (12.5, 25, 50, 100, and 200 μM) for 6 days during differentiation. On day 6, cell viability was determined by MTT assay. Numbers are mean ± S.E. (n= 10). Means with different letters are significantly different at $P< 0.05$.

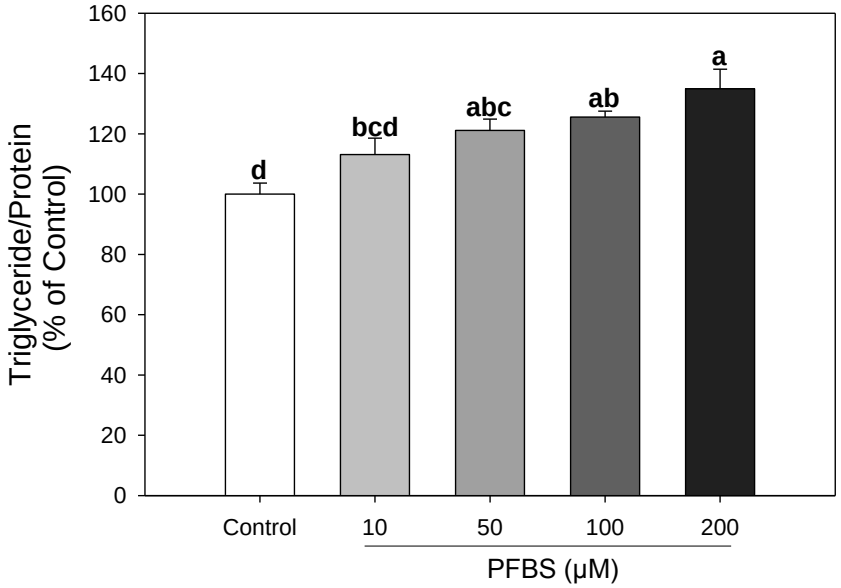

Figure 5.2 PFBS promotes triglyceride accumulation in 3T3-L1 cells. After treatment for 6 days, adipocytes were harvested and measured for triglyceride content that were normalized by protein. Numbers are mean ± S.E. (n=4). Means with different letters are significantly different at $P< 0.05$.

5.3.2 PFBS upregulates the expression of adipogenic genes

Next, we assessed whether PFBS potentiated adipogenesis through the upregulation of genes known to be involved in adipogenic differentiation and/or lipid metabolism. Treatment with 100 μM PFBS for 6 days significantly increased the mRNA levels of genes encoding two master regulators of adipogenic differentiation; CCAAT/enhancer-binding protein alpha (C/EBPα, 84%, P=0.0047) and peroxisome-proliferator activated receptor gamma (PPARγ, 29%, P<0.0001), as well as their target gene fatty acid binding protein 4 (FABP4, 159%, P<0.0001) (Figure 5.2) when compared with the control. The mRNA expression level of key regulatory enzymes involved in *de novo* lipogenesis; fatty acid synthase (FAS, 84%, P<0.0001) and acetyl-CoA carboxylase (ACC, 37%, P=0.0049), were also significantly increased by 100 μM PFBS treatments compared with the control (Figure 5.3). Likewise, 100 μM PFBS treatments also significantly increased the protein expression levels of PPARγ and C/EBPα compared with the control by 76% (P=0.006) and 77% (P=0.0017), respectively (Figure 5.4 B and C). In a similar manner, the protein expression of ACC was also increased by PFBS (69%, P=0.0021, Figure 5.4 D) compared to the control.

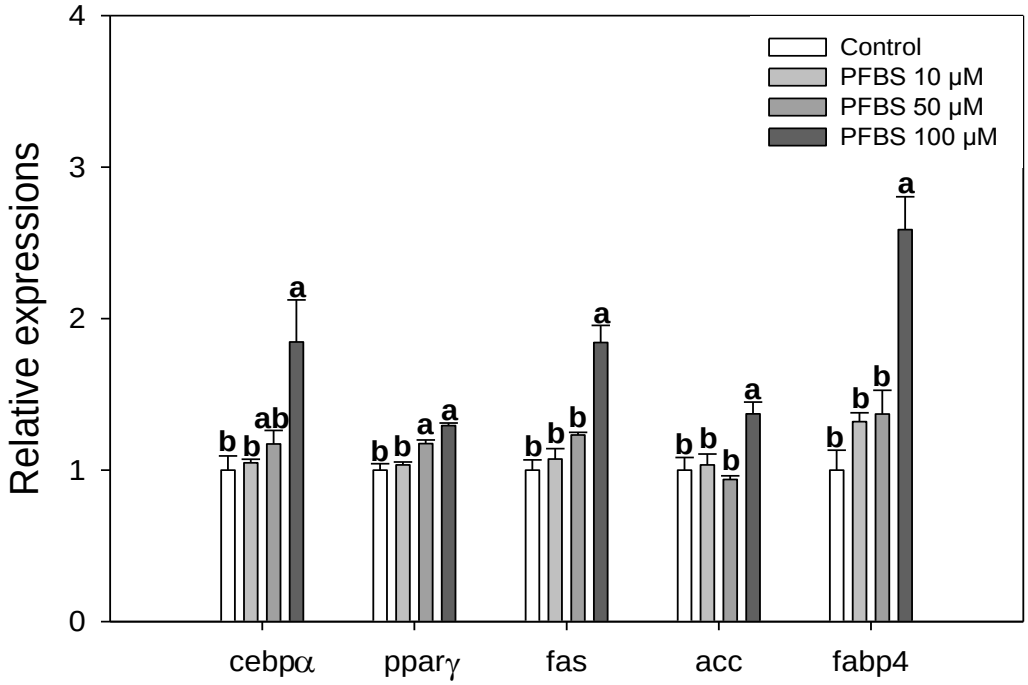

Figure 5.3 Effects of PFBS on adipogenic gene expression. Cells were induced to differentiation for 6 days with or without PFBS (10, 50, 100 μM). mRNA levels of indicated genes were quantified by real-time PCR and the ddCt was determined using 18S RNA as a housekeeping gene. C/EBPα, CAATT element binding protein alpha; PPARγ, Peroxisome proliferator-activated receptor gamma; FAS, Fatty acid synthase; ACC, Acetyl-CoA carboxylase; and FABP4, Fatty acid binding protein 4. Numbers are mean ± S.E. (n=3). Means with different letters are significantly different at $P< 0.05$.

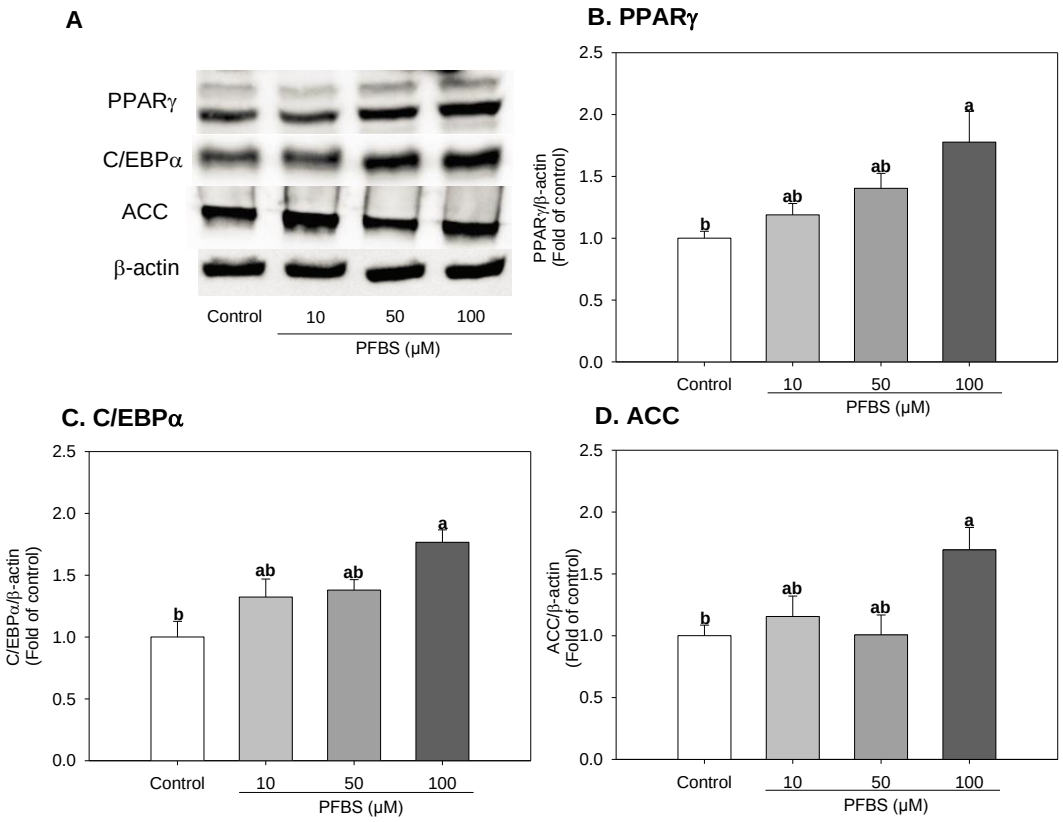

Figure 5.4 Effects of PFBS on protein levels of molecular mediators of adipogenesis. Cells were induced to differentiation for 6 days with or without PFBS (10, 50, 100 μM). Protein levels of indicated genes were quantified by Western blot. A. Representative results; B. PPARγ, Peroxisome proliferator-activated receptor gamma; C. C/EBPα, CAATT element binding protein alpha; D. ACC, Acetyl-CoA carboxylase. Numbers represent mean ± S.E. (n=3). Means with different letters were significantly different at $P< 0.05$.

5.3.3 PFBS potentiates fat accumulation by targeting early phase of adipogenesis

To determine the specific adipogenic developmental stage targeted by PFBS, we next examined the effect of PFBS on lipid accumulation at different exposure intervals. A significant increase in lipid accumulation was observed in cells treated with PFBS at day 0-2 (P=0.0078), day 0-4 (P=0.0020) and day 0-6 (P<0.0001), while treatment after day 2 showed no effect compared to the control (Figure 5.5). It is apparent that longer treatment of PFBS potentiated fat accumulation (from day 0 to 2-6 days). These finding suggested that PFBS induced adipogenesis, particularly targeting events in early adipogenesis.

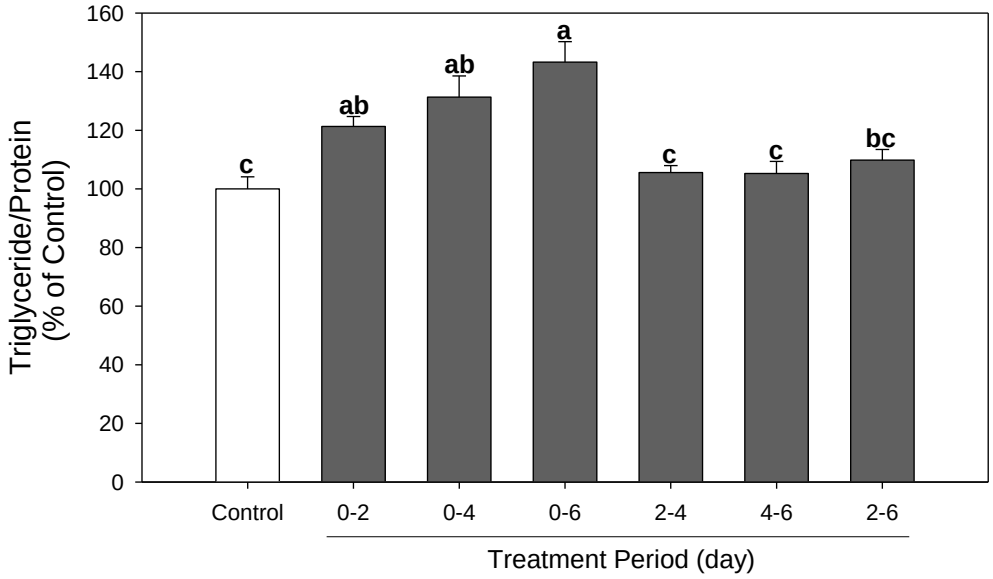

Figure 5.5 Effects of PFBS on fat accumulation with different treatment periods. Cells were exposed to PFBS (100 μM) on indicated time period and harvested at day 6. Numbers are mean ± S.E. (n=4). Means with different letters are significantly different at $P<0.05$.

5.3.4 PFBS activates mitotic clonal expansion

Upon exposure to adipogenic inducers, such as methylisobutylxanthin, dexamethasone, and insulin, growth-arrested preadipocytes re-enter the cell cycle and undergo two rounds of cell division in the subsequent 2 days, a process called mitotic clonal expansion (MCE). MCE is a prerequisite for the expression of adipogenic genes that produce the terminal differentiated phenotype. As observed in Figure 5, the effect of PFBS targets the early stage of differentiation in 3T3-L1 cells when MCE is triggered. Therefore, we next examined whether MCE was affected by PFBS. Treatments with PFBS (50 & 100 μM) for 48 h significantly increased the relative cell number compared to the control by 13% (P=0.0076) and 20% (P=0.0005) compared to the control, respectively, which implied the activation of MCE by PFBS treatment (Figure 5.6).

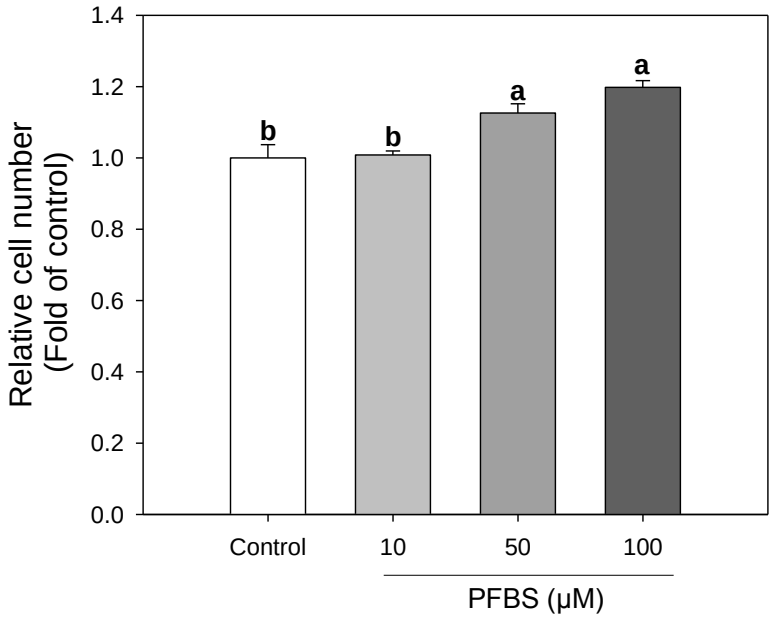

Figure 5.6 Activation of mitotic clonal expansion in preadipocytes by PFBS. Upon induction of differentiation, preadipocytes were treated by PFBS (10, 50 and 100 μM) for 48 hours. Then, cell numbers were determined by hemocytometer. Numbers are mean ± S.E. (n=6). Means with different letters are significantly different at $P< 0.05$.

5.3.5 PFBS induces adipogenesis via MEK/ERK pathway

The activation of ERK is one of the crucial steps in the early stages of adipogenesis. The inhibition of ERK phosphorylation during the early adipogenesis has been shown to significantly inhibit fat accumulation in the later stages (Prusty et al., 2002). Also, ERK activation was reported to be essential to MCE. Therefore, we next determine whether the effect of PFBS was dependent on the activation of ERK. The treatment of PFBS (100 μM) for 4 hours significantly increased the ratio of pERK and ERK by 38% compared to the control (Figure 5.7, P=0.047).

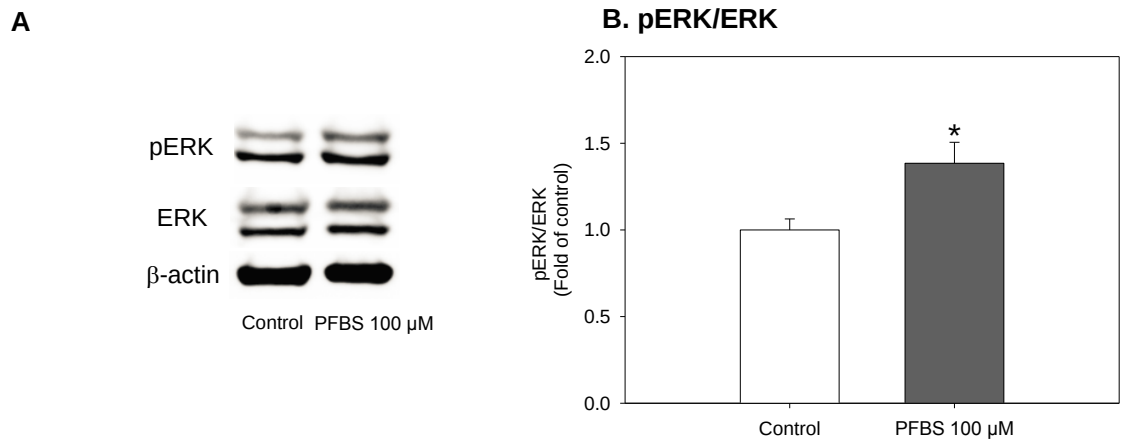

Figure 5.7 Activation of ERK pathway by PFBS. Upon induction of differentiation, preadipocytes were treated by PFBS (100 μM) for 4 hours. Then, phosphorylation of ERK was determined by immunoblotting. A. Representative results; B. Ratio of phospho-ERK to ERK. Numbers are mean ± S.E. (n=3). * indicates a significant difference against the control ($P< 0.05$).

To further confirm if the enhanced adipogenesis by PFBS is mediated by ERK activation, we next co-treated the cells with PFBS (100 μM) and U0126 (50 μM), a specific MEK/ERK pathway blocker, for 6 days. PFBS significantly increased fat accumulation consistent with the results shown in Fig. 1 ($P<0.0001$), while U0126 treatment alone did not change the fat content. However, the increased fat accumulation induced by PFBS was abolished with co-treatment of U0126 (Figure 5.8). These results suggested that PFBS increased fat accumulation, in part, via a MEK/ERK-dependent manner.

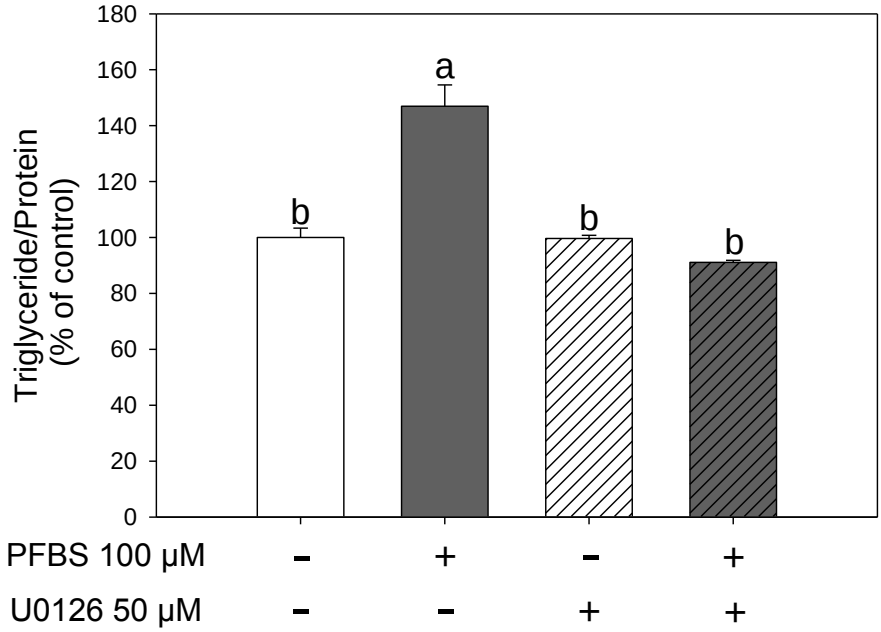

Figure 5.8 Activation of ERK with PFBS was abolished by MEK1/2 specific inhibitor U0126. During differentiation, the cells were treated with PFBS (100 μM) and U0126 (50 μM). On day 6, triglyceride contents were measured. Numbers are mean ± S.E. (n=4). Means with different letters are significantly different at $P< 0.05$.

5.4 Discussion

In this study, we demonstrated that PFBS exposure contributes to increased adipogenesis of 3T3-L1 adipocytes. To our knowledge, this is the first report on the correlation between PFBS exposure and adipogenesis. Further, we found that the effect of PFBS on adipogenesis occurs primarily during early stage of adipogenesis, and mitotic clonal expansion (MCE) is induced by PFBS treatment during this developmental interval. The current results also suggest that PFBS influence adipogenesis, in part, via the up regulation of the MEK/ERK-dependent pathway, which affects MCE in the early stages of adipogenesis that is a crucial step of adipogenesis and the activation of this step has been reported to induce adipogenesis (Tang et al., 2003b).

ERK1/2 are activated by phosphorylation of threonine and tyrosine residues by the dual specificity kinase MAPK/ERK kinase 1/2 (MEK1/2), which is essential to the induction of MCE and the subsequent adipogenesis (Bost et al., 2005; Qiu et al., 2001). The activation of this

pathway during early adipogenesis promotes adipogenesis by activating the transcription factors to initiate the expression of PPARγ and C/EBPα. Conversely, the inhibition of MEK/ERK pathway by U0126 has been suggested to inhibit adipogenesis (Prusty et al., 2002). Our results suggest that the effect of PFBS on increase adipogenesis is in part dependent on the activation of the MEK/ERK pathway. Thus, PFBS appears to initially activate the MEK/ERK pathway, which further induces an accelerated MCE, showing increase in cell number after 48-hour treatment. Other PFASs, including PFOS, have been reported to increase cell number of 3T3-L1 cells (Watkins et al., 2015), and PFOS activates ERK in multiple cell lines, including HAPI microglial cells and cerebellar granule cells (Lee et al., 2013; Wang et al., 2015), which are consistent to the current results. Similar effects were likewise observed following treatments with PFOA or perfluorohexanesulfonic acid (PFHxS) (Lee et al., 2014; Upham et al., 2009). Therefore, we speculate that other PFASs might share common mechanism for adipogenesis as PFBS. However, this is the first to report on the role of PFBS in adipogenesis.

It is not clear how PFBS activates ERK in the current study, however, previously it was reported that PFOS and PFOA elevate cytoplasmic calcium levels by releasing calcium ions from intracellular calcium stores (Liu et al., 2011), where elevated calcium levels can subsequently activate ERK through calmodulin kinase I (CaMKI) (Chuderland and Seger, 2008; Schmitt et al., 2004). Alternatively, elevated calcium levels can activate phospholipase C and protein kinase C, leading to ERK activation (Huang, 1989; Orton et al., 2005). Further studies are needed to determine if PFBS activates ERK via modulating calcium levels.

PFBS is generally believed to be less toxic than PFOS due to its shorter biological half-life of a month in comparison to 5.4 years for PFOS (Olsen et al., 2007; Olsen et al., 2009a). In our study, PFOS treatment had no effect on adipogenesis (Supplementary Figure S2). This is consistent with a previous study reporting no effect of PFOS on adipocyte differentiation in 3T3-L1 adipocytes (Yamamoto et al., 2015). Others reported that PFOS was less potent than perfluorohexane sulfonate (PFHxS), a short-chain cognate of PFOS, in adipogenesis (Watkins et

al., 2015; Xu et al., 2016). Even though PFBS is more potent in adipogenesis than PFOS, tissue levels of PFBS are relatively low compared to other PFASs: 5-40 fold lower than that of PFOS (Bogdanska et al., 2014). However, it is reported that PFBS and PFOS have similar tissue distribution (Bogdanska et al., 2014) and the concentration of PFBS in humans currently is rising. Thus, more attention should be paid to the potential effects of long-term exposure of PFBS as well as interactions with other PFASs including PFOS on adipogenesis.

A few studies have examined the concentration of PFBS in humans or animals and have led to a 7 μg/L (23 nM) health risk limit for ground water established in Minnesota, and the EPA has set a subchronic reference dose of 0.2 mg/kg/d and chronic reference dose of 0.02 mg/kg/d (EPA, 2014). In a 90-day oral administration study on rats, the no-observed-adverse-effect level (NOAEL) for PFBS was set at 60 mg/kg/d for males and 600 mg/kg/d for females (Lieder et al., 2009). In a pharmacokinetic study following the exposure to 16 mg/kg/d of ^{35}S-labeled PFBS, ^{35}S labeled PFBS was found to distribute to epididymal fat and blood at 5 μmol/kg and 19 μmol/kg (~19 μM), respectively (Bogdanska et al., 2014). Serum PFBS levels of factory workers have been found to be approximately 23 ng/ml (77 nM) (Fu et al., 2015). Given this limited data set, the doses used in the current study may not be achievable. Nevertheless, the effects of obesogens can be aggravated by dietary fat as previous studies have shown the interaction between obesogens and dietary fat (Sun et al., 2017; Sun et al., 2016b; Xiao et al., 2015; Xiao et al., 2018).

5.5 Conclusions

To summarize, our current study reports the effects of PFBS, the replacement compound for PFOS, on adipogenesis. These results are significant in elucidating a potential link between the risk of developing obesity and the exposure to the replacement of PFOS, which is a known obesogens. However, the current results are limited to an *in vitro* model using relatively high concentrations of PFBS. Further studies in animals, as well as epidemiology studies, are needed to further confirm our *in vitro* results.

CHAPTER 6

Perfluorobutanesulfonic Acid (PFBS) induces fat accumulation in HepG2 liver cells

6.1 Introduction

Nonalcoholic fatty liver disease (NAFLD) is the excessive accumulation of fat in liver without routine alcohol intake, which is considered one of the most prevalent chronic liver diseases (Younossi et al., 2016). The surpassed storage of fat disrupts normal hepatic lipid metabolism, and contributes to a number of metabolic syndromes, including dyslipidemia, hypertension, and type 2 diabetes. In recent decades, it has been reported that the exposure to environmental contaminants could be positively associated with the development of NAFLD (Arciello et al., 2013; Armstrong and Guo, 2019).

Perfluoroalkyl substances (PFAS) are a large group of surface-active compounds. PFAS, especially PFOS, have been extensively used as water, oil, and stain repellents in food packaging, non-stick cookware, textile, etc. for over 50 years, which makes them among the most ubiquitous environmental contaminants (Boulanger et al., 2005; Hoffman et al., 2011; Post et al., 2012). These compounds are relatively stable (Lemal, 2004), highly persistent in the environment (Li et al., 2018), and tend to accumulate in living organisms, causing a growing concern for their potential adverse effects on human health. In fact, accumulating evidence has revealed the correlation between the exposure to PFAS and the increased risks for metabolic syndromes, including NAFLD (Das et al., 2017), which has led to regulatory restrictions on their usages. As a replacement for PFOS, its four-carbon cognate, PFBS, was widely used due to the shorter biological half-life since early 2000s (Olsen et al., 2009a). PFBS is also expected to be the final degradation product from some of the perfluorobutanesulfonyl fluoride-based chemicals (D'eon et al., 2006). After production and usage for over 15 years, PFBS has become a growing concern. PFBS has been detected in the human serum, with an increase in PFBS level in humans during 2006-2010 (Glynn et al., 2012). Similar to PFOS, PFBS was found to distribute to the liver

(Bogdanska et al., 2014; Olsen et al., 2009a), where it is metabolized, although the potential adverse effects are largely unknown. However, slight increases in liver weight and hepatocellular hypertrophy were reported in rats exposed to high doses of PFBS (300 and 1000 mg/kg/day) for 70 days (Lieder et al., 2009). Besides, PFBS was reported to induce adipogenesis in 3T3-L1 cells (Qi et al., 2018b), suggesting a potential disruption on lipid metabolisms. In addition, PFAS have been reported to disrupt lipogenesis (Zhang et al., 2019), fatty acid uptake (Huck et al., 2018), fatty acid β oxidation (Wan et al., 2012), reactive oxygen species (ROS) generation (Qian et al., 2010), endoplasmic reticulum (ER) stress (Oh et al., 2017), and calcium homeostasis (Liu et al., 2011), which are related to the hepatic TG accumulation. Thus, the aim of the current work was to determine the role of PFBS in hepatic lipid metabolism, as well as the potential mechanisms behind the effects, using HepG2 cell as a model system.

6.2 Material and Methods

6.2.1 Materials

HepG2 human hepatocytes were obtained from American Type Culture Collection (Manassas, VA). Fetal bovine serum (FBS), Dulbecco's modified Eagle's medium (DMEM), bovine serum albumin (BSA, >98%), dimethyl sulfoxide (DMSO), and perfluorobutanesulfonic acid (PFBS, 97%) were purchased from Sigma Aldrich Co. (St. Louis, MO). Penicillin streptomycin (100X) solution was purchased from GE Healthcare Life Sciences (Uppsala, Sweden). Palmitic acid (> 99%) and oleic acid (>99%) was from Nu-Chek Prep, Inc. (Elysian, MN). 3-(4,5-Dimethylthiazol-2-yl)-2,5-diphenyltetrazolium bromide (MTT) was purchased from Biosynth International (Itasca, IL). The amounts of triglyceride and protein were quantified using Infinity triglycerides kit and Pierce BCA protein assay kit, respectively, both from Thermo Fisher Scientifics (Middletown, VA). Trizol and High-Capacity cDNA Reverse Transcription Kit were purchased from Life Technologies (Carlsbad, CA). Taqman Universal Master Mix II was obtained from Applied Biosystems (Carlsbad, CA). 2′,7′-Dichlorofluorescin diacetate (DCFDA,

>95%) and GW9662 (>98%) was purchased from Cayman Chemical (Ann Arbor, MI). Fura-2-acetoxymethyl ester (Fura-2 AM, >95%) was purchased from Abcam (Cambridge, MA).

6.2.2 Cell culture

HepG2 cells were maintained in DMEM supplemented with 10% (v/v) FBS, 10,000 U/mL penicillin and 10 mg/mL streptomycin. Cells were sub-cultured every 48–72 h at a confluency of 80–90%. After confluent, HepG2 cells were exposed to PFBS with or without 300 μM fatty acid (FA) mixture conjugated by bovine serum albumin (oleic acid:palmitic acid = 2:1) as an inducer of steatosis for 48 h (Dhami-Shah et al., 2018; Yang et al., 2019a). All treatments included DMSO at a final concentration of 0.1%.

6.2.3 Measurement of cell viability

Cell viability was determined by 3-(4,5-dimethylthiazol-2-yl)-2,5-diphenyltetrazolium bromide (MTT)-based assay (Gerlier and Thomasset, 1986). HepG2 cells were seeded in a 96-well plate, and cells were treated with PFBS at various concentrations for 2 days. The cells were then treated with 5 mg/ml MTT at 37 °C for 4 h. Cell viability was then assessed by the formation of formazan from MTT. The purple formazan was dissolved in DMSO and the absorbance at 540 nm was determined using a SpectraMax i3 microplate reader (Molecular Devices, Sunnyvale, CA).

6.2.4 Triglyceride quantification

Triglyceride levels were determined using a commercial kit (Infinity™ Triglycerides Reagent). Briefly, after 48 h, cells were washed twice with phosphate-buffered saline (PBS) and harvested by scraping the cells from the culture plate in PBS containing 1% Triton-X. Cell homogenates were obtained by sonication using Fisherbrand™ Model 50 Sonic Dismembrator (Fisher Scientific), and TG concentrations were determined according to the manufacturer's instructions. Protein concentrations were measured using Pierce BCA Protein Assay Kit and used for normalization of samples.

6.2.5 Reverse transcriptase quantitative PCR (RT-qPCR) analysis

Total RNA was isolated from cells using TRIzol Reagent (Life Technologies, Carlsbad, CA) according to manufacturer's instruction. Conversion of total RNA to single stranded cDNA was performed using the High-Capacity cDNA Reverse Transcription Kit (Life Technologies, Carlsbad, CA). Gene expression assays for sterol regulatory element-binding protein 1 (SREBP1, Hs01088679_g1), acetyl-CoA carboxylase (ACC, Hs01046047_m1), fatty acid synthase (FAS, Hs00236330_m1), peroxisome proliferator-activated receptor α (PPARα, Hs00947536_m1), peroxisome proliferator-activated receptor γ (PPARγ, HsXXXXXX_m1), carnitine palmitoyltransferase 1α (CPT1α, Hs00912671_m1), cluster of differentiation 36 (CD36, Hs00354519_m1), diacylglycerol O-acyltransferase 2 (DGAT2, Hs01045913_m1) and DNA damage-inducible transcript 3 (DDIT3, Hs00358796_g1) were performed with Taqman Universal Master Mix II (Applied Biosystems, Carlsbad, CA) on a StepOne Plus Real Time PCR System (Applied Biosystems, Carlsbad, CA). The results of target gene expression levels were normalized to the expression level of the eukaryotic18S rRNA gene (Hs99999901_s1) using the $2^{-\Delta\Delta Ct}$ method (Livak and Schmittgen, 2001).

6.2.6 Measurement of intracellular reactive oxygen species (ROS)

Intracellular ROS were measured by fluorescence dye 2′,7′-dichlorofluorescin diacetate (DCFDA) assay as described (LeBel et al., 1992; Yang et al., 2018a). DCFDA was first dissolved in DMSO and 25 μM DCFDA solution was freshly prepared in HEPES buffer. Cells were pre-incubated with DCFDA for 45 min at 37 °C. DCFDA was then replaced by PFBS treatment and fluorescence was measured at excitation 485 nm and emission 535 nm at 1, 3, and 12 h after treatment (SpectraMax i3, Molecular Devices LLC, San Jose, CA).

6.2.7 Measurement of cytosolic calcium

Cytosolic calcium levels were measured by cell permeate fluorescence dye, Fura-2-acetoxymethyl ester (Fura-2 AM), using the ratiometric method (Roe et al., 1990; Yang et al.,

2018a). The conformation of fluorescent dye changes when chelated with Ca^{2+}, resulting in change of excitation wavelength from 380 nm to 340 nm, but did not influence the emission wavelength and 510 nm. Fura-2 AM was diluted in HEPES buffer containing 0.01% pluronic acid. Before PFBS treatment, cells were pre-incubated with 2 μM Fura-2 AM for 60 min at room temperature. Dye was then removed, and cells were incubated with HEPES buffer for another 30 min at room temperature for ester hydrolysis without the further compartmentation of Fura-2 AM into intracellular organelles, for example ER. Cells were then treated with PFBS and cytosolic calcium levels were estimated by the ratio of fluorescence intensities detected at emission 510 nm with excitation wavelengths of 340 nm and 380 nm (510 nm/340 nm vs. 510 nm/380 nm) (SpectraMax i3, Molecular Devices LLC, San Jose, CA).

6.2.8 Data Analysis

Data in Figures 1-7 were analyzed with two-way ANOVA. Data in Figures 8 were analyzed with one-way ANOVA. Data in Figures 9 were analyzed with three-way ANOVA. All data were analyzed using the Statistical Analysis System 9.3 (SAS Institute, Cary, NC). All data are expressed as the mean ± standard error of the mean. Multiple comparisons among groups were performed using Tukey's test. *P* values less than 0.05 are reported as statistically significant. N is defined as the number of replicates in each experiment.

6.3 Results

6.3.1 PFBS enhances fat accumulation in HepG2 cells

To investigate the effects of PFBS on fat accumulation in liver cells, HepG2 cells were treated with PFBS with or without 300 μM fatty acid mixture conjugated by bovine serum albumin (oleic acid:palmitic acid= 2:1, FA) as the inducer of steatosis. The cytotoxicity of PFBS on HepG2 cells was first determined. As shown in Figure 6.1, there was no interaction between FA and PFBS with respect to cell viability (P=0.0865). 300 μM FA treatment significantly reduced the percentage of viable cell (P<0.0001). PFBS from 50 to 200 μM has no cytotoxic

effect on HepG2 cells with or without FA (*P*=0.1592). From these results, it was decided to use PFBS concentrations up to 200 µM for the following experiments.

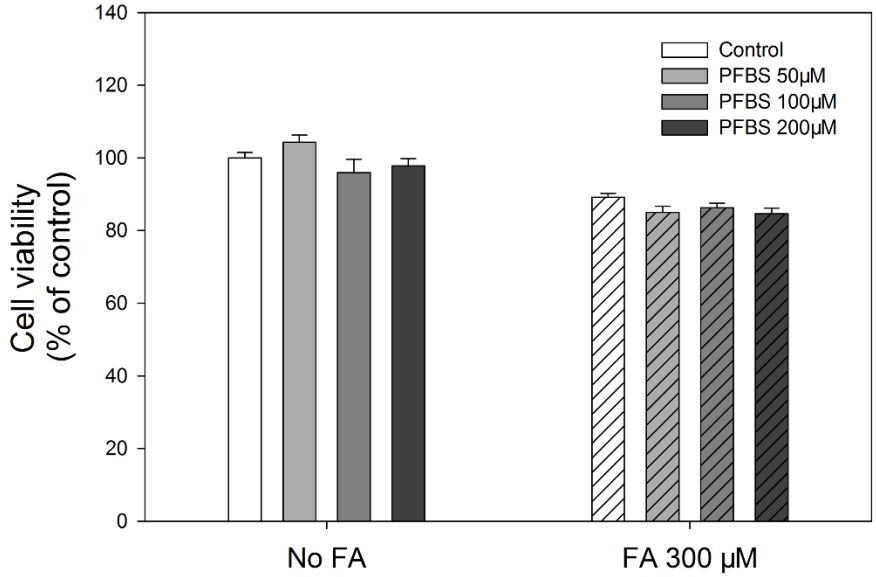

	PFBS	FA	Interaction
P value	n.s.	<0.0001	n.s.

Figure 6.1 Cytotoxicity of PFBS in HepG2 hepatocytes. HepG2 cells in 96-well culture plates were treated with PFBS (0, 50, 100, and 200 µM) with or without fatty acid mixture for 48 hours. After 48 hours, cell viability was determined by MTT assay. Numbers are mean ± S.E. (n= 10).

Next, we investigated the role of PFBS in fat accumulation in hepatocytes (Figure 6.2). As expected, FA treatment significantly elevated TG content (P<0.0001), with significant interaction between PFBS and FA treatment (*P*=0.0023). After 48h treatment, our data showed that PFBS at 200 µM supplemented with 300 µM FA significantly increases the fat accumulation by 27% compared with FA control (*P*=0.0001). However, we observed no effects of PFBS treatment without FA compared with control.

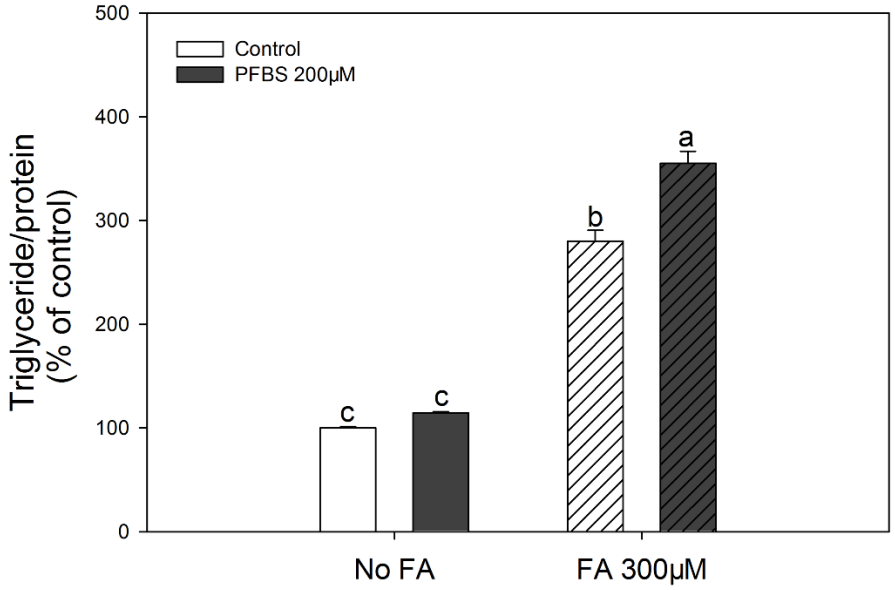

	PFBS	FA	Interaction
P value	<0.0001	<0.0001	0.0023

Figure 6.2 PFBS promotes triglyceride accumulation in HepG2 cells. After treatment for 48 hours, hepatocytes were harvested and measured for triglyceride content that were normalized by protein. Numbers are mean ± S.E. (n=4). Means with different letters are significantly different at P< 0.05.

6.3.2 Effects of PFBS on lipogenesis pathways

To understand the role of PFBS in hepatic lipid metabolism, as well as the potential interaction between PFBS and FA supplementation, we next tested whether PFBS treatment could induce mRNA expression of lipogenesis-related genes in HepG2 cells with or without induction of steatosis. Figure 6.3 shows the influence of PFBS exposure for 48 hours on the expression levels of lipogenesis related genes. No interaction between PFBS and FA treatment can be observed in the expression of these genes. FA treatment significantly increased the expression levels of key genes in *de novo* fatty acid synthesis; acetyl-CoA carboxylase (ACC, Figure 6.3A, 35%, *P*=0.0453), fatty acid synthase (FAS, Figure 6.3B, 42%, *P*=0.0038), and sterol regulatory element-binding protein 1 (SREBP1, Figure 6.3C, 39%, *P*=0.0446), while diacylglycerol acyltransferase 2 (DGAT2), a key regulator in TG synthesis expression, was not

affected by FA treatment (Figure 6.3D, *P*=0.4531). Treatment with 200 µM PFBS significantly enhanced the mRNA expression levels of ACC (Figure 6.3A, 75%, *P*=0.0014), FAS (Figure 6.3B, 98%, *P*<0.0001), and SREBP1 (Figure 6.3C, 74%, *P*=0.0028), as well as DGAT2 (Figure 6.3D, 39%, *P*=0.0008).

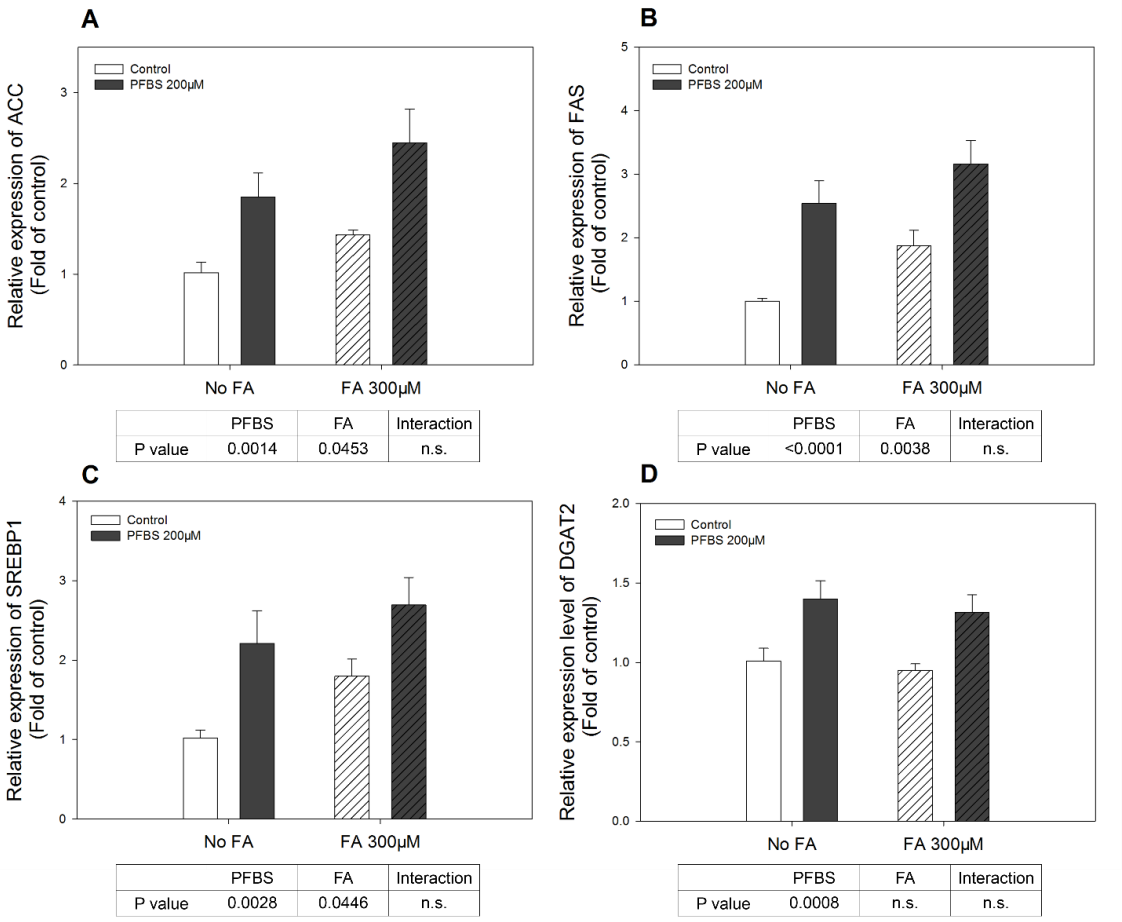

Figure 6.3 Effects of PFBS on lipogenesis gene expression in HepG2. Cells were treated with PFBS (200 µM) and FA (300 µM) for 48 hours. mRNA levels of indicated genes were quantified by RT-qPCR and the ΔΔCt was determined using eukaryotic 18S rRNA as a housekeeping gene. FAS, fatty acid synthase (A); ACC, acetyl-CoA carboxylase (B); SREBP1, sterol regulatory element-binding protein 1 (C); DGAT2, diglyceride acyltransferase 2 (D). Numbers are mean ± S.E. (n=4).

6.3.3 Effects of PFBS on fatty acid uptake pathways

Besides lipogenesis pathways, the uptake of circulating free fatty acid also plays an important role in the accumulation of hepatic lipid (Vergani, 2017). Therefore, we next

investigated the potential effects of PFBS on fatty acid translocase (FAT/CD36), a major lipid trafficking gene, and peroxisome proliferator-activated receptor gamma (PPARγ), its major regulator (Huck et al., 2018; Wan et al., 2012). Similar to the results for lipogenesis related genes, no significant interaction between PFBS and FA can be observed. FA treatment significantly promoted the expressions of these genes (CD36, 47%, *P*=0.0019; PPARγ, 45%, *P*=0.0036), while PFBS significantly increased the expressions of CD36 (Figure 6.4A, 26%, *P*=0.0012) and PPARγ (Figure 6.4B, 47%, *P*=0.0032).

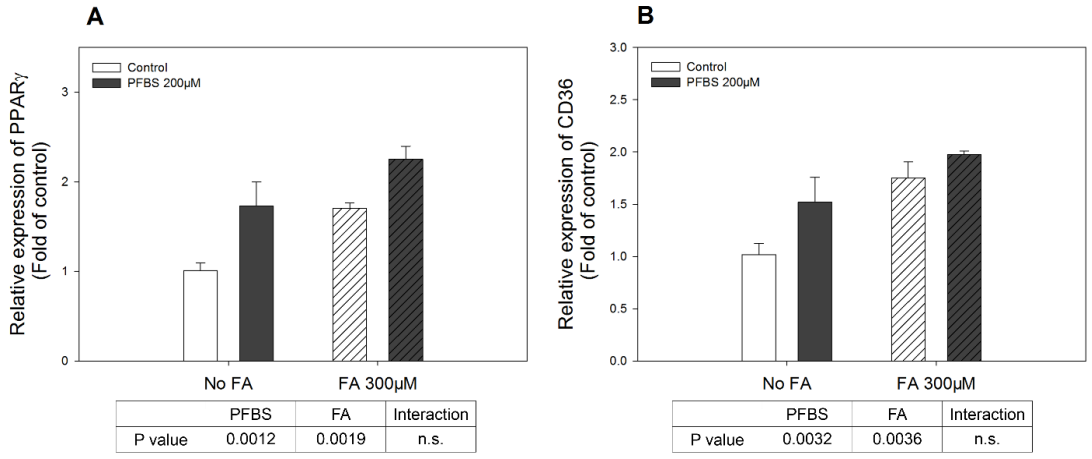

Figure 6.4 Effects of PFBS on fatty acid uptake gene expression in HepG2. Cells were treated with PFBS (200 μM) and FA (300 μM) for 48 hours. mRNA levels of indicated genes were quantified by RT-qPCR and the ΔΔCt was determined using eukaryotic 18S rRNA as a housekeeping gene. PPARγ, peroxisome proliferator-activated receptor gamma (A); CD36, fatty acid translocase (B). Numbers are mean ± S.E. (n=4).

6.3.4 Effects of PFBS on PPARα and CPT1α

The inhibition of mitochondrial β oxidation could be another potential mechanism in the accumulation of TG. In order to verify the role of mitochondrial β oxidation in the effects of PFBS on TG accumulation, we next investigated whether PFBS exposure could affect the expression of carnitine palmitoyltransferase 1 alpha (CPT1α), the key regulator of β oxidation, as well as its upstream regulator, peroxisome proliferator activated receptor alpha (PPARα). In the present study, neither interaction nor FA effects can be observed on the expression of these genes.

On the other hand, PFBS significantly induced the expressions of PPARα (Figure 6.5A, 67%, *P*=0.0019), and CPT1α (Figure 6.5B, 149%, *P*=0.0002).

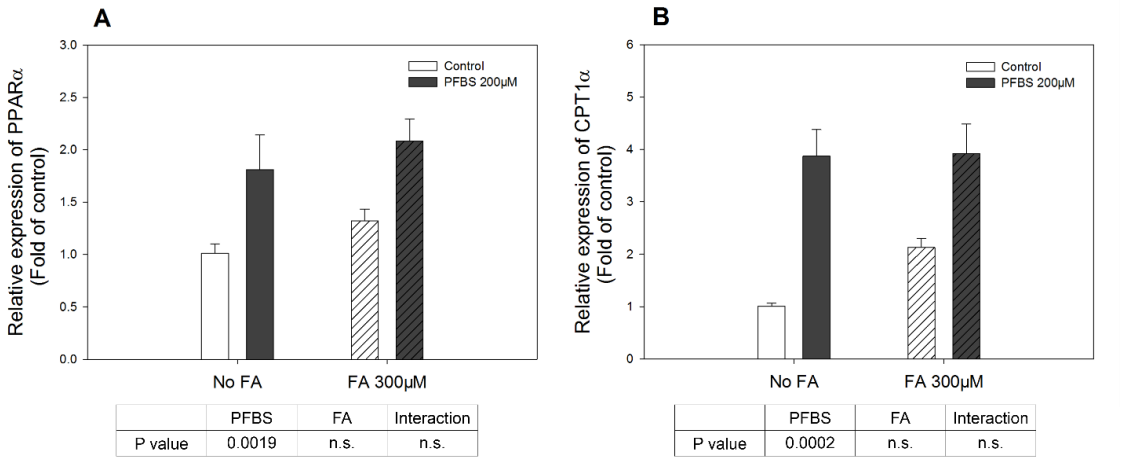

Figure 6.5 Effects of PFBS on fatty acid oxidation gene expression in HepG2. Cells were treated with PFBS (200 μM) and FA (300 μM) for 48 hours. mRNA levels of indicated genes were quantified by RT-qPCR and the ΔΔCt was determined using eukaryotic 18S rRNA as a housekeeping gene. PPARα, peroxisome proliferator-activated receptor alpha (A); CPT1α, carnitine palmitoyltransferase 1 alpha (B). Numbers are mean ± S.E. (n=4).

6.3.5 Effects of PFBS on ROS, ER stress pathways, and cytosolic calcium

Next, we examined how PFBS could affect the production of reactive oxygen species (Figure 6.6), which is also a potential mechanism of liver steatosis (Masarone et al., 2018). Thus, effects of PFBS on ROS production after 1, 3, and 12-hour treatment of PFBS were investigated. Among the three time points, significant interactions between PFBS and FA were observed only at 3 hours (*P*=0.0009) and 12 hours (*P*<0.0001); while the PFBS treatment effect was observed independent of the FA effect at 1 hour. FA significantly increase ROS at all time points (1 hour, 179%, *P*<0.001; 3 hours, 248%, *P*<0.001; 12 hours, 187%, *P*<0.001). Also, significant increases can be observed on ROS production after treatment of PFBS for 1, 3, and 12 hours (1 hour, 18%, *P*<0.001; 3 hours, 30%, *P*<0.001; 12 hours, 59%, *P*<0.001).

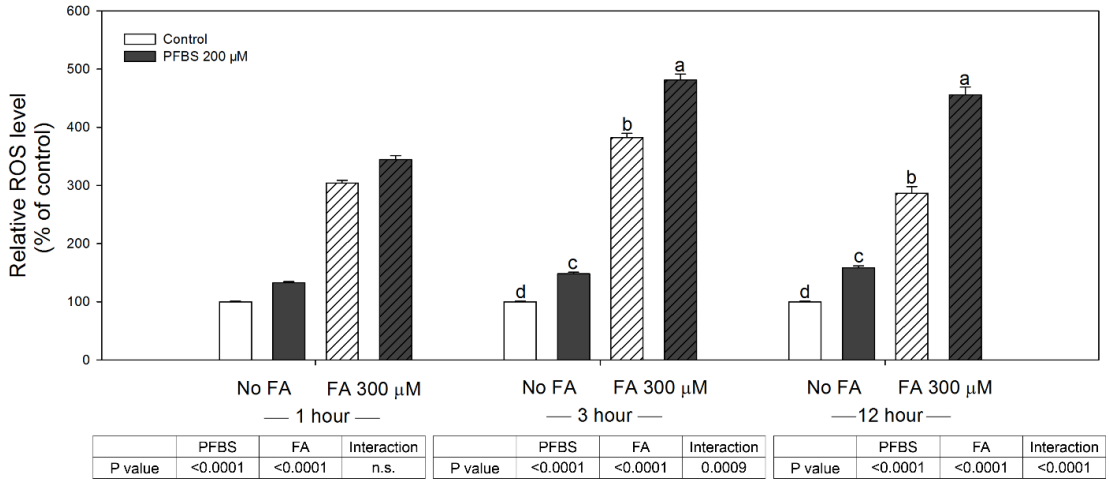

	PFBS	FA	Interaction
P value	<0.0001	<0.0001	n.s.

	PFBS	FA	Interaction
P value	<0.0001	<0.0001	0.0009

	PFBS	FA	Interaction
P value	<0.0001	<0.0001	<0.0001

Figure 6.6 Effects of PFBS on reactive oxygen species (ROS) production in HepG2. HepG2 cells were preincubated with 25 μM DCFDA as ROS probe and treated with PFBS (200 μM) and FA (300 μM), and ROS levels were measured at 1, 3, and 12 hours. Numbers are mean ± S.E. (n=6). Means with different letters are significantly different at P< 0.05.

Endoplasmic reticulum (ER) stress results from the unfolded protein response (UPR) induced by accumulation of misfolded or unfolded protein in ER, which is also one of the modulators in lipogenesis (Lebeaupin et al., 2018). Besides, ER stress is largely connected to the production of ROS, as ER accounts for 25% of total cellular ROS generation (Shimizu and Hendershot, 2009). CCAAT/enhancer-binding homologous protein (CHOP), one of the key markers in ER stress, is also responsible for the UPR-mediated ROS generation (van Galen et al., 2014). Thus, we tested whether PFBS treatment could affect CHOP. As shown in Figure 6.7, interaction was not found between PFBS and FA treatment on CHOP expression. Increased expression of CHOP can also be observed after FA treatment (23%, *P*=0.0446), while PFBS significantly increased the transcript level of CHOP (82%, *P*<0.0001).

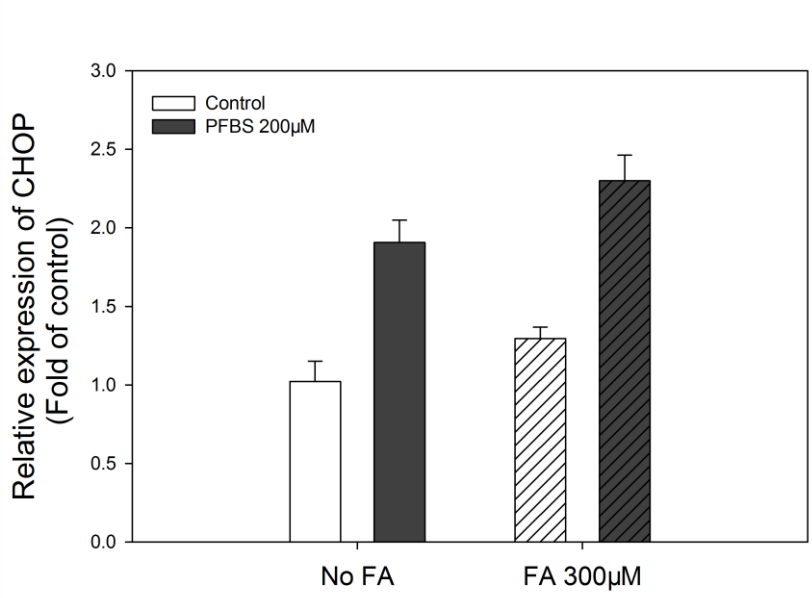

	PFBS	FA	Interaction
P value	<0.0001	0.0446	n.s.

Figure 6.7 Effects of PFBS on ER stress pathway in HepG2. Cells were treated with PFBS (200 μM) and FA (300 μM) for 48 hours. mRNA levels of indicated genes were quantified by RT-qPCR and the ΔΔCt was determined using eukaryotic 18S rRNA as a housekeeping gene. CHOP, C/EBP homologous protein. Numbers are mean ± S.E. (n=4).

As calcium homeostasis is crucial in hepatic lipid metabolism, and it is intertwined with oxidative stress and ER stress (Bahar et al., 2016; Berridge et al., 2003; Brookes et al., 2004), here we also investigated the effect of PFBS on cytosolic calcium (Figure 6.8). As a result, 200 μM PFBS treatment for 1 hour significantly increased the cytosolic calcium by 17% (P=0.0278).

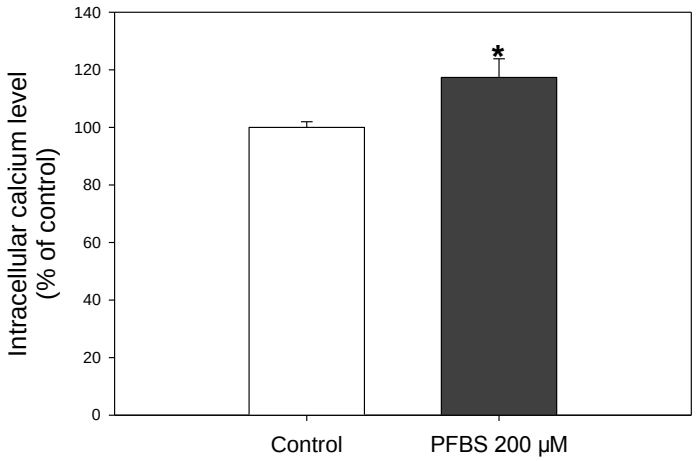

Figure 6.8 Effects of PFBS on cytosolic calcium in HepG2. HepG2 cells were pre-treated with 2 µM Fura-2 AM, and then treated with PFBS (200 µM). Cytosolic calcium was measured after 1 hour. Numbers are mean ± S.E. (n=6). * indicates a significant difference against the respective control ($P < 0.05$)

6.3.6 PFBS promotes fat accumulation in HepG2 cells via PPARγ mediated pathway

PPARγ is the one of key regulators modulating lipid metabolism in liver regulating both lipogenesis and FA uptake (Schadinger et al., 2005; Zhou et al., 2008). We further investigated whether the promoted accumulation of fat caused by PFBS is mediated by the activation of PPARγ. To determine whether the effect of PFBS is PPARγ-mediated, GW9662 (an antagonist of PPARγ) was used to determine if the inhibition of PPARγ could reverse the promoted hepatic fat accumulation induced by PFBS. HepG2 cells were exposed under the combination treatment of 200 µM PFBS, 300 µM FA, and 40 µM GW9662. Since there was significant three-way interaction among PFBS, FA, and GW9662, all treatment groups were compared separately (Figure 6.9). PFBS increased the TG content with or without the addition of FA by 18% and 28%, although the increase in non-FA group is insignificant. However, with the addition of GW9662, the increases induced by PFBS were eliminated both with and without FA. These results suggested that PFBS promotes fat accumulation via a PPARγ-dependent pathway.

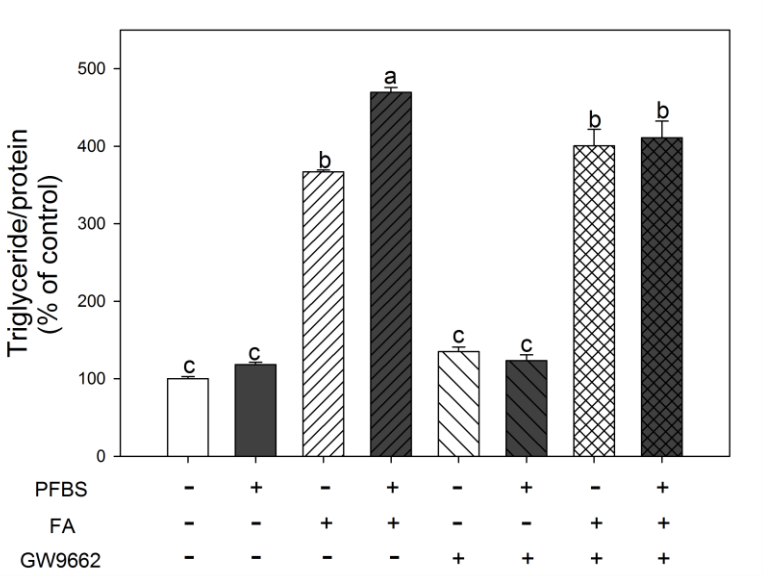

	PFBS	FA	GW9662	PFBS*FA	PFBS* GW9662	FA* GW9662	PFBS*FA *GW9662
P value	<0.0001	<0.0001	n.s.	<0.0001	<0.0001	0.0026	0.0036

Figure 6.9 Increase in triglyceride accumulation caused by PFBS were abolished by GW9662. Cells were treated with PFBS (200 µM), FA (300 µM), and GW9662 (40 µM). After treatment for 48 hours, hepatocytes were harvested and measured for triglyceride content that were normalized by protein. Numbers are mean ± S.E. (n=4). Means with different letters are significantly different at P< 0.05.

6.4 Discussion

The liver is known as the major site for regulating lipid in the body, playing a crucial role in normal lipid homeostasis. In the current study, we demonstrated that PFBS increased fat accumulation in HepG2 hepatocytes. We further investigated the effects of PFBS on hepatic lipid metabolism, as well as its interaction with FA. It was also found that PFBS may trigger oxidative stress, ER stress, and the impairment in calcium homeostasis. Finally, the increase hepatic fat accumulation was mediated in part by PPARγ regulated pathway.

PPARγ is the master regulator of whole-body lipid metabolism. PPARγ is most highly expressed in adipose tissue, where it regulates the adipocyte differentiation (Siersbæk et al., 2010). In addition, PPARγ is also well known to promote hepatic steatosis. Indeed, hepatic PPARγ expression is increased in the mice with high-fat-diet induced steatosis (Inoue et al.,

2005). The overexpression of hepatic PPARγ has been reported to induce steatosis by activating lipogenesis genes, ACC, FAS, and SREBP1 (Schadinger et al., 2005; Yu et al., 2003), and free fatty acid uptake transporter, CD36 (Zhou et al., 2008). In this study, PFBS significantly elevated the expression of PPARγ (Figure 6.4A), and genes regulating lipogenesis (Figure 6.3) and FA uptake (Figure 6.4B) were both activated by PFBS treatment. Also, the current results suggested that the effect of PFBS on increased fat accumulation is dependent on the activation of PPARγ (Figure 6.9). As shown in Figure 6.2, effect of PFBS on TG accumulation was enhanced when FA is available in the media, which implies an important role of PPARγ/CD36-mediated FA uptake in the effects of PFBS. Consistent with our finding, in a recent study using liver-specific PPARγ knockdown model, CD36-mediated FA uptake was reported to be the major target of hepatic PPARγ in steatosis, while genes regulating de novo lipogenesis and TG synthesis, including ACC, FAS, SREBP1, and DGAT2, were not affected by the knockdown of PPARγ specifically in liver (Wolf Greenstein et al., 2017). Thus, PFBS appears to activate PPARγ, which mainly promotes FA uptake and leads to increased hepatic fat accumulation. However, although PFBS has been reported to activate human PPARγ, the activation potency was relatively low compared with PFOS (Zhang et al., 2014). Based on the current data, it remained unclear whether the activation of PPARγ is induced directly by the exposure to PFBS, or it is induced by the upstream effectors.

Besides PPARγ, PPARα is a known target for PFAS, including PFBS (Wolf et al., 2008). Previous studies have suggested the upregulation of key enzymes in fatty acid β oxidation, including CPT1α, upon PFOS exposure in rodents (Wan et al., 2012), which is regulated by the activation of PPARα (Song et al., 2010). However, another study on PPARα-null mice revealed the PPARα-independent effects of PFOS (Rosen et al., 2010). In the current study, as expected, PFBS significantly activated the expression of both PPARα and CPT1α (Figure 6.5). However, since FA are ligands of PPARs (Grygiel-Górniak, 2014), it is possible that the hepatic

accumulation of FA might activate PPARα and subsequently CPT1α, which is the secondary effect of PFBS-induced fat accumulation. Therefore, although mitochondrial β oxidation was activated by PFBS treatment, it might not be relevant to the fat accumulation induced by PFBS.

On the other hand, mitochondrial β-oxidation could be a source of the increased ROS production. The increased amounts or activities of fatty acid oxidation enzymes have been reported to be associated with the net production of ROS in liver (Tahara et al., 2009). Besides, accumulating evidences have supported the strong connections between oxidative stress and ER stress. The primary function of ER is folding and assembling proteins, but its function can be disrupted when the cells are under stress, for example lipid overload. Unfolded and misfolded proteins can accumulate in ER lumen and activate unfolded protein response (UPR) (Malhotra and Kaufman, 2007). A prolonged ER stress and UPR can result in excessive production of ROS by the activation of CHOP (van Galen et al., 2014). The protein folding process is also dependent largely on the redox homeostasis. Oxidative stress could potentially interfere the protein folding process, which generates misfolded or unfolded protein, and subsequently ER stress (van der Vlies et al., 2003). Besides, oxidative stress and ER stress can also be mediated by the imbalance of calcium. The increased level of cytosolic calcium could lead to the activation of ER stress (Bahar et al., 2016; Berridge et al., 2003). On the other hand, increased metabolic rate caused by increased calcium results in increased respiratory chain electron leakage and ROS production (Brookes et al., 2004). From the current data, significant increases in ROS production (Figure 6.6), CHOP expression (Figure 6.7), and cytosolic calcium (Figure 6.8) were identified, which is consistent with the studies on PFOS, the higher molecular weight cognate of PFBS (Eriksen et al., 2010; Liu et al., 2011; Oh et al., 2017; Qian et al., 2010). Therefore, it is possible that PFBS could potentially induce hepatic fat accumulation through the activation of oxidative stress, ER stress, and calcium imbalance. However, the interaction between these factors on PFBS-induced fat accumulation is needed to be further investigated.

PFBS is generally believed to be less toxic than PFOS due to its shorter biological half-life in human (~1 month). A 7 μg/L (23 nM) health risk limit in groundwater for PFBS was established in Minnesota, and the EPA has set a sub-chronic reference dose of 0.2 mg/kg/d and chronic reference dose of 0.02 mg/kg/d (EPA, 2014). The no-observed-adverse-effect level (NOAEL) for PFBS was determined to be 60 mg/kg/d for males and 600 mg/kg/d for females in rats after a 90-day oral study (Lieder et al., 2009). The levels of PFBS in the liver after single or repeated oral dose have been reported in rats and mice. In Sprague-Dawley rats, liver PFBS concentration at day 4 after a single dose of 30 mg/kg was 0.45 μmol/kg for male and 1.14 μmol/kg for female (Olsen et al., 2009a). In male C57BL/6 mice exposed to 16 mg/kg/d of ^{35}S-labeled PFBS for 3 days, ^{35}S labeled PFBS was found to distribute to the liver at 31 μmol/kg, being as much as 1.6-fold the level in blood (19 μmol/kg), suggesting a potential accumulation in the liver (Bogdanska et al., 2014). In human, serum PFBS levels of factory workers have been found to be approximately 23 ng/ml (77 nM) (Fu et al., 2015). Given this limited data set, the doses used in the current study may not be achievable. Nevertheless, the effects of obesogens can be aggravated by dietary fat intake as previous studies have shown the interaction between obesogens treatment and dietary fat (Sun et al., 2017; Sun et al., 2016b; Xiao et al., 2017a; Xiao et al., 2018). Therefore, despite the high concentration used in this study, the effects of PFBS on hepatic fat accumulation could elucidate a potential risk on the development of NAFLD.

6.5 Conclusion

In conclusion, this study investigated the effects of PFBS, a replacement of PFOS, on hepatic lipid metabolism, as well as its interaction with FA overloads. Potential link between PFBS exposure, high fat diet, and the risk of developing NAFLD was elucidated. The current results, however, are limited to an *in vitro* model with relatively high concentrations of treatment. Further well-designed studies in animals, as well as epidemiology studies, are needed to confirm the current results.

CHAPTER 7

Concluding Remarks

The incidence of metabolic diseases associated with disrupted lipid metabolisms, including obesity, and non-alcoholic fatty liver disease (NAFLD), have been increasing in the last few decades. Western diet, sedentary lifestyle, and genetic profile have been associated with the pathogenesis of these diseases. However, the dramatic increases cannot be completely explained by these contributing factors. Recently, accumulating literatures have elucidated the potential connections between environmental contaminants and the development of obesity and NAFLD (Arciello et al., 2013; Armstrong and Guo, 2019; Wang et al., 2016). However, there is a big knowledge gap on the potential mechanisms of these effects. Thus, the objective is to clarify the mechanisms of altered lipid metabolism in adipocytes and hepatocytes induced by environmental contaminants (ivermectin and PFBS). By understanding molecular mechanisms by which exposure to environmental contaminants may induce or prevent the development of obesity and type 2 diabetes, we will be able to direct more efficient prevention and/or treatment strategies for these and related pathologies in the future.

Ivermectin, a member of the avermectins, is one of the most extensively used anti-parasitic agents worldwide, and acts by binding to glutamate-gated chloride channels in invertebrate nerve cells. There is limited information, however, on the effects of ivermectin in non-neural cell, such as mammalian adipocytes. Our current study aimed to investigate the role of ivermectin in adipogenesis using 3T3-L1 preadipocytes. From our data, ivermectin inhibited the differentiation of preadipocytes and TG accumulation. In particular, the effects of ivermectin was found to focus on middle to late stage of the differentiation. Ivermectin treatment also significantly reduced the mRNA expression of key markers in adipogenesis, modulated the expression of genes regulating fatty acid synthesis, uptake, and oxidation, and enhanced the gene expression of two subunits of the glycine receptor (GlyR). Specifically, the protein levels of

peroxisome proliferator-activated receptor gamma (PPARγ), CCAAT/enhancer-binding protein alpha (C/EBPα), and acetyl-CoA carboxylase (ACC) were reduced by ivermectin treatment. Of interest, the suppression of TG accumulation by ivermectin was partially abolished by rosiglitazone, a specific PPARγ agonist, but Z-guggulsterone, a selective FXR antagonist, failed to rescue the ivermectin-induced effect on adipogenesis. Lastly, ivermectin prevented adipogenesis induced by permethrin and fipronil.

PFBS is used as the replacement of PFOS since 2000 because of the concern on PFOS' persistence in the environment and the bioaccumulation in animals. Accumulating evidence has shown the correlation between the exposure to perfluorinated compounds and enhanced adipogenesis. There is no report, however, of the effect of PFBS on adipogenesis. Here, we investigated the role of PFBS in adipogenesis using 3T3-L1 adipocytes. PFBS treatment extensively promoted the differentiation of 3T3-L1 preadipocytes to adipocytes. In particular, the treatments of PFBS at the early adipogenic differentiation period (day 0-2) were positively correlated with increased the triglyceride accumulation on day 6. PFBS treatments significantly increased the protein and mRNA levels of the master transcription factors in adipocyte differentiation; C/EBPα and PPARγ, along with ACC and FAS, the key proteins in lipogenesis. PFBS significantly activated the phosphorylation of extracellular signal-regulated kinase1/2 (ERK1/2) after 4-hour treatment, and PFBS' effect on triglyceride was abolished by U0126, a specific MAPK/ERK kinase (MEK) inhibitor.

To elucidate the potential role of PFBS on the development of NAFLD, we next investigated the effects of PFBS on hepatic lipid metabolism using HepG2 cells as model. PFBS treatment for 48 hours significantly increased the triglyceride level with fatty acid (FA) mixture (oleic acid:palmitic acid = 2:1), but not without FA. Moreover, the expression levels of genes regulating lipogenesis were enhanced by PFBS treatment. PFBS also induced hepatic FA uptake implied by the upregulation of key genes modulating the capacity of FA trafficking to liver.

PFBS' effect on triglyceride was abolished by GW9662, a specific peroxisome proliferator-activated receptor gamma (PPARγ) antagonist. Besides, PFBS treatment also promoted the production of reactive oxygen species (ROS), endoplasmic reticulum (ER) stress marker and cytosolic calcium.

Collectively, environmental contaminants (ivermectin and PFBS) interrupt lipid metabolisms in adipose tissue and liver with different mechanisms. With further study on animals or humans, our results might provide some insights for the design of strategies against the development of diseases associated with lipid metabolisms.

BIBLIOGRAPHY

Abdelkarim, M., Caron, S., Duhem, C., Prawitt, J., Dumont, J., Lucas, A., Bouchaert, E., Briand, O., Brozek, J., Kuipers, F., Fievet, C., Cariou, B., Staels, B., 2010. The farnesoid X receptor regulates adipocyte differentiation and function by promoting peroxisome proliferator-activated receptor-gamma and interfering with the Wnt/beta-catenin pathways. The Journal of biological chemistry. 285, 36759-36767.

Adelsberger, H., Lepier, A., Dudel, J., 2000. Activation of rat recombinant α1β2γ2S GABAA receptor by the insecticide ivermectin. European journal of pharmacology. 394, 163-170.

Ahrens, L., Ebinghaus, R., 2010. Spatial distribution of polyfluoroalkyl compounds in dab (Limanda limanda) bile fluids from Iceland and the North Sea. Marine pollution bulletin. 60, 145-148.

Alderete, T.L., Jin, R., Walker, D.I., Valvi, D., Chen, Z., Jones, D.P., Peng, C., Gilliland, F.D., Berhane, K., Conti, D.V., Goran, M.I., Chatzi, L., 2019. Perfluoroalkyl substances, metabolomic profiling, and alterations in glucose homeostasis among overweight and obese Hispanic children: A proof-of-concept analysis. Environ Int. 126, 445-453.

Altiok, S., Xu, M., Spiegelman, B.M., 1997. PPARγ induces cell cycle withdrawal: inhibition of E2F/DP DNA-binding activity via down-regulation of PP2A. Genes & development. 11, 1987-1998.

Ameduri, B., Boutevin, B., 2004. Chapter 1 - Telomerisation reactions of fluorinated alkenes, in: B. Ameduri, B. Boutevin (Eds.), Well-Architectured Fluoropolymers: Synthesis, Properties and Applications. Elsevier Science, Amsterdam, pp. 1-99.

Andersen, C.S., Fei, C., Gamborg, M., Nohr, E.A., Sørensen, T.I., Olsen, J., 2010. Prenatal exposures to perfluorinated chemicals and anthropometric measures in infancy. American journal of epidemiology. 172, 1230-1237.

Andersen, C.S., Fei, C., Gamborg, M., Nohr, E.A., Sørensen, T.I., Olsen, J., 2013. Prenatal exposures to perfluorinated chemicals and anthropometry at 7 years of age. American journal of epidemiology. 178, 921-927.

Antignac, J.P., Veyrand, B., Kadar, H., Marchand, P., Oleko, A., Le Bizec, B., Vandentorren, S., 2013. Occurrence of perfluorinated alkylated substances in breast milk of French women and relation with socio-demographical and clinical parameters: results of the ELFE pilot study. Chemosphere. 91, 802-808.

Apelberg, B.J., Goldman, L.R., Calafat, A.M., Herbstman, J.B., Kuklenyik, Z., Heidler, J., Needham, L.L., Halden, R.U., Witter, F.R., 2007. Determinants of fetal exposure to polyfluoroalkyl compounds in Baltimore, Maryland. Environmental science & technology. 41, 3891-3897.

Arciello, M., Gori, M., Maggio, R., Barbaro, B., Tarocchi, M., Galli, A., Balsano, C., 2013. Environmental pollution: a tangible risk for NAFLD pathogenesis. Int J Mol Sci. 14, 22052-22066.

Armstrong, L.E., Guo, G.L., 2019. Understanding Environmental Contaminants' Direct Effects on Non-alcoholic Fatty Liver Disease Progression. Current environmental health reports.

Bach, C.C., Vested, A., Jorgensen, K.T., Bonde, J.P., Henriksen, T.B., Toft, G., 2016. Perfluoroalkyl and polyfluoroalkyl substances and measures of human fertility: a systematic review. Critical reviews in toxicology. 46, 735-755.

Bahar, E., Kim, H., Yoon, H., 2016. ER Stress-Mediated Signaling: Action Potential and Ca(2+) as Key Players. Int J Mol Sci. 17, 1558.

Banerjee, S.S., Feinberg, M.W., Watanabe, M., Gray, S., Haspel, R.L., Denkinger, D.J., Kawahara, R., Hauner, H., Jain, M.K., 2003. The Krüppel-like factor KLF2 inhibits peroxisome proliferator-activated receptor-γ expression and adipogenesis. Journal of biological chemistry. 278, 2581-2584.

Baraka, O., Mahmoud, B., Marschke, C., Geary, T., Homeida, M., Williams, J., 1996. Ivermectin distribution in the plasma and tissues of patients infected with Onchocerca volvulus. European journal of clinical pharmacology. 50, 407-410.

Bassler, J., Ducatman, A., Elliott, M., Wen, S., Wahlang, B., Barnett, J., Cave, M.C., 2019. Environmental perfluoroalkyl acid exposures are associated with liver disease characterized by apoptosis and altered serum adipocytokines. Environmental Pollution. 247, 1055-1063.

Begley, T.H., Hsu, W., Noonan, G., Diachenko, G., 2008. Migration of fluorochemical paper additives from food-contact paper into foods and food simulants. Food additives & contaminants. Part A, Chemistry, analysis, control, exposure & risk assessment. 25, 384-390.

Begley, T.H., White, K., Honigfort, P., Twaroski, M.L., Neches, R., Walker, R.A., 2005. Perfluorochemicals: Potential sources of and migration from food packaging. Food Addit. Contam. 22, 1023-1031.

Berridge, M.J., Bootman, M.D., Roderick, H.L., 2003. Calcium signalling: dynamics, homeostasis and remodelling. Nature reviews. Molecular cell biology. 4, 517-529.

Birsoy, K., Chen, Z., Friedman, J., 2008. Transcriptional regulation of adipogenesis by KLF4. Cell metabolism. 7, 339-347.

Blake, B.E., Pinney, S.M., Hines, E.P., Fenton, S.E., Ferguson, K.K., 2018. Associations between longitudinal serum perfluoroalkyl substance (PFAS) levels and measures of thyroid hormone, kidney function, and body mass index in the Fernald Community Cohort. Environmental pollution. 242, 894-904.

Bloom, R.A., Matheson III, J.C., 1993. Environmental assessment of avermectins by the US Food and Drug Administration. Veterinary parasitology. 48, 281-294.

Bogdanska, J., Sundström, M., Bergström, U., Borg, D., Abedi-Valugerdi, M., Bergman, Å., DePierre, J., Nobel, S., 2014. Tissue distribution of 35S-labelled perfluorobutanesulfonic acid in adult mice following dietary exposure for 1–5 days. Chemosphere. 98, 28-36.

Bost, F., Aouadi, M., Caron, L., Even, P., Belmonte, N., Prot, M., Dani, C., Hofman, P., Pagès, G., Pouysségur, J., 2005. The extracellular signal–regulated kinase isoform ERK1 is specifically required for in vitro and in vivo adipogenesis. Diabetes. 54, 402-411.

Boulanger, B., Vargo, J.D., Schnoor, J.L., Hornbuckle, K.C., 2005. Evaluation of perfluorooctane surfactants in a wastewater treatment system and in a commercial surface protection product. Environmental science & technology. 39, 5524-5530.

Braun, J.M., Chen, A., Romano, M.E., Calafat, A.M., Webster, G.M., Yolton, K., Lanphear, B.P., 2016. Prenatal perfluoroalkyl substance exposure and child adiposity at 8 years of age: The HOME study. Obesity. 24, 231-237.

Brookes, P.S., Yoon, Y., Robotham, J.L., Anders, M.W., Sheu, S.S., 2004. Calcium, ATP, and ROS: a mitochondrial love-hate triangle. American journal of physiology. Cell physiology. 287, C817-833.

Buck, R.C., Franklin, J., Berger, U., Conder, J.M., Cousins, I.T., de Voogt, P., Jensen, A.A., Kannan, K., Mabury, S.A., van Leeuwen, S.P., 2011. Perfluoroalkyl and polyfluoroalkyl substances in the environment: terminology, classification, and origins. Integrated environmental assessment and management. 7, 513-541.

Butt, C.M., Muir, D.C., Mabury, S.A., 2014. Biotransformation pathways of fluorotelomer-based polyfluoroalkyl substances: a review. Environmental toxicology and chemistry. 33, 243-267.

Campbell, W., Fisher, M., Stapley, E., Albers-Schonberg, G., Jacob, T., 1983. Ivermectin: a potent new antiparasitic agent. Science. 221, 823-828.

Canga, A.G., Prieto, A.M.S., Liébana, M.J.D., Martínez, N.F., Vega, M.S., Vieitez, J.J.G., 2008. The pharmacokinetics and interactions of ivermectin in humans—a mini-review. The AAPS journal. 10, 42-46.

Cardenas, A., Gold, D.R., Hauser, R., Kleinman, K.P., Hivert, M.F., Calafat, A.M., Ye, X.Y., Webster, T.F., Horton, E.S., Oken, E., 2017. Plasma Concentrations of Per- and Polyfluoroalkyl Substances at Baseline and Associations with Glycemic Indicators and Diabetes Incidence among High-Risk Adults in the Diabetes Prevention Program Trial. Environmental Health Perspectives. 125.

Cardenas, A., Hauser, R., Gold, D.R., Kleinman, K.P., Hivert, M.-F., Fleisch, A.F., Lin, P.-I.D., Calafat, A.M., Webster, T.F., Horton, E.S., 2018. Association of Perfluoroalkyl and Polyfluoroalkyl Substances With Adiposity. JAMA network open. 1, e181493-e181493.

Cariou, B., 2008. The farnesoid X receptor (FXR) as a new target in non-alcoholic steatohepatitis. Diabetes & metabolism. 34, 685-691.

Cariou, B., van Harmelen, K., Duran-Sandoval, D., van Dijk, T.H., Grefhorst, A., Abdelkarim, M., Caron, S., Torpier, G., Fruchart, J.-C., Gonzalez, F.J., 2006. The farnesoid X receptor modulates adiposity and peripheral insulin sensitivity in mice. Journal of biological chemistry. 281, 11039-11049.

Carr, R.M., Reid, A.E., 2015. FXR agonists as therapeutic agents for non-alcoholic fatty liver disease. Current atherosclerosis reports. 17, 16.

Chang, E.T., Adami, H.O., Boffetta, P., Cole, P., Starr, T.B., Mandel, J.S., 2014. A critical review of perfluorooctanoate and perfluorooctanesulfonate exposure and cancer risk in humans. Critical reviews in toxicology. 44 Suppl 1, 1-81.

Chang, E.T., Adami, H.O., Boffetta, P., Wedner, H.J., Mandel, J.S., 2016. A critical review of perfluorooctanoate and perfluorooctanesulfonate exposure and immunological health conditions in humans. Critical reviews in toxicology. 46, 279-331.

Chawla, A., Schwarz, E.J., Dimaculangan, D.D., Lazar, M.A., 1994. Peroxisome proliferator-activated receptor (PPAR) gamma: adipose-predominant expression and induction early in adipocyte differentiation. Endocrinology. 135, 798-800.

Chen, W.L., Bai, F.Y., Chang, Y.C., Chen, P.C., Chen, C.Y., 2018. Concentrations of perfluoroalkyl substances in foods and the dietary exposure among Taiwan general population and pregnant women. Journal of food and drug analysis. 26, 994-1004.

Cheng, J., Lv, S., Nie, S., Liu, J., Tong, S., Kang, N., Xiao, Y., Dong, Q., Huang, C., Yang, D., 2016. Chronic perfluorooctane sulfonate (PFOS) exposure induces hepatic steatosis in zebrafish. Aquatic toxicology (Amsterdam, Netherlands). 176, 45-52.

Chicoine, A.L., Durden, D.A., MacNaughton, G., Dowling, P.M., 2007. Ivermectin use and resulting milk residues on 4 Canadian dairy herds. The canadian veterinary journal. 48, 836.

Christensen, K.Y., Raymond, M., Meiman, J., 2019. Perfluoroalkyl substances and metabolic syndrome. International journal of hygiene and environmental health. 222, 147-153.

Christensen, K.Y., Raymond, M., Thompson, B.A., Anderson, H.A., 2016. Perfluoroalkyl substances in older male anglers in Wisconsin. Environment International. 91, 312-318.

Chuderland, D., Seger, R., 2008. Calcium regulates ERK signaling by modulating its protein-protein interactions. Communicative & integrative biology. 1, 4-5.

Cipriani, S., Mencarelli, A., Palladino, G., Fiorucci, S., 2010. FXR activation reverses insulin resistance and lipid abnormalities and protects against liver steatosis in Zucker (fa/fa) obese rats. Journal of lipid research. 51, 771-784.

Conway, B., Innes, K.E., Long, D., 2016. Perfluoroalkyl substances and beta cell deficient diabetes. Journal of Diabetes and its Complications. 30, 993-998.

Costa, J., Diazgranados, J., 1994. Ivermectin for spasticity in spinal-cord injury. The lancet. 343, 739.

Crooks, S., Ross, P., Thompson, C., Haggan, S., Elliott, C., 2000. Detection of unwanted residues of ivermectin in bovine milk by dissociation-enhanced lanthanide fluoroimmunoassay. Luminescence. 15, 371-376.

Crooks, S.R., Baxter, A.G., McCaughey, W.J., 1998. Detection of ivermectin residues in bovine liver using an enzyme immunoassay. Analyst. 123, 355-358.

D'Eon J, C., Crozier, P.W., Furdui, V.I., Reiner, E.J., Libelo, E.L., Mabury, S.A., 2009. Perfluorinated phosphonic acids in Canadian surface waters and wastewater treatment plant effluent: discovery of a new class of perfluorinated acids. Environmental toxicology and chemistry. 28, 2101-2107.

D'eon, J.C., Hurley, M.D., Wallington, T.J., Mabury, S.A., 2006. Atmospheric chemistry of N-methyl perfluorobutane sulfonamidoethanol, C4F9SO2N (CH3) CH2CH2OH: Kinetics and mechanism of reaction with OH. Environmental science & technology. 40, 1862-1868.

Darrow, L.A., Groth, A.C., Winquist, A., Shin, H.-M., Bartell, S.M., Steenland, K., 2016. Modeled Perfluorooctanoic Acid (PFOA) Exposure and Liver Function in a Mid-Ohio Valley Community. Environmental health perspectives. 124, 1227-1233.

Das, K.P., Wood, C.R., Lin, M.T., Starkov, A.A., Lau, C., Wallace, K.B., Corton, J.C., Abbott, B.D., 2017. Perfluoroalkyl acids-induced liver steatosis: Effects on genes controlling lipid homeostasis. Toxicology. 378, 37-52.

de Cock, M., de Boer, M., Lamoree, M., Legler, J., van de Bor, M., 2014. First year growth in relation to prenatal exposure to endocrine disruptors—a Dutch prospective cohort study. International journal of environmental research and public health. 11, 7001-7021.

Dhami-Shah, H., Vaidya, R., Udipi, S., Raghavan, S., Abhijit, S., Mohan, V., Balasubramanyam, M., Vaidya, A., 2018. Picroside II attenuates fatty acid accumulation in HepG2 cells via modulation of fatty acid uptake and synthesis. Clinical and molecular hepatology. 24, 77-87.

Dinglasan, M.J., Ye, Y., Edwards, E.A., Mabury, S.A., 2004. Fluorotelomer alcohol biodegradation yields poly- and perfluorinated acids. Environmental science & technology. 38, 2857-2864.

Domazet, S.L., Grontved, A., Timmermann, A.G., Nielsen, F., Jensen, T.K., 2016. Longitudinal Associations of Exposure to Perfluoroalkylated Substances in Childhood and Adolescence and Indicators of Adiposity and Glucose Metabolism 6 and 12 Years Later: The European Youth Heart Study. Diabetes Care. 39, 1745-1751.

Donat-Vargas, C., Bergdahl, I.A., Tornevi, A., Wennberg, M., Sommar, J., Kiviranta, H., Koponen, J., Rolandsson, O., Åkesson, A., 2019. Perfluoroalkyl substances and risk of type II diabetes: A prospective nested case-control study. Environment International. 123, 390-398.

Dourmishev, A., Serafimova, D., Dourmishev, L., 1998. Efficacy and tolerance of oral ivermectin in scabies. Journal of the European Academy of Dermatology and Venereology. 11, 247-251.

Ebnesajjad, S., 2013. 7 - Manufacturing Polytetrafluoroethylene, in: S. Ebnesajjad (Ed.), Introduction to Fluoropolymers. William Andrew Publishing, Oxford, pp. 91-124.

Edwards, G., Dingsdale, A., Helsby, N., Orme, M.E., Breckenridge, A., 1988. The relative systemic availability of ivermectin after administration as capsule, tablet, and oral solution. European journal of clinical pharmacology. 35, 681-684.

Egeghy, P.P., Lorber, M., 2010. An assessment of the exposure of Americans to perfluorooctane sulfonate: A comparison of estimated intake with values inferred from NHANES data. Journal Of Exposure Science And Environmental Epidemiology. 21, 150.

Emmett, E.A., Shofer, F.S., Zhang, H., Freeman, D., Desai, C., Shaw, L.M., 2006. Community exposure to perfluorooctanoate: relationships between serum concentrations and exposure sources. Journal of occupational and environmental medicine. 48, 759-770.

EPA, 2014. Provisional Peer-Reviewed Toxicity Values for Perfluorobutane Sulfonate (CASRN 375-73-5) and Related Compound Potassium Perfluorobutane Sulfonate (CASRN 29420-49-3).

Eriksen, K.T., Raaschou-Nielsen, O., Sorensen, M., Roursgaard, M., Loft, S., Moller, P., 2010. Genotoxic potential of the perfluorinated chemicals PFOA, PFOS, PFBS, PFNA and PFHxA in human HepG2 cells. Mutation research. 700, 39-43.

Fajas, L., Schoonjans, K., Gelman, L., Kim, J.B., Najib, J., Martin, G., Fruchart, J.-C., Briggs, M., Spiegelman, B.M., Auwerx, J., 1999. Regulation of peroxisome proliferator-activated receptor γ expression by adipocyte differentiation and determination factor 1/sterol regulatory element binding protein 1: implications for adipocyte differentiation and metabolism. Molecular and cellular biology. 19, 5495-5503.

Favreau, P., Poncioni-Rothlisberger, C., Place, B.J., Bouchex-Bellomie, H., Weber, A., Tremp, J., Field, J.A., Kohler, M., 2017. Multianalyte profiling of per- and polyfluoroalkyl substances (PFASs) in liquid commercial products. Chemosphere. 171, 491-501.

Fei, C., McLaughlin, J.K., Tarone, R.E., Olsen, J., 2007. Perfluorinated chemicals and fetal growth: a study within the Danish National Birth Cohort. Environ Health Perspect. 115, 1677-1682.

Feldstein, A.E., Wieckowska, A., Lopez, A.R., Liu, Y.C., Zein, N.N., McCullough, A.J., 2009. Cytokeratin-18 fragment levels as noninvasive biomarkers for nonalcoholic steatohepatitis: a multicenter validation study. Hepatology (Baltimore, Md.). 50, 1072-1078.

Fisher, M., Arbuckle, T.E., Wade, M., Haines, D.A., 2013. Do perfluoroalkyl substances affect metabolic function and plasma lipids?--Analysis of the 2007-2009, Canadian Health Measures Survey (CHMS) Cycle 1. Environ Res. 121, 95-103.

Fitz-Simon, N., Fletcher, T., Luster, M.I., Steenland, K., Calafat, A.M., Kato, K., Armstrong, B., 2013. Reductions in serum lipids with a 4-year decline in serum perfluorooctanoic acid and perfluorooctanesulfonic acid. Epidemiology. 24, 569-576.

Fleisch, A.F., Rifas-Shiman, S.L., Mora, A.M., Calafat, A.M., Ye, X.Y., Luttmann-Gibson, H., Gillman, M.W., Oken, E., Sagiv, S.K., 2017. Early-Life Exposure to Perfluoroalkyl Substances and Childhood Metabolic Function. Environmental Health Perspectives. 125, 481-487.

Fletcher, T., Galloway, T.S., Melzer, D., Holcroft, P., Cipelli, R., Pilling, L.C., Mondal, D., Luster, M., Harries, L.W., 2013. Associations between PFOA, PFOS and changes in the expression of genes involved in cholesterol metabolism in humans. Environ Int. 57-58, 2-10.

Fraser, A.J., Webster, T.F., Watkins, D.J., Nelson, J.W., Stapleton, H.M., Calafat, A.M., Kato, K., Shoeib, M., Vieira, V.M., McClean, M.D., 2012. Polyfluorinated compounds in serum linked to indoor air in office environments. Environmental science & technology. 46, 1209-1215.

Frömel, T., Knepper, T.P., 2010. Biodegradation of Fluorinated Alkyl Substances, in: P. De Voogt (Ed.), Reviews of Environmental Contamination and Toxicology Volume 208: Perfluorinated alkylated substances. Springer New York, New York, NY, pp. 161-177.

Fromme, H., Tittlemier, S.A., Volkel, W., Wilhelm, M., Twardella, D., 2009. Perfluorinated compounds--exposure assessment for the general population in Western countries. Int J Hyg Environ Health. 212, 239-270.

Fu, J., Gao, Y., Wang, T., Liang, Y., Zhang, A., Wang, Y., Jiang, G., 2015. Elevated levels of perfluoroalkyl acids in family members of occupationally exposed workers: the importance of dust transfer. Scientific reports. 5, 9313.

Gallo, V., Leonardi, G., Genser, B., Lopez-Espinosa, M.J., Frisbee, S.J., Karlsson, L., Ducatman, A.M., Fletcher, T., 2012. Serum perfluorooctanoate (PFOA) and perfluorooctane

sulfonate (PFOS) concentrations and liver function biomarkers in a population with elevated PFOA exposure. Environ Health Perspect. 120, 655-660.

Gebbink, W.A., Berger, U., Cousins, I.T., 2015. Estimating human exposure to PFOS isomers and PFCA homologues: the relative importance of direct and indirect (precursor) exposure. Environ Int. 74, 160-169.

Gerlier, D., Thomasset, N., 1986. Use of MTT colorimetric assay to measure cell activation. Journal of immunological methods. 94, 57-63.

Gleason, J.A., Post, G.B., Fagliano, J.A., 2015. Associations of perfluorinated chemical serum concentrations and biomarkers of liver function and uric acid in the US population (NHANES), 2007-2010. Environ Res. 136, 8-14.

Glynn, A., Berger, U., Bignert, A., Ullah, S., Aune, M., Lignell, S., Darnerud, P.O., 2012. Perfluorinated alkyl acids in blood serum from primiparous women in Sweden: serial sampling during pregnancy and nursing, and temporal trends 1996-2010. Environmental science & technology. 46, 9071-9079.

Grygiel-Górniak, B., 2014. Peroxisome proliferator-activated receptors and their ligands: nutritional and clinical implications--a review. Nutr J. 13, 17-17.

Guelfo, J.L., Adamson, D.T., 2018. Evaluation of a national data set for insights into sources, composition, and concentrations of per- and polyfluoroalkyl substances (PFASs) in U.S. drinking water. Environmental pollution (Barking, Essex : 1987). 236, 505-513.

Gupta, R.K., Arany, Z., Seale, P., Mepani, R.J., Ye, L., Conroe, H.M., Roby, Y.A., Kulaga, H., Reed, R.R., Spiegelman, B.M., 2010. Transcriptional control of preadipocyte determination by Zfp423. Nature. 464, 619.

Guzzo, C.A., Furtek, C.I., Porras, A.G., Chen, C., Tipping, R., Clineschmidt, C.M., Sciberras, D.G., Hsieh, J.Y.K., Lasseter, K.C., 2002. Safety, tolerability, and pharmacokinetics of escalating high doses of ivermectin in healthy adult subjects. The journal of clinical pharmacology. 42, 1122-1133.

Hagen, D.F., Belisle, J., Johnson, J.D., Venkateswarlu, P., 1981. Characterization of fluorinated metabolites by a gas chromatographic-helium microwave plasma detector--the biotransformation of 1H, 1H, 2H, 2H-perfluorodecanol to perfluorooctanoate. Analytical biochemistry. 118, 336-343.

Halldorsson, T.I., Rytter, D., Haug, L.S., Bech, B.H., Danielsen, I., Becher, G., Henriksen, T.B., Olsen, S.F., 2012. Prenatal exposure to perfluorooctanoate and risk of overweight at 20 years of age: a prospective cohort study. Environmental health perspectives. 120, 668-673.

Harrad, S., de Wit, C.A., Abdallah, M.A.-E., Bergh, C., Björklund, J.A., Covaci, A., Darnerud, P.O., de Boer, J., Diamond, M., Huber, S., Leonards, P., Mandalakis, M., Östman, C., Haug, L.S., Thomsen, C., Webster, T.F., 2010. Indoor Contamination with Hexabromocyclododecanes, Polybrominated Diphenyl Ethers, and Perfluoroalkyl Compounds: An Important Exposure Pathway for People? Environmental science & technology. 44, 3221-3231.

Hartman, T.J., Calafat, A.M., Holmes, A.K., Marcus, M., Northstone, K., Flanders, W.D., Kato, K., Taylor, E.V., 2017. Prenatal exposure to perfluoroalkyl substances and body fatness in girls. Childhood Obesity. 13, 222-230.

Haug, L.S., Huber, S., Becher, G., Thomsen, C., 2011. Characterisation of human exposure pathways to perfluorinated compounds — Comparing exposure estimates with biomarkers of exposure. Environment International. 37, 687-693.

He, L., Deng, L., Zhang, Q., Guo, J., Zhou, J., Song, W., Yuan, F., 2017. Diagnostic Value of CK-18, FGF-21, and Related Biomarker Panel in Nonalcoholic Fatty Liver Disease: A Systematic Review and Meta-Analysis. BioMed research international. 2017, 9729107.

He, X.W., Liu, Y.X., Xu, B., Gu, L.B., Tang, W., 2018. PFOA is associated with diabetes and metabolic alteration in US men: National Health and Nutrition Examination Survey 2003-2012. Science of the Total Environment. 625, 566-574.

Heindel, J.J., Skalla, L.A., Joubert, B.R., Dilworth, C.H., Gray, K.A., 2017. Review of developmental origins of health and disease publications in environmental epidemiology. Reproductive toxicology (Elmsford, N.Y.). 68, 34-48.

Henderson, W.M., Smith, M.A., 2007. Perfluorooctanoic acid and perfluorononanoic acid in fetal and neonatal mice following in utero exposure to 8-2 fluorotelomer alcohol. Toxicological sciences : an official journal of the Society of Toxicology. 95, 452-461.

Herzke, D., Olsson, E., Posner, S., 2012. Perfluoroalkyl and polyfluoroalkyl substances (PFASs) in consumer products in Norway - a pilot study. Chemosphere. 88, 980-987.

Hoffman, K., Webster, T.F., Bartell, S.M., Weisskopf, M.G., Fletcher, T., Vieira, V.M., 2011. Private drinking water wells as a source of exposure to perfluorooctanoic acid (PFOA) in communities surrounding a fluoropolymer production facility. Environ Health Perspect. 119, 92-97.

Hölzer, J., Midasch, O., Rauchfuss, K., Kraft, M., Reupert, R., Angerer, J., Kleeschulte, P., Marschall, N., Wilhelm, M., 2008. Biomonitoring of perfluorinated compounds in children and adults exposed to perfluorooctanoate-contaminated drinking water. Environmental health perspectives. 116, 651-657.

Houtz, E.F., Sutton, R., Park, J.S., Sedlak, M., 2016. Poly- and perfluoroalkyl substances in wastewater: Significance of unknown precursors, manufacturing shifts, and likely AFFF impacts. Water research. 95, 142-149.

Howard, P.H., Muir, D.C., 2010. Identifying new persistent and bioaccumulative organics among chemicals in commerce. Environmental science & technology. 44, 2277-2285.

Høyer, B.B., Ramlau-Hansen, C.H., Vrijheid, M., Valvi, D., Pedersen, H.S., Zviezdai, V., Jönsson, B.A., Lindh, C.H., Bonde, J.P., Toft, G., 2015. Anthropometry in 5-to 9-year-old Greenlandic and Ukrainian children in relation to prenatal exposure to perfluorinated alkyl substances. Environmental health perspectives. 123, 841-846.

Hu, X.C., Andrews, D.Q., Lindstrom, A.B., Bruton, T.A., Schaider, L.A., Grandjean, P., Lohmann, R., Carignan, C.C., Blum, A., Balan, S.A., Higgins, C.P., Sunderland, E.M., 2016. Detection of Poly- and Perfluoroalkyl Substances (PFASs) in U.S. Drinking Water Linked to Industrial Sites, Military Fire Training Areas, and Wastewater Treatment Plants. Environmental science & technology letters. 3, 344-350.

Huang, K.-P., 1989. The mechanism of protein kinase C activation. Trends in neurosciences. 12, 425-432.

Huck, I., Beggs, K., Apte, U., 2018. Paradoxical Protective Effect of Perfluorooctanesulfonic Acid Against High-Fat Diet-Induced Hepatic Steatosis in Mice. International journal of toxicology. 37, 383-392.

Hwang, H.-H., Moon, P.-G., Lee, J.-E., Kim, J.-G., Lee, W., Ryu, S.-H., Baek, M.-C., 2011. Identification of the target proteins of rosiglitazone in 3T3-L1 adipocytes through proteomic analysis of cytosolic and secreted proteins. Molecules and cells. 31, 239-246.

Inoue, K., Okada, F., Ito, R., Kato, S., Sasaki, S., Nakajima, S., Uno, A., Saijo, Y., Sata, F., Yoshimura, Y., Kishi, R., Nakazawa, H., 2004. Perfluorooctane sulfonate (PFOS) and related perfluorinated compounds in human maternal and cord blood samples: assessment of PFOS exposure in a susceptible population during pregnancy. Environ Health Perspect. 112, 1204-1207.

Inoue, M., Ohtake, T., Motomura, W., Takahashi, N., Hosoki, Y., Miyoshi, S., Suzuki, Y., Saito, H., Kohgo, Y., Okumura, T., 2005. Increased expression of PPARgamma in high fat diet-induced liver steatosis in mice. Biochem Biophys Res Commun. 336, 215-222.

Jaacks, L., Boyd Barr, D., Sundaram, R., Grewal, J., Zhang, C., Buck Louis, G., 2016. Pre-pregnancy maternal exposure to persistent organic pollutants and gestational weight gain: a prospective cohort study. International journal of environmental research and public health. 13, 905.

Jain, R.B., 2018a. Contribution of diet and other factors to the observed levels of selected perfluoroalkyl acids in serum among US children aged 3-11 years. Environ Res. 161, 268-275.

Jain, R.B., 2018b. Time trends over 2003–2014 in the concentrations of selected perfluoroalkyl substances among US adults aged ≥20 years: Interpretational issues. Science of The Total Environment. 645, 946-957.

Jain, R.B., Ducatman, A., 2019. Roles of gender and obesity in defining correlations between perfluoroalkyl substances and lipid/lipoproteins. Science of The Total Environment. 653, 74-81.

Jensen, R.C., Glintborg, D., Timmermann, C.A.G., Nielsen, F., Kyhl, H.B., Andersen, H.R., Grandjean, P., Jensen, T.K., Andersen, M., 2018. Perfluoroalkyl substances and glycemic status in pregnant Danish women: The Odense Child Cohort. Environ Int. 116, 101-107.

Jimenez, M.A., Åkerblad, P., Sigvardsson, M., Rosen, E.D., 2007. Critical role for Ebf1 and Ebf2 in the adipogenic transcriptional cascade. Molecular and cellular biology. 27, 743-757.

Jin, L., Feng, X., Rong, H., Pan, Z., Inaba, Y., Qiu, L., Zheng, W., Lin, S., Wang, R., Wang, Z., 2013. The antiparasitic drug ivermectin is a novel FXR ligand that regulates metabolism. Nature communications. 4, 1937.

Jin, L., Wang, R., Zhu, Y., Zheng, W., Han, Y., Guo, F., Ye, F.B., Li, Y., 2015. Selective targeting of nuclear receptor FXR by avermectin analogues with therapeutic effects on nonalcoholic fatty liver disease. Scientific reports. 5, 17288.

Joensen, U.N., Bossi, R., Leffers, H., Jensen, A.A., Skakkebæk, N.E., Jørgensen, N., 2009. Do perfluoroalkyl compounds impair human semen quality? Environmental health perspectives. 117, 923.

Jones, J.R., Barrick, C., Kim, K.-A., Lindner, J., Blondeau, B., Fujimoto, Y., Shiota, M., Kesterson, R.A., Kahn, B.B., Magnuson, M.A., 2005. Deletion of PPARγ in adipose

tissues of mice protects against high fat diet-induced obesity and insulin resistance. Proceedings of the national academy of sciences. 102, 6207-6212.

Kadowaki, T., Hara, K., Kubota, N., Tobe, K., Terauchi, Y., Yamauchi, T., Eto, K., Kadowaki, H., Noda, M., Hagura, R., 2002. The role of PPARγ in high-fat diet-induced obesity and insulin resistance. Journal of diabetes and its complications. 16, 41-45.

Kang, H., Choi, K., Lee, H.S., Kim, D.H., Park, N.Y., Kim, S., Kho, Y., 2016. Elevated levels of short carbon-chain PFCAs in breast milk among Korean women: Current status and potential challenges. Environ Res. 148, 351-359.

Karlsen, M., Grandjean, P., Weihe, P., Steuerwald, U., Oulhote, Y., Valvi, D., 2017. Early-life exposures to persistent organic pollutants in relation to overweight in preschool children. Reproductive Toxicology. 68, 145-153.

Karnes, C., Winquist, A., Steenland, K., 2014. Incidence of type II diabetes in a cohort with substantial exposure to perfluorooctanoic acid. Environ. Res. 128, 78-83.

Karsa, D.R., 1995. Fluorinated surfactants: synthesis properties applications, by Erik Kissa. Marcel Dekker Inc., New York, 1994, pp. vii + 469, price US$165.00. ISBN 0-8247-9011-1. Polymer International. 36, 101-101.

Khalil, N., Ebert, J.R., Honda, M., Lee, M., Nahhas, R.W., Koskela, A., Hangartner, T., Kannan, K., 2018. Perfluoroalkyl substances, bone density, and cardio-metabolic risk factors in obese 8-12 year old children: A pilot study. Environ. Res. 160, 314-321.

Khansari, M.R., Yousefsani, B.S., Kobarfard, F., Faizi, M., Pourahmad, J., 2017. In vitro toxicity of perfluorooctane sulfonate on rat liver hepatocytes: probability of distructive binding to CYP 2E1 and involvement of cellular proteolysis. Environmental science and pollution research international. 24, 23382-23388.

Kim, J., Park, Y., Yoon, K.S., Clark, J.M., Park, Y., 2014. Permethrin Alters Adipogenesis in 3T3-L1 Adipocytes and Causes Insulin Resistance in C2C12 Myotubes. Journal of biochemical and molecular toxicology. 28, 418-424.

Kim, J., Sun, Q., Yue, Y., Yoon, K.S., Whang, K.-Y., Clark, J.M., Park, Y., 2016a. 4, 4′-Dichlorodiphenyltrichloroethane (DDT) and 4, 4′-dichlorodiphenyldichloroethylene (DDE) promote adipogenesis in 3T3-L1 adipocyte cell culture. Pesticide biochemistry and physiology. 131, 40-45.

Kim, J.H., Park, H.Y., Jeon, J.D., Kho, Y., Kim, S.K., Park, M.S., Hong, Y.C., 2016b. The modifying effect of vitamin C on the association between perfluorinated compounds and insulin resistance in the Korean elderly: a double-blind, randomized, placebo-controlled crossover trial. Eur. J. Nutr. 55, 1011-1020.

Kim, M.J., Moon, S., Oh, B.C., Jung, D., Ji, K., Choi, K., Park, Y.J., 2018. Association between perfluoroalkyl substances exposure and thyroid function in adults: A meta-analysis. PloS one. 13, e0197244.

Konig, S., Beguet, A., Bader, C.R., Bernheim, L., 2006. The calcineurin pathway links hyperpolarization (Kir2.1)-induced Ca2+ signals to human myoblast differentiation and fusion. Development (Cambridge, England). 133, 3107-3114.

Koshy, T.T., Attina, T.M., Ghassabian, A., Gilbert, J., Burdine, L.K., Marmor, M., Honda, M., Chu, D.B., Han, X.X., Shao, Y.Z., Kannan, K., Urbina, E.M., Trasande, L., 2017. Serum perfluoroalkyl substances and cardiometabolic consequences in adolescents exposed to the World Trade Center disaster and a matched comparison group. Environment International. 109, 128-135.

Lam, J.C., Lyu, J., Kwok, K.Y., Lam, P.K., 2016. Perfluoroalkyl Substances (PFASs) in Marine Mammals from the South China Sea and Their Temporal Changes 2002-2014: Concern for Alternatives of PFOS? Environmental science & technology. 50, 6728-6736.

Lanusse, C., Lifschitz, A., Virkel, G., Alvarez, L., Sanchez, S., Sutra, J., Galtier, P., Alvinerie, M., 1997. Comparative plasma disposition kinetics of ivermectin, moxidectin and doramectin in cattle. Journal of veterinary pharmacology and therapeutics. 20, 91-99.

Lau, C., Butenhoff, J.L., Rogers, J.M., 2004. The developmental toxicity of perfluoroalkyl acids and their derivatives. Toxicology and applied pharmacology. 198, 231-241.

Lauritzen, H.B., Larose, T.L., Øien, T., Sandanger, T.M., Odland, J.Ø., Van de Bor, M., Jacobsen, G.W., 2018. Prenatal exposure to persistent organic pollutants and child overweight/obesity at 5-year follow-up: a prospective cohort study. Environmental Health. 17, 9.

Lebeaupin, C., Vallee, D., Hazari, Y., Hetz, C., Chevet, E., Bailly-Maitre, B., 2018. Endoplasmic reticulum stress signalling and the pathogenesis of non-alcoholic fatty liver disease. Journal of hepatology. 69, 927-947.

LeBel, C.P., Ischiropoulos, H., Bondy, S.C., 1992. Evaluation of the probe 2',7'-dichlorofluorescin as an indicator of reactive oxygen species formation and oxidative stress. Chem Res Toxicol. 5, 227-231.

Lee, H., Mabury, S.A., 2011. A Pilot Survey of Legacy and Current Commercial Fluorinated Chemicals in Human Sera from United States Donors in 2009. Environmental science & technology. 45, 8067-8074.

Lee, S., Kim, S., Park, J., Kim, H.J., Choi, G., Choi, S., Kim, S., Kim, S.Y., Kim, S., Choi, K., Moon, H.B., 2018. Perfluoroalkyl substances (PFASs) in breast milk from Korea: Time-course trends, influencing factors, and infant exposure. The Science of the total environment. 612, 286-292.

Lee, Y.J., Choi, S.-Y., Yang, J.-H., 2014. PFHxS induces apoptosis of neuronal cells via ERK1/2-mediated pathway. Chemosphere. 94, 121-127.

Lee, Y.J., Lee, H.-G., Yang, J.-H., 2013. Perfluorooctane sulfonate-induced apoptosis of cerebellar granule cells is mediated by ERK 1/2 pathway. Chemosphere. 90, 1597-1602.

Lehmler, H.J., 2005. Synthesis of environmentally relevant fluorinated surfactants--a review. Chemosphere. 58, 1471-1496.

Lemal, D.M., 2004. Perspective on fluorocarbon chemistry. J. Org. Chem. 69, 1-11.

Leonard, R.C., Kreckmann, K.H., Sakr, C.J., Symons, J.M., 2008. Retrospective cohort mortality study of workers in a polymer production plant including a reference population of regional workers. Annals of epidemiology. 18, 15-22.

Lespine, A., Alvinerie, M., Sutra, J.-F., Pors, I., Chartier, C., 2005. Influence of the route of administration on efficacy and tissue distribution of ivermectin in goat. Veterinary parasitology. 128, 251-260.

Li, Y., Fletcher, T., Mucs, D., Scott, K., Lindh, C.H., Tallving, P., Jakobsson, K., 2018. Half-lives of PFOS, PFHxS and PFOA after end of exposure to contaminated drinking water. Occup Environ Med. 75, 46-51.

Lieder, P.H., Chang, S.-C., York, R.G., Butenhoff, J.L., 2009. Toxicological evaluation of potassium perfluorobutanesulfonate in a 90-day oral gavage study with Sprague–Dawley rats. Toxicology. 255, 45-52.

Lin, C.Y., Chen, P.C., Lin, Y.C., Lin, L.Y., 2009. Association Among Serum Perfluoroalkyl Chemicals, Glucose Homeostasis, and Metabolic Syndrome in Adolescents and Adults. Diabetes Care. 32, 702-707.

Lind, L., Zethelius, B., Salihovic, S., van Bavel, B., Lind, P.M., 2014. Circulating levels of perfluoroalkyl substances and prevalent diabetes in the elderly. Diabetologia. 57, 473-479.

Liu, G., Dhana, K., Furtado, J.D., Rood, J., Zong, G., Liang, L., Qi, L., Bray, G.A., DeJonge, L., Coull, B., 2018a. Perfluoroalkyl substances and changes in body weight and resting metabolic rate in response to weight-loss diets: A prospective study. PLoS medicine. 15, e1002502.

Liu, H.S., Wen, L.L., Chu, P.L., Lin, C.Y., 2018b. Association among total serum isomers of perfluorinated chemicals, glucose homeostasis, lipid profiles, serum protein and metabolic syndrome in adults: NHANES, 2013-2014. Environmental pollution (Barking, Essex : 1987). 232, 73-79.

Liu, X., Jin, Y., Liu, W., Wang, F., Hao, S., 2011. Possible mechanism of perfluorooctane sulfonate and perfluorooctanoate on the release of calcium ion from calcium stores in primary cultures of rat hippocampal neurons. Toxicology in vitro. 25, 1294-1301.

Liu, X., Zhang, L., Chen, L., Li, J., Wang, Y., Wang, J., Meng, G., Chi, M., Zhao, Y., Chen, H., Wu, Y., 2019. Structure-based investigation on the association between perfluoroalkyl acids exposure and both gestational diabetes mellitus and glucose homeostasis in pregnant women. Environ Int. 127, 85-93.

Livak, K.J., Schmittgen, T.D., 2001. Analysis of relative gene expression data using real-time quantitative PCR and the 2− ΔΔCT method. Methods. 25, 402-408.

Lopez, Y.R., Perez-Torres, I., Zuniga-Munoz, A., Lans, V.G., Diaz-Diaz, E., Castro, E.S., Espejel, R.V., 2016. Effect of Glycine on Adipocyte Hypertrophy in a Metabolic Syndrome Rat Model. Current drug delivery. 13, 158-169.

Lundin, J.I., Alexander, B.H., Olsen, G.W., Church, T.R., 2009. Ammonium perfluorooctanoate production and occupational mortality. Epidemiology. 921-928.

Lynagh, T., Lynch, J.W., 2010. An improved ivermectin-activated chloride channel receptor for inhibiting electrical activity in defined neuronal populations. Journal of Biological Chemistry. 285, 14890-14897.

Macheka-Tendenguwo, L.R., Olowoyo, J.O., Mugivhisa, L.L., Abafe, O.A., 2018. Per- and polyfluoroalkyl substances in human breast milk and current analytical methods. Environmental science and pollution research international. 25, 36064-36086.

MacNeil, J., Steenland, N.K., Shankar, A., Ducatman, A., 2009. A cross-sectional analysis of type II diabetes in a community with exposure to perfluorooctanoic acid (PFOA). Environ. Res. 109, 997-1003.

Maisonet, M., Terrell, M.L., McGeehin, M.A., Christensen, K.Y., Holmes, A., Calafat, A.M., Marcus, M., 2012. Maternal concentrations of polyfluoroalkyl compounds during

pregnancy and fetal and postnatal growth in British girls. Environmental health perspectives. 120, 1432-1437.

Malhotra, J.D., Kaufman, R.J., 2007. The endoplasmic reticulum and the unfolded protein response. Seminars in cell & developmental biology. 18, 716-731.

Mancini, F.R., Rajaobelina, K., Praud, D., Dow, C., Antignac, J.P., Kvaskoff, M., Severi, G., Bonnet, F., Boutron-Ruault, M.C., Fagherazzi, G., 2018. Nonlinear associations between dietary exposures to perfluorooctanoic acid (PFOA) or perfluorooctane sulfonate (PFOS) and type 2 diabetes risk in women: Findings from the E3N cohort study. Int J Hyg Environ Health. 221, 1054-1060.

Martin, J.W., Mabury, S.A., O'Brien, P.J., 2005. Metabolic products and pathways of fluorotelomer alcohols in isolated rat hepatocytes. Chemico-biological interactions. 155, 165-180.

Martinez-Moral, M.P., Tena, M.T., 2012. Determination of perfluorocompounds in popcorn packaging by pressurised liquid extraction and ultra-performance liquid chromatography-tandem mass spectrometry. Talanta. 101, 104-109.

Marty, F.M., Lowry, C.M., Rodriguez, M., Milner, D.A., Pieciak, W.S., Sinha, A., Fleckenstein, L., Baden, L.R., 2005. Treatment of human disseminated strongyloidiasis with a parenteral veterinary formulation of ivermectin. Clinical infectious diseases. 41, e5-e8.

Masarone, M., Rosato, V., Dallio, M., Gravina, A.G., Aglitti, A., Loguercio, C., Federico, A., Persico, M., 2018. Role of Oxidative Stress in Pathophysiology of Nonalcoholic Fatty Liver Disease. Oxid Med Cell Longev. 2018, 9547613-9547613.

Matilla-Santander, N., Valvi, D., Lopez-Espinosa, M.J., Manzano-Salgado, C.B., Ballester, F., Ibarluzea, J., Santa-Marina, L., Schettgen, T., Guxens, M., Sunyer, J., Vrijheid, M., 2017. Exposure to Perfluoroalkyl Substances and Metabolic Outcomes in Pregnant Women: Evidence from the Spanish INMA Birth Cohorts. Environ Health Perspect. 125, 117004.

McCarty, M.F., Barroso-Aranda, J., Contreras, F., 2009. The hyperpolarizing impact of glycine on endothelial cells may be anti-atherogenic. Medical hypotheses. 73, 263-264.

Melotti, A., Mas, C., Kuciak, M., Lorente-Trigos, A., Borges, I., i Altaba, A.R., 2014. The river blindness drug Ivermectin and related macrocyclic lactones inhibit WNT-TCF pathway responses in human cancer. EMBO molecular medicine. 6, 1263-1278.

Midasch, O., Drexler, H., Hart, N., Beckmann, M.W., Angerer, J., 2007. Transplacental exposure of neonates to perfluorooctanesulfonate and perfluorooctanoate: a pilot study. International archives of occupational and environmental health. 80, 643-648.

Mora, A.M., Oken, E., Rifas-Shiman, S.L., Webster, T.F., Gillman, M.W., Calafat, A.M., Ye, X., Sagiv, S.K., 2016. Prenatal exposure to perfluoroalkyl substances and adiposity in early and mid-childhood. Environmental health perspectives. 125, 467-473.

Mori, T., Sakaue, H., Iguchi, H., Gomi, H., Okada, Y., Takashima, Y., Nakamura, K., Nakamura, T., Yamauchi, T., Kubota, N., 2005. Role of Krüppel-like factor 15 (KLF15) in transcriptional regulation of adipogenesis. Journal of biological chemistry. 280, 12867-12875.

Neal, J.W., Clipstone, N.A., 2002. Calcineurin mediates the calcium-dependent inhibition of adipocyte differentiation in 3T3-L1 cells. Journal of biological chemistry. 277, 49776-49781.

Nelson, J.W., Hatch, E.E., Webster, T.F., 2010. Exposure to polyfluoroalkyl chemicals and cholesterol, body weight, and insulin resistance in the general US population. Environmental health perspectives. 118, 197-202.

Nian, M., Li, Q.-Q., Bloom, M., Qian, Z., Syberg, K.M., Vaughn, M.G., Wang, S.-Q., Wei, Q., Zeeshan, M., Gurram, N., Chu, C., Wang, J., Tian, Y.-P., Hu, L.-W., Liu, K.-K., Yang, B.-Y., Liu, R.-Q., Feng, D., Zeng, X.-W., Dong, G.-H., 2019. Liver function biomarkers disorder is associated with exposure to perfluoroalkyl acids in adults: Isomers of C8 Health Project in China. Environ. Res. 172, 81-88.

Nyberg, E., Awad, R., Bignert, A., Ek, C., Sallsten, G., Benskin, J.P., 2018. Inter-individual, inter-city, and temporal trends of per- and polyfluoroalkyl substances in human milk from Swedish mothers between 1972 and 2016. Environmental science. Processes & impacts. 20, 1136-1147.

Oh, J.H., Kim, E.-Y., Choi, Y.H., Nam, T.-J., 2017. Negative regulation of ERK1/2 by PI3K is required for the protective effects of Pyropia yezoensis peptide against perfluorooctane sulfonate-induced endoplasmic reticulum stress. Mol Med Rep. 15, 2583-2587.

Oishi, Y., Manabe, I., Tobe, K., Tsushima, K., Shindo, T., Fujiu, K., Nishimura, G., Maemura, K., Yamauchi, T., Kubota, N., 2005. Krüppel-like transcription factor KLF5 is a key regulator of adipocyte differentiation. Cell metabolism. 1, 27-39.

Okada, E., Kashino, I., Matsuura, H., Sasaki, S., Miyashita, C., Yamamoto, J., Ikeno, T., Ito, Y.M., Matsumura, T., Tamakoshi, A., Kishi, R., 2013. Temporal trends of perfluoroalkyl acids in plasma samples of pregnant women in Hokkaido, Japan, 2003–2011. Environment International. 60, 89-96.

Olsen, G.W., Burris, J.M., Ehresman, D.J., Froehlich, J.W., Seacat, A.M., Butenhoff, J.L., Zobel, L.R., 2007. Half-life of serum elimination of perfluorooctanesulfonate,perfluorohexanesulfonate, and perfluorooctanoate in retired fluorochemical production workers. Environmental health perspectives. 115, 1298-1305.

Olsen, G.W., Chang, S.-C., Noker, P.E., Gorman, G.S., Ehresman, D.J., Lieder, P.H., Butenhoff, J.L., 2009a. A comparison of the pharmacokinetics of perfluorobutanesulfonate (PFBS) in rats, monkeys, and humans. Toxicology. 256, 65-74.

Olsen, G.W., Chang, S.C., Noker, P.E., Gorman, G.S., Ehresman, D.J., Lieder, P.H., Butenhoff, J.L., 2009b. A comparison of the pharmacokinetics of perfluorobutanesulfonate (PFBS) in rats, monkeys, and humans. Toxicology. 256, 65-74.

Olsen, G.W., Lange, C.C., Ellefson, M.E., Mair, D.C., Church, T.R., Goldberg, C.L., Herron, R.M., Medhdizadehkashi, Z., Nobiletti, J.B., Rios, J.A., Reagen, W.K., Zobel, L.R.,

2012. Temporal Trends of Perfluoroalkyl Concentrations in American Red Cross Adult Blood Donors, 2000–2010. Environmental science & technology. 46, 6330-6338.

Orton, R.J., Sturm, O.E., Vyshemirsky, V., Calder, M., Gilbert, D.R., Kolch, W., 2005. Computational modelling of the receptor-tyrosine-kinase-activated MAPK pathway. Biochemical journal. 392, 249-261.

Papadopoulou, E., Poothong, S., Koekkoek, J., Lucattini, L., Padilla-Sanchez, J.A., Haugen, M., Herzke, D., Valdersnes, S., Maage, A., Cousins, I.T., Leonards, P.E.G., Smastuen Haug, L., 2017. Estimating human exposure to perfluoroalkyl acids via solid food and drinks: Implementation and comparison of different dietary assessment methods. Environ Res. 158, 269-276.

Park, Y., Kim, Y., Kim, J., Yoon, K.S., Clark, J., Lee, J., Park, Y., 2012. Imidacloprid, a neonicotinoid insecticide, potentiates adipogenesis in 3T3-L1 adipocytes. Journal of agricultural and food chemistry. 61, 255-259.

Patel, C.J., Cullen, M.R., Ioannidis, J.P., Butte, A.J., 2012. Systematic evaluation of environmental factors: persistent pollutants and nutrients correlated with serum lipid levels. International Journal of Epidemiology. 41, 828-843.

Pei, H., Yao, Y., Yang, Y., Liao, K., Wu, J., 2011. Krüppel-like factor KLF9 regulates PPARγ transactivation at the middle stage of adipogenesis. Cell death and differentiation. 18, 315.

Pérez, F., Nadal, M., Navarro-Ortega, A., Fàbrega, F., Domingo, J.L., Barceló, D., Farré, M., 2013. Accumulation of perfluoroalkyl substances in human tissues. Environment international. 59, 354-362.

Poothong, S., Boontanon, S.K., Boontanon, N., 2012. Determination of perfluorooctane sulfonate and perfluorooctanoic acid in food packaging using liquid chromatography coupled with tandem mass spectrometry. Journal of hazardous materials. 205-206, 139-143.

Post, G.B., Cohn, P.D., Cooper, K.R., 2012. Perfluorooctanoic acid (PFOA), an emerging drinking water contaminant: A critical review of recent literature. Environ. Res. 116, 93-117.

Predieri, B., Iughetti, L., Guerranti, C., Bruzzi, P., Perra, G., Focardi, S.E., 2015. High Levels of Perfluorooctane Sulfonate in Children at the Onset of Diabetes. Int. J. Endocrinol.

Prevedouros, K., Cousins, I.T., Buck, R.C., Korzeniowski, S.H., 2006. Sources, fate and transport of perfluorocarboxylates. Environmental science & technology. 40, 32-44.

Prusty, D., Park, B.-H., Davis, K.E., Farmer, S.R., 2002. Activation of MEK/ERK signaling promotes adipogenesis by enhancing peroxisome proliferator-activated receptor γ (PPARγ) and C/EBPα gene expression during the differentiation of 3T3-L1 preadipocytes. Journal of biological chemistry. 277, 46226-46232.

Qi, W., Clark, J.M., Timme-Laragy, A.R., Park, Y., 2018a. Perfluorobutanesulfonic acid (PFBS) potentiates adipogenesis of 3T3-L1 adipocytes. Food and chemical toxicology. 120, 340-345.

Qi, W., Clark, J.M., Timme-Laragy, A.R., Park, Y., 2018b. Perfluorobutanesulfonic acid (PFBS) potentiates adipogenesis of 3T3-L1 adipocytes. Food and chemical toxicology : an international journal published for the British Industrial Biological Research Association. 120, 340-345.

Qian, Y., Ducatman, A., Ward, R., Leonard, S., Bukowski, V., Lan Guo, N., Shi, X., Vallyathan, V., Castranova, V., 2010. Perfluorooctane sulfonate (PFOS) induces reactive oxygen species (ROS) production in human microvascular endothelial cells: role in endothelial permeability. Journal of toxicology and environmental health. Part A. 73, 819-836.

Qiu, Z., Wei, Y., Chen, N., Jiang, M., Wu, J., Liao, K., 2001. DNA synthesis and mitotic clonal expansion is not a required step for 3T3-L1 preadipocyte differentiation into adipocytes. Journal of biological chemistry. 276, 11988-11995.

Rahman, M.L., Zhang, C.L., Smarr, M.M., Lee, S., Honda, M., Kannan, K., Tekola-Ayele, F., Louis, G.M.B., 2019. Persistent organic pollutants and gestational diabetes: A multi-center prospective cohort study of healthy US women. Environment International. 124, 249-258.

Rao, N.S., Baker, B.E., 1994. Textile Finishes and Fluorosurfactants, in: R.E. Banks, B.E. Smart, J.C. Tatlow (Eds.), Organofluorine Chemistry: Principles and Commercial Applications. Springer US, Boston, MA, pp. 321-338.

Rhoads, K.R., Janssen, E.M., Luthy, R.G., Criddle, C.S., 2008. Aerobic biotransformation and fate of N-ethyl perfluorooctane sulfonamidoethanol (N-EtFOSE) in activated sludge. Environmental science & technology. 42, 2873-2878.

Rizzo, G., Disante, M., Mencarelli, A., Renga, B., Gioiello, A., Pellicciari, R., Fiorucci, S., 2006. FXR promotes adipocyte differentiation and regulates adipose cell function in vivo. Molecular pharmacology. 70, 1164-1173.

Roe, M.W., Lemasters, J.J., Herman, B., 1990. Assessment of Fura-2 for measurements of cytosolic free calcium. Cell Calcium. 11, 63-73.

Rosen, E.D., MacDougald, O.A., 2006. Adipocyte differentiation from the inside out. Nature reviews: molecular cell biology. 7, 885.

Rosen, M.B., Lee, J.S., Ren, H., Vallanat, B., Liu, J., Waalkes, M.P., Abbott, B.D., Lau, C., Corton, J.C., 2008. Toxicogenomic dissection of the perfluorooctanoic acid transcript profile in mouse liver: evidence for the involvement of nuclear receptors PPARα and CAR. Toxicological Sciences. 103, 46-56.

Rosen, M.B., Schmid, J.R., Corton, J.C., Zehr, R.D., Das, K.P., Abbott, B.D., Lau, C., 2010. Gene Expression Profiling in Wild-Type and PPARα-Null Mice Exposed to Perfluorooctane Sulfonate Reveals PPARα-Independent Effects. PPAR Res. 2010, 794739.

Ruan, T., Lin, Y., Wang, T., Liu, R., Jiang, G., 2015. Identification of Novel Polyfluorinated Ether Sulfonates as PFOS Alternatives in Municipal Sewage Sludge in China. Environmental science & technology. 49, 6519-6527.

Salihovic, S., Stubleski, J., Karrman, A., Larsson, A., Fall, T., Lind, L., Lind, P.M., 2018. Changes in markers of liver function in relation to changes in perfluoroalkyl substances - A longitudinal study. Environ Int. 117, 196-203.

Schadinger, S.E., Bucher, N.L., Schreiber, B.M., Farmer, S.R., 2005. PPARgamma2 regulates lipogenesis and lipid accumulation in steatotic hepatocytes. American journal of physiology. Endocrinology and metabolism. 288, E1195-1205.

Schlummer, M., Solch, C., Meisel, T., Still, M., Gruber, L., Wolz, G., 2015. Emission of perfluoroalkyl carboxylic acids (PFCA) from heated surfaces made of polytetrafluoroethylene (PTFE) applied in food contact materials and consumer products. Chemosphere. 129, 46-53.

Schmitt, J.M., Wayman, G.A., Nozaki, N., Soderling, T.R., 2004. Calcium activation of ERK mediated by calmodulin kinase I. Journal of biological chemistry. 279, 24064-24072.

Schué, F., 1999. Modern fluoropolymers Edited by John Scheirs John Wiley & Sons, Chichester, 1997 637 pp, price: ?145.00 ISBN 0-471-97055-7. Polymer International. 48, 426-426.

Seo, S.-H., Son, M.-H., Choi, S.-D., Lee, D.-H., Chang, Y.-S., 2018. Influence of exposure to perfluoroalkyl substances (PFASs) on the Korean general population: 10-year trend and health effects. Environment international. 113, 149-161.

Shan, Q., Haddrill, J.L., Lynch, J.W., 2001. Ivermectin, an unconventional agonist of the glycine receptor chloride channel. Journal of biological chemistry. 276, 12556-12564.

Sharmeen, S., Skrtic, M., Sukhai, M.A., Hurren, R., Gronda, M., Wang, X., Fonseca, S.B., Sun, H., Wood, T.E., Ward, R., 2010. The anti-parasitic agent ivermectin induces chloride-dependent membrane hyperpolarization and cell death in leukemia cells. Blood. 116, 3593-3603.

Shi, H., HALVORSEN, Y.-D., ELLIS, P.N., WILKISON, W.O., ZEMEL, M.B., 2000. Role of intracellular calcium in human adipocyte differentiation. Physiological genomics. 3, 75-82.

Shimizu, Y., Hendershot, L.M., 2009. Oxidative folding: cellular strategies for dealing with the resultant equimolar production of reactive oxygen species. Antioxidants & redox signaling. 11, 2317-2331.

Shu, H., Lindh, C.H., Wikström, S., Bornehag, C.-G., 2019. Temporal trends and predictors of perfluoroalkyl substances serum levels in Swedish pregnant women in the SELMA study. PloS one. 13, e0209255.

Siersbæk, R., Nielsen, R., Mandrup, S., 2010. PPARγ in adipocyte differentiation and metabolism–Novel insights from genome-wide studies. FEBS letters. 584, 3242-3249.

Simons, J.H., 1949. THE ELECTROCHEMICAL PROCESS FOR THE PRODUCTION OF FLUOROCARBONS. J. Electrochem. Soc. 95, 47-47.

Skutlarek, D., Exner, M., Farber, H., 2006. Perfluorinated surfactants in surface and drinking waters. Environmental science and pollution research international. 13, 299.

Song, S., Attia, R.R., Connaughton, S., Niesen, M.I., Ness, G.C., Elam, M.B., Hori, R.T., Cook, G.A., Park, E.A., 2010. Peroxisome proliferator activated receptor alpha (PPARalpha) and PPAR gamma coactivator (PGC-1alpha) induce carnitine palmitoyltransferase IA (CPT-1A) via independent gene elements. Molecular and cellular endocrinology. 325, 54-63.

Steenland, K., Zhao, L., Winquist, A., 2015. A cohort incidence study of workers exposed to perfluorooctanoic acid (PFOA). Occup Environ Med. 72, 373-380.

Su, T.C., Kuo, C.C., Hwang, J.J., Lien, G.W., Chen, M.F., Chen, P.C., 2016. Serum perfluorinated chemicals, glucose homeostasis and the risk of diabetes in working-aged Taiwanese adults. Environment International. 88, 15-22.

Sun, Q., Qi, W., Xiao, X., Yang, S.-H., Kim, D., Yoon, K.S., Clark, J.M., Park, Y., 2017. Imidacloprid Promotes High Fat Diet-Induced Adiposity in Female C57BL/6J Mice and Enhances Adipogenesis in 3T3-L1 Adipocytes via the AMPKα-Mediated Pathway. Journal of agricultural and food chemistry. 65, 6572-6581.

Sun, Q., Qi, W., Yang, J.J., Yoon, K.S., Clark, J.M., Park, Y., 2016a. Fipronil promotes adipogenesis via AMPKα-mediated pathway in 3T3-L1 adipocytes. Food and chemical toxicology. 92, 217-223.

Sun, Q., Xiao, X., Kim, Y., Kim, D., Yoon, K.S., Clark, J.M., Park, Y., 2016b. Imidacloprid promotes high fat diet-induced adiposity and insulin resistance in male C57BL/6J mice. Journal of agricultural and food chemistry. 64, 9293-9306.

Sun, Q., Zong, G., Valvi, D., Nielsen, F., Coull, B., Grandjean, P., 2018. Plasma Concentrations of Perfluoroalkyl Substances and Risk of Type 2 Diabetes: A Prospective Investigation among U.S. Women. Environ Health Perspect. 126, 037001.

Sundstrom, M., Ehresman, D.J., Bignert, A., Butenhoff, J.L., Olsen, G.W., Chang, S.C., Bergman, A., 2011. A temporal trend study (1972-2008) of perfluorooctanesulfonate, perfluorohexanesulfonate, and perfluorooctanoate in pooled human milk samples from Stockholm, Sweden. Environ Int. 37, 178-183.

Tahara, E.B., Navarete, F.D., Kowaltowski, A.J., 2009. Tissue-, substrate-, and site-specific characteristics of mitochondrial reactive oxygen species generation. Free radical biology & medicine. 46, 1283-1297.

Tang, Q.-Q., Lane, M.D., 1999. Activation and centromeric localization of CCAAT/enhancer-binding proteins during the mitotic clonal expansion of adipocyte differentiation. Genes & development. 13, 2231-2241.

Tang, Q.-Q., Lane, M.D., 2000. Role of C/EBP homologous protein (CHOP-10) in the programmed activation of CCAAT/enhancer-binding protein-β during adipogenesis. Proceedings of the national academy of sciences. 97, 12446-12450.

Tang, Q.-Q., Otto, T.C., Lane, M.D., 2003a. CCAAT/enhancer-binding protein β is required for mitotic clonal expansion during adipogenesis. Proceedings of the national academy of sciences. 100, 850-855.

Tang, Q.-Q., Otto, T.C., Lane, M.D., 2003b. Mitotic clonal expansion: a synchronous process required for adipogenesis. Proceedings of the National Academy of Sciences. 100, 44-49.

Tang, Q.-Q., Zhang, J.-W., Lane, M.D., 2004. Sequential gene promoter interactions by C/EBPβ, C/EBPα, and PPARγ during adipogenesis. Biochemical and biophysical research communications. 318, 213-218.

Tian, Y.-P., Zeng, X.-W., Bloom, M.S., Lin, S., Wang, S.-Q., Yim, S.H.L., Yang, M., Chu, C., Gurram, N., Hu, L.-W., 2019. Isomers of perfluoroalkyl substances and overweight status among Chinese by sex status: Isomers of C8 Health Project in China. Environment international. 124, 130-138.

Tian, Y., Zhou, Y., Miao, M., Wang, Z., Yuan, W., Liu, X., Wang, X., Wang, Z., Wen, S., Liang, H., 2018. Determinants of plasma concentrations of perfluoroalkyl and polyfluoroalkyl substances in pregnant women from a birth cohort in Shanghai, China. Environ Int. 119, 165-173.

Timchenko, N.A., Wilde, M., Nakanishi, M., Smith, J.R., Darlington, G.J., 1996. CCAAT/enhancer-binding protein alpha (C/EBP alpha) inhibits cell proliferation through the p21 (WAF-1/CIP-1/SDI-1) protein. Genes & development. 10, 804-815.

Timmermann, C.A.G., Rossing, L.I., Grontved, A., Ried-Larsen, M., Dalgard, C., Andersen, L.B., Grandjean, P., Nielsen, F., Svendsen, K.D., Scheike, T., Jensen, T.K., 2014. Adiposity and Glycemic Control in Children Exposed to Perfluorinated Compounds. J. Clin. Endocrinol. Metab. 99, E608-E614.

Tittlemier, S.A., Pepper, K., Edwards, L., 2006. Concentrations of perfluorooctanesulfonamides in Canadian total diet study composite food samples collected between 1992 and 2004. Journal of agricultural and food chemistry. 54, 8385-8389.

Tittlemier, S.A., Pepper, K., Seymour, C., Moisey, J., Bronson, R., Cao, X.L., Dabeka, R.W., 2007. Dietary exposure of Canadians to perfluorinated carboxylates and perfluorooctane sulfonate via consumption of meat, fish, fast foods, and food items prepared in their packaging. Journal of agricultural and food chemistry. 55, 3203-3210.

Tong, Q., Dalgin, G., Xu, H., Ting, C.-N., Leiden, J.M., Hotamisligil, G.S., 2000. Function of GATA transcription factors in preadipocyte-adipocyte transition. Science. 290, 134-138.

Tontonoz, P., Hu, E., Spiegelman, B.M., 1995. Regulation of adipocyte gene expression and differentiation by peroxisome proliferator activated receptor γ. Current opinion in genetics & development. 5, 571-576.

Toutain, P., Campan, M., Galtier, P., Alvinerie, M., 1988. Kinetic and insecticidal properties of ivermectin residues in the milk of dairy cows. Journal of veterinary pharmacology and therapeutics. 11, 288-291.

Trebak, M., Jr., J.W.P., 2017. ORAI Calcium Channels. Physiology. 32, 332-342.

Tsai, M.-S., Miyashita, C., Araki, A., Itoh, S., Bamai, Y., Goudarzi, H., Okada, E., Kashino, I., Matsuura, H., Kishi, R., 2018. Determinants and Temporal Trends of Perfluoroalkyl Substances in Pregnant Women: The Hokkaido Study on Environment and Children's Health. International journal of environmental research and public health. 15, 989.

Turner, M., Schaeffer, J., 1989. Mode of action of ivermectin, in: W. Campbell (Ed.), Ivermectin and abamectin, 1 ed. Springer, New York, NY, pp. 73-88.

Upham, B.L., Park, J.-S., Babica, P., Sovadinova, I., Rummel, A.M., Trosko, J.E., Hirose, A., Hasegawa, R., Kanno, J., Sai, K., 2009. Structure-Activity–Dependent Regulation of Cell Communication by Perfluorinated Fatty Acids using in Vivo and in Vitro Model Systems. Environmental health perspectives. 117, 545.

Urizar, N.L., Liverman, A.B., D'nette, T.D., Silva, F.V., Ordentlich, P., Yan, Y., Gonzalez, F.J., Heyman, R.A., Mangelsdorf, D.J., Moore, D.D., 2002. A natural product that lowers cholesterol as an antagonist ligand for FXR. Science. 296, 1703-1706.

van der Vlies, D., Makkinje, M., Jansens, A., Braakman, I., Verkleij, A.J., Wirtz, K.W., Post, J.A., 2003. Oxidation of ER resident proteins upon oxidative stress: effects of altering cellular redox/antioxidant status and implications for protein maturation. Antioxidants & redox signaling. 5, 381-387.

van Galen, P., Kreso, A., Mbong, N., Kent, D.G., Fitzmaurice, T., Chambers, J.E., Xie, S., Laurenti, E., Hermans, K., Eppert, K., Marciniak, S.J., Goodall, J.C., Green, A.R., Wouters, B.G., Wienholds, E., Dick, J.E., 2014. The unfolded protein response governs integrity of the haematopoietic stem-cell pool during stress. Nature. 510, 268-272.

Vanden Heuvel, J.P., Thompson, J.T., Frame, S.R., Gillies, P.J., 2006. Differential activation of nuclear receptors by perfluorinated fatty acid analogs and natural fatty acids: a comparison of human, mouse, and rat peroxisome proliferator-activated receptor-α,-β, and-γ, liver X receptor-β, and retinoid X receptor-α. Toxicological Sciences. 92, 476-489.

Vergani, L., 2017. Fatty acids and effects on in vitro and in vivo models of liver steatosis. Current medicinal chemistry.

Vestergren, R., Berger, U., Glynn, A., Cousins, I.T., 2012. Dietary exposure to perfluoroalkyl acids for the Swedish population in 1999, 2005 and 2010. Environ Int. 49, 120-127.

Vestergren, R., Cousins, I.T., 2009. Tracking the Pathways of Human Exposure to Perfluorocarboxylates. Environmental science & technology. 43, 5565-5575.

Wahlang, B., Beier, J.I., Clair, H.B., Bellis-Jones, H.J., Falkner, K.C., McClain, C.J., Cave, M.C., 2012. Toxicant-associated Steatohepatitis. Toxicologic Pathology. 41, 343-360.

Waki, H., Nakamura, M., Yamauchi, T., Wakabayashi, K.-i., Yu, J., Hirose-Yotsuya, L., Take, K., Sun, W., Iwabu, M., Okada-Iwabu, M., 2011. Global mapping of cell type–specific open chromatin by FAIRE-seq reveals the regulatory role of the NFI family in adipocyte differentiation. PLoS genetics. 7, e1002311.

Wan, H.T., Zhao, Y.G., Wei, X., Hui, K.Y., Giesy, J.P., Wong, C.K., 2012. PFOS-induced hepatic steatosis, the mechanistic actions on beta-oxidation and lipid transport. Biochimica et biophysica acta. 1820, 1092-1101.

Wang, C., Nie, X., Zhang, Y., Li, T., Mao, J., Liu, X., Gu, Y., Shi, J., Xiao, J., Wan, C., 2015. Reactive oxygen species mediate nitric oxide production through ERK/JNK MAPK signaling in HAPI microglia after PFOS exposure. Toxicology and applied pharmacology. 288, 143-151.

Wang, H., Iakova, P., Wilde, M., Welm, A., Goode, T., Roesler, W.J., Timchenko, N.A., 2001. C/EBPα arrests cell proliferation through direct inhibition of Cdk2 and Cdk4. Molecular cell. 8, 817-828.

Wang, H.X., Yang, J.Q., Du, H.Y., Xu, L.J., Liu, S.P., Yi, J.P., Qian, X., Chen, Y., Jiang, Q.W., He, G.S., 2018. Perfluoroalkyl substances, glucose homeostasis, and gestational diabetes mellitus in Chinese pregnant women: A repeat measurement-based prospective study. Environment International. 114, 12-20.

Wang, Y., Hollis-Hansen, K., Ren, X., Qiu, Y., Qu, W., 2016. Do environmental pollutants increase obesity risk in humans? Obesity reviews : an official journal of the International Association for the Study of Obesity. 17, 1179-1197.

Watkins, A.M., Wood, C.R., Lin, M.T., Abbott, B.D., 2015. The effects of perfluorinated chemicals on adipocyte differentiation in vitro. Molecular and cellular endocrinology. 400, 90-101.

Winquist, A., Lally, C., Shin, H.M., Steenland, K., 2013. Design, methods, and population for a study of PFOA health effects among highly exposed mid-Ohio valley community residents and workers. Environ Health Perspect. 121, 893-899.

Wolf, C.J., Takacs, M.L., Schmid, J.E., Lau, C., Abbott, B.D., 2008. Activation of Mouse and Human Peroxisome Proliferator−Activated Receptor Alpha by Perfluoroalkyl Acids of Different Functional Groups and Chain Lengths. Toxicological Sciences. 106, 162-171.

Wolf Greenstein, A., Majumdar, N., Yang, P., Subbaiah, P.V., Kineman, R.D., Cordoba-Chacon, J., 2017. Hepatocyte-specific, PPARγ-regulated mechanisms to promote steatosis in adult mice. J Endocrinol. 232, 107-121.

Wu, Z., Xie, Y., Bucher, N., Farmer, S.R., 1995. Conditional ectopic expression of C/EBP beta in NIH-3T3 cells induces PPAR gamma and stimulates adipogenesis. Genes & development. 9, 2350-2363.

Xiao, X., Kim, Y., Kim, D., Yoon, K.S., Clark, J.M., Park, Y., 2015. A pyrethroid pesticide, permethrin, alters lipid metabolism and voluntary activities in mice. The FASEB Journal. 29, 776.772.

Xiao, X., Kim, Y., Kim, D., Yoon, K.S., Clark, J.M., Park, Y., 2017a. Permethrin alters glucose metabolism in conjunction with high fat diet by potentiating insulin resistance and decreases voluntary activities in female C57BL/6J mice. Food and chemical toxicology. 108, 161-170.

Xiao, X., Qi, W., Clark, J.M., Park, Y., 2017b. Permethrin potentiates adipogenesis via intracellular calcium and endoplasmic reticulum stress-mediated mechanisms in 3T3-L1 adipocytes. Food and chemical toxicology. 109, 123-129.

Xiao, X., Sun, Q., Kim, Y., Yang, S.-H., Qi, W., Kim, D., Yoon, K.S., Clark, J.M., Park, Y., 2018. Exposure to permethrin promotes high fat diet-induced weight gain and insulin resistance in male C57BL/6J mice. Food and chemical toxicology. 111, 405-416.

Xu, J., Shimpi, P., Armstrong, L., Salter, D., Slitt, A.L., 2016. PFOS induces adipogenesis and glucose uptake in association with activation of Nrf2 signaling pathway. Toxicology and applied pharmacology. 290, 21-30.

Yamaguchi, M., Arisawa, K., Uemura, H., Katsuura-Kamano, S., Takami, H., Sawachika, F., Nakamoto, M., Juta, T., Toda, E., Mori, K., Hasegawa, M., Tanto, M., Shima, M., Sumiyoshi, Y., Morinaga, K., Kodama, K., Suzuki, T., Nagai, M., Satoh, H., 2013.

Consumption of seafood, serum liver enzymes, and blood levels of PFOS and PFOA in the Japanese population. Journal of occupational health. 55, 184-194.

Yamamoto, J., Yamane, T., Oishi, Y., Kobayashi-Hattori, K., 2015. Perfluorooctanoic acid binds to peroxisome proliferator-activated receptor γ and promotes adipocyte differentiation in 3T3-L1 adipocytes. Bioscience, biotechnology, and biochemistry. 79, 636-639.

Yang, J.S., Qi, W., Farias-Pereira, R., Choi, S., Clark, J.M., Kim, D., Park, Y., 2019a. Permethrin and ivermectin modulate lipid metabolism in steatosis-induced HepG2 hepatocyte. Food and chemical toxicology : an international journal published for the British Industrial Biological Research Association. 125, 595-604.

Yang, J.S., Qi, W., Pereira, R.F., Choi, S., Clark, J.M., Kim, D., Park, Y., 2019b. Permethrin and ivermectin modulate lipid metabolism in steatosis-induced HepG2 hepatocyte. Food and chemical toxicology. 125, 595-604.

Yang, J.S., Symington, S., Clark, J.M., Park, Y., 2018a. Permethrin, a pyrethroid insecticide, regulates ERK1/2 activation through membrane depolarization-mediated pathway in HepG2 hepatocytes. Food and chemical toxicology : an international journal published for the British Industrial Biological Research Association. 121, 387-395.

Yang, J.Y., Della-Fera, M.A., Baile, C.A., 2008. Guggulsterone inhibits adipocyte differentiation and induces apoptosis in 3T3-L1 cells. Obesity. 16, 16-22.

Yang, Q., Guo, X., Sun, P., Chen, Y., Zhang, W., Gao, A., 2018b. Association of serum levels of perfluoroalkyl substances (PFASs) with the metabolic syndrome (MetS) in Chinese male adults: A cross–sectional study. Science of the total environment. 621, 1542-1549.

Young, C.J., Mabury, S.A., 2010. Atmospheric perfluorinated acid precursors: chemistry, occurrence, and impacts. Reviews of environmental contamination and toxicology. 208, 1-109.

Younossi, Z.M., Koenig, A.B., Abdelatif, D., Fazel, Y., Henry, L., Wymer, M., 2016. Global epidemiology of nonalcoholic fatty liver disease-Meta-analytic assessment of prevalence, incidence, and outcomes. Hepatology (Baltimore, Md.). 64, 73-84.

Youssef, M.Y., Sadaka, H.A., Eissa, M.M., El-Ariny, A.F., 1995. Topical application of ivermectin for human ectoparasites. American journal of tropical medicine and hygiene. 53, 652-653.

Yu, S., Matsusue, K., Kashireddy, P., Cao, W.Q., Yeldandi, V., Yeldandi, A.V., Rao, M.S., Gonzalez, F.J., Reddy, J.K., 2003. Adipocyte-specific gene expression and adipogenic steatosis in the mouse liver due to peroxisome proliferator-activated receptor gamma1 (PPARgamma1) overexpression. The Journal of biological chemistry. 278, 498-505.

Yuan, G., Peng, H., Huang, C., Hu, J., 2016. Ubiquitous Occurrence of Fluorotelomer Alcohols in Eco-Friendly Paper-Made Food-Contact Materials and Their Implication for Human Exposure. Environmental science & technology. 50, 942-950.

Zebisch, K., Voigt, V., Wabitsch, M., Brandsch, M., 2012. Protocol for effective differentiation of 3T3-L1 cells to adipocytes. Analytical biochemistry. 425, 88-90.

Zhang, C., Sundaram, R., Maisog, J., Calafat, A.M., Barr, D.B., Buck Louis, G.M., 2015. A prospective study of prepregnancy serum concentrations of perfluorochemicals and the risk of gestational diabetes. Fertility and sterility. 103, 184-189.

Zhang, H., He, J., Li, N., Gao, N., Du, Q., Chen, B., Chen, F., Shan, X., Ding, Y., Zhu, W., Wu, Y., Tang, J., Jia, X., 2019. Lipid accumulation responses in the liver of Rana nigromaculata induced by perfluorooctanoic acid (PFOA). Ecotoxicology and environmental safety. 167, 29-35.

Zhang, L., Ren, X.-M., Wan, B., Guo, L.-H., 2014. Structure-dependent binding and activation of perfluorinated compounds on human peroxisome proliferator-activated receptor γ. Toxicology and applied pharmacology. 279, 275-283.

Zhou, J., Febbraio, M., Wada, T., Zhai, Y., Kuruba, R., He, J., Lee, J.H., Khadem, S., Ren, S., Li, S., Silverstein, R.L., Xie, W., 2008. Hepatic fatty acid transporter Cd36 is a common target of LXR, PXR, and PPARgamma in promoting steatosis. Gastroenterology. 134, 556-567.

Zhou, Z., Liang, Y., Shi, Y., Xu, L., Cai, Y., 2013a. Occurrence and transport of perfluoroalkyl acids (PFAAs), including short-chain PFAAs in Tangxun Lake, China. Environmental science & technology. 47, 9249-9257.

Zhou, Z., Liang, Y., Shi, Y., Xu, L., Cai, Y., 2013b. Occurrence and transport of perfluoroalkyl acids (PFAAs), including short-chain PFAAs in Tangxun Lake, China. Environmental science & technology. 47, 9249-9257.